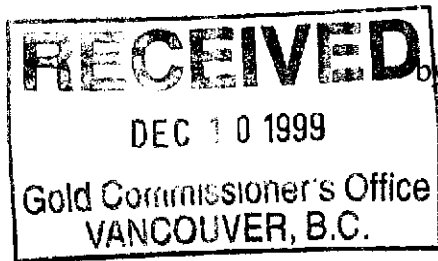


TO ACCOMPANY TUZEX CLAIMS, REPORT OF FIELD WORK
ENZYME LEACH SOILS SURVEY, AND DATA COMPILATION
ALBERNI M.D. SOUTHERN VANCOUVER IS. B.C. NTS 092C-119
BY H.V. WAHL, P. ENG. B.C. AUGUST 1999

Interpretation of Enzyme LeachSM Data for the H. Wahl and J. Ruza Tuzex Project



by: Gregory T. Hill, Enzyme Laboratories, Inc.

12 November 1999

Summary

Enzyme LeachSM data were generated from soils collected at 37 sample sites along two lines within the Tuzex claim block. The Flora zone is indicated by apical base metals anomalies along Line 57A and as either apical anomalies, or a central low along Line TX. Although the Flora zone is strongly indicated, the Enzyme LeachSM signature above this feature along Line TX is unclear because of a paucity of samples near this shear zone. Oxidation halos are present to the north of the Flora zone on both lines. The oxidation halo along Line 57A brackets a central low centered near 900NW. The halo along Line TX is of higher contrast, and contains much higher base metals values than the halo along Line 57A. This TX halo occurs within a quartz-sericite-pyrite alteration zone and surrounds apparent apical base metals anomalies that coincide with a photo linear at sample TX-11. These apical anomalies are interpreted to mark either a mineralized fault zone or a post-mineral fault that cuts mineralization in the subsurface. For these reasons, the subsurface beneath TX-11 is ranked as the highest priority drill target within the sampled area.

Introduction and Evaluation Procedure

Enzyme LeachSM data were generated from soils collected at 37 sample sites along two lines within the Tuzex claim block. Profiles of each detected element, except for some of the heavy rare earth elements, were constructed for each sample line, and are included with this report. Several groups of elements were plotted together in order to better illustrate the distributions of oxidation halos within the sampled area. The groups of elements chosen to be plotted together were identified through inspection of individual plots and cataloguing the distributions of each. Oxidation halos are typically heterogeneous in composition, where one or more elements are most concentrated into one portion of a halo, and other elements are most concentrated into other portions. In order to produce these composite plots, some elements were normalized so that each would be given roughly equal weighting.

Enzyme LeachSM Patterns

It is important to briefly reiterate the types of anomalies revealed by Enzyme LeachSM in areas covered by alluvial or glacial overburden, volcanic units, or barren bedrock. Enzyme LeachSM

anomalies tend to form two predominant patterns: oxidation halo anomalies and diffusion or apical anomalies.

The more important oxidation anomaly patterns tend to be characterized by oxidation halos where reduced material in the subsurface is undergoing very subtle oxidation. These halos flank the reduced body, and a "central low" is found over a "reduced chimney" located between the reduced body and the surface. The elements in these halos characteristically include at least part of the oxidation suite: Cl, Br, I, Mo, As, Sb, W, Re, V, Se, Te, U, Th, and sometimes Au, Hg and rare earth elements. Oxidation halos are typically asymmetrical, and often require comparison of a number of trace element patterns before they become apparent. Where a strong oxidation cell is present in the subsurface, some or all of the metals will migrate into the halo.

Apical or diffusion anomaly patterns tend to form apical highs directly over the source of the anomaly rather than forming a halo around the source. The source of the anomaly can be the actual source of the anomalous trace elements, or it can be a fault, unconformity or other feature that facilitates the movement of the trace elements to the surface. In either case the anomaly will usually be almost directly over the source. In simple diffusion anomalies, the trace element suite does not include the oxidation suite elements. In fault-related diffusion anomalies, the trace element suite can contain many of the oxidation suite elements. Typically, diffusion anomalies exhibit a more diminished contrast above background than do oxidation anomalies. Alternatively, fault-related anomalies can have extreme anomaly/background contrast.

In the real world, mineralized bodies tend to be geologically complex and the anomalies frequently are combined or partially overlap each other. For example, where a deeply buried reduced body is intersected by a fault, many of the oxidation suite elements will commonly form an extremely high contrast anomaly directly over the trace of the buried fault. This high contrast anomaly may partially mask the oxidation anomaly. In another example, in moderately strong oxidation cells some base metals will migrate into the halo, while others will migrate into the apical anomaly. Another pattern is the multi-sample, multi-line high values or platform anomaly. These platform anomalies will often have high contrast boundaries and will often flank oxidation anomalies. Sometimes, linear low trends occur internal to the platform and the high contrast flanks. In many instances, these trends represent the underlying structural fabric of the area.

The key to interpretation of Enzyme LeachSM data is pattern recognition in multiple trace element distributions in conjunction with available geologic information. In addition to variances in composition around the circumferences of oxidation halos, they are often concentrically zoned, with some elements forming halos proximal to central lows and others forming halos more distally. Recognition of this zonation can be important for determining the morphologies of oxidation halos which are typically irregular and discontinuous. The element patterns are often more important than the absolute values, although high values of oxidation suite elements do mark many economic mineral deposits and petroleum reservoirs. The interpretation of Enzyme LeachSM data is enhanced by comparison and integration with all other available project data.

Geologic Setting and Distribution of Enzyme LeachSM Samples

These Enzyme LeachSM data were measured from samples collected at the Tuzex project operated by H. Wahl and J. Ruza. Samples were collected at most 100 m intervals on two traverses along forest roads. B-horizons soils were collected from an average depth of 20 cm. Sixteen samples were collected from traverse 57A and 21 samples were collected along traverse TX.

Descriptions of geology and work history on the Tuzex claims are given by H.J. Wahl in "TUZEX CLAIMS Report on Field Work, Enzyme Leach Soils Survey, and Data Compilation (Non-destructive geological work) Minfile 092C-119." The following geologic descriptions are excerpted or summarized from this report. The Tuzex claims are situated on a 1.5 X 1.0 km quartz-pyrite-sericite-kaolin alteration zone within Bonanza volcanics of estimated Jurassic age. Large deformation zones occur within and adjacent to this alteration zone and contain a number of Pb, Zn, Ag occurrences. Substantial conventional soil and IP anomalies are also present. A 500 m wide zone containing 50-150 m thick discontinuous intercalated carbonate beds also occurs within the claims.

The property is located within rugged, forested, mountainous terrain with elevations ranging from 40 to 800 meters above sea level. Overburden consists of glacial drift estimated to be 2-10 m thick. Much of the drift is orange, reflecting the large alteration zone.

Interpretation

Line TX

Oxidation Suite Elements

Chlorine forms a moderate contrast rabbit ears pattern that indicates an oxidation halo with a central low centered near sample TX-11, the location of an east northeast trending photo linear. A second oxidation halo, possibly associated with the Flora zone, is present at the southern end of the line, with a central low near TX-18 or TX-19. This halo is narrower and of higher contrast, but the central low associated with this feature is poorly defined. The lack of definition could result from the paucity of samples between the two peaks at TX-16 and TX-21.

The two highest bromine peaks occur at either end of Line TX, at TX-2 and TX-21 and bracket the quartz-sericite-pyrite alteration zone. Overall, the Br distribution is similar to that of Cl, with corresponding peaks and valleys in many places. However, the magnitudes of these peaks are quite different among these two elements. The Br distribution suggests that one oxidation halo, marking the quartz-sericite-pyrite zone, with several internal structural (?) interruptions occurs along Line TX. While Br indicates this broad alteration zone, the distributions of other elements suggest Zn, Cu and/or Ag zones within the bounds of this feature.

Iodine forms a moderate contrast halo that roughly corresponds with the Cl rabbit ears pattern along the north-center of Line TX. A second iodine low is also apparent between TX-16 and

TX-21, with a moderate high near the Flora zone at TX-18. It is suspected that the iodine halo surrounding the Flora zone is wider than those of Cl and Br, and the southern margin of this iodine halo occurs to the south at TX-21.

The summary plot of the halogens and base metals along Line TX shows superimposed Cl, Br, and I distributions. This plot shows that the moderate iodine high at TX-18 occurs near the center of the Cl and Br peaks which bracket the Flora shear zone. Bromine may also form an apical high at TX-18, but this is not resolvable because of the lack of samples between TX-17 and TX-18. The Cl halo, and a portion of the Br halo bracketing the Flora zone are of higher contrast than the halogen halos bracketing central lows along the northern part of Line TX. This could indicate that mineralization is more intense within the Flora zone than beneath other portions of Line TX. However, differences in the depths of glacial cover or the depths to mineralization, or the presence of structural conduits within or near the Flora zone could also account for the lower Cl and Br contrasts along the northern portion of Line TX. Iodine appears to form halos of similar contrast at both anomalies.

Vanadium is enriched in three peaks near both ends and the center of Line TX, forming central lows that partially correspond with those of the halogens described above. A deep V central low is present between TX-6 and TX-7 and corresponds with Cl, Br and I lows of similar dimensions, as marked by asymmetrical low to moderate contrast rabbit ears patterns in this area. Although difficult to discern, zonation among the halogens appears to occur about this central low. Chlorine highs at TX-5 and TX-9 form the narrowest halo, while Br highs at TX-2 and TX-10, and I highs at TX-2 and TX-13 form successively wider halos. This halogen zonation has been noted among a number Enzyme Leachsm studies and can be useful in determining the presence of the most persistent oxidation halos and central lows. This is particularly important in an area such as this, where several oxidation halos may overlap and obscure one another. Zonation such as this may occur because there are large differences in the oxidation potentials required to oxidize chloride, bromide, and iodide to elemental chlorine, bromine, and iodine, respectively (Table 1). Because the voltage required to oxidize iodide is smallest, iodine is sometimes mobilized farthest within an electrochemical cell while Cl is the least dispersed of the halogens, thereby producing nested Cl, Br, and I halos.

Table 1. Standard electrode potentials for the oxidation of halides to halogens.

Reaction	E° volts
$2\text{Cl}^- = \text{Cl}_2 + 2\text{e}^-$	+1.39
$2\text{Br}^- = \text{Br}_2 + 2\text{e}^-$	+1.08
$2\text{I}^- = \text{I}_2 + 2\text{e}^-$	+0.62

Arsenic and molybdenum form low contrast patterns near the detection limits for these elements. Nonetheless, both elements form central lows centered near TX-8, that correspond with the apparent oxidation halo defined by Cl, Br, I, and V. Arsenic and vanadium do not provide good evidence of an oxidation halo near the southern end of Line TX.

Antimony, thorium, and uranium were only detected in a few samples at the detection limits for these elements, and do not indicate any oxidation anomalies.

Tungsten, selenium, tellurium, and rhenium were not detected in any samples.

The oxidation suite elements are thought to be the most important for defining Enzyme LeachSM anomalies that indicate reduced mineralized zones in the subsurface. The remainder of the elements detected by Enzyme LeachSM analysis can also provide important information about covered bedrock and mineralizing systems as is discussed below. Perhaps more important is the fact that many elements that are not part of the oxidation suite also enter oxidation halos where there is a strong oxidation cell associated with a reduced body in the subsurface. This can be useful in ranking the importance of the best developed oxidation suite anomalies.

Metals

The base metals, Cu, Pb, and Zn are plotted beneath the halogens on the summary plot of the halogens and base metals for Line TX. The distributions of these elements are also shown as individual plots contained within this report. Central lows between TX-8 and TX-12 are consistently developed among these elements. The Cu values within these samples are the lowest of any samples along Line TX. Three of these five samples contain lower Zn values than any other Line TX samples. The exception, TX-11, contains a relatively high Zn value and corresponds with the photo linear indicated on maps supplied by H. Wahl. Lead and copper form very weak highs at TX-11 within the Pb and Cu central lows spanning from TX-8 to TX-12. These relationships, and the corresponding oxidation suite halos, suggest that a mineralized zone is centered between TX-8 and TX-12 and contains a fault that corresponds with the photo linear and may be either pre-mineral or post mineral in origin. The apparent fault beneath TX-11 could be mineralized itself, or could cut the mineralized zone at depth. Copper, lead, and zinc each form peaks at the northern end of Line TX, suggesting that these elements are enriched in an oxidation halo surrounding the quartz-sericite-pyrite zone. Like iodine, the Cu, Pb, and Zn peaks marking the southern margin of the halo, likely occur to the south of TX-21.

Cadmium, manganese, and cobalt each halo central lows at TX-8 to TX-12. Cadmium was measured at fairly high levels relative to many Enzyme LeachSM surveys. This element is distributed similarly to Zn except that no Cd peak is present at the northern end of Line TX. Cadmium, Mn, and Co, like Cu and Zn, form well defined, deep central lows between TX-8 and TX-12. For each of these elements, the values within these lows are the lowest of any along Line TX. This suggests that a reduced chimney, due to a reduced body in the subsurface, is present in this area. This reduced chimney may extend to the surface producing reducing conditions that are strong enough to immobilize these elements within this central low. Under such conditions, concentrations of these elements with the soil would not be taken up by amorphous manganese oxides resulting in lower background levels.

Nickel appears to be enriched in an oxidation halo that surrounds the large quartz-sericite-pyrite alteration zone.

Gallium and bismuth were detected near the detection limits for these elements and do not produce patterns that clearly indicate the presence of mineralization in the subsurface.

Rare Earth Elements

The rare earth elements (REE) are geochemically similar and, as such, tend to yield similar patterns. Plots of La, Ce, Pr, and Nd are included with this report. Although there are slight differences in the La, Pr, and Nd distributions in this study, the patterns generated by these elements are generally the same. These REE are concentrated into a peak at TX-5 that coincides with the edges of the quartz-sericite-pyrite alteration zone. On the southern end of Line TX the REE values increase from TX-20 to TX-21 and may form similar peaks just beyond the southern edge of Line TX which corresponds with the edge of the mapped alteration zone. The highest Ce peak is defined by samples TX-5 and TX-6. Central lows that correspond with the Flora zone or the photo linear are not well developed.

Lithophile Elements

Sometimes the lithophile elements produce patterns related to lithologic units in the subsurface. Strontium, Rb, and Ba commonly occur as trace elements in feldspars and are released from these minerals during hydrothermal alteration. At times their Enzyme LeachSM patterns can indicate alteration patterns, or altered lithologies in the bedrock. When strong oxidation cells are present, one or more of them can migrate into halos, similar to, but not exactly mimicking some of the oxidation suite elements.

Strontium appears to be enriched in an oxidation halo at TX-4 and TX-18 while Ba appears to form a slightly wider halo. A strong Ba high occurs at TX-11 suggesting the presence of a fault in this location. These elements form highs near the Flora zone at TX-18. These apical highs may result from Ba and Sr being liberated from feldspars through alteration of granitic fragments within the Flora shear zone.

The rubidium distribution does not indicate any oxidation halos or central lows. However, the relatively low Rb values at samples TX-1, TX-18, and TX-20 suggest that an apical Rb high may partially correspond with the large alteration zone as is seen in some Enzyme LeachSM surveys.

Cesium and lithium were detected in only a small number of samples near the detection limits.

High Field Strength Elements

The zirconium, yttrium, and titanium distributions each suggest that an oxidation halo is present in the northern part of Line TX with central lows centered near TX-8. The strongest peaks in

these elements are developed along the northern margin of this halo. Interestingly, these Zr, Ti, and Y peaks occur at three separate samples, TX-2, TX-3, and TX-5, respectively. This strongly suggests that these elements are enriched in an oxidation halo and are not simply enriched apically above a fault. If these were fault related highs one would expect them to coincide more closely. However, Zr tends to form apical anomalies above faults as has been noted in many Enzyme LeachSM surveys. The Zr high at TX-2 corresponds to highs developed among many elements and could be developed above a fault in the subsurface. Zirconium, yttrium, and titanium all form low contrast highs over TX-11, further suggesting that these highs and the photo linear coincide with a fault in the subsurface.

Niobium was detected near the detection limit in about half of the samples along the northern half of Line TX.

Scandium was not measured above the detection limit in any samples.

Precious Metals

Gold was detected in only one sample at 0.7 ppb. This value occurs near the northern edge of the >1.9 ppm Ag in conventional soils zone and may indicate that Au is enriched in the subsurface near this sample. However, Au is rarely found at significant levels in Enzyme LeachSM surveys and this sample may or may not represent Au enrichment in the subsurface. This 0.7 ppb Au value could result from the scavenging of soil-derived gold chloride formed at the surface and not from Au that has migrated vertically from the subsurface.

Silver, platinum, palladium, ruthenium, and osmium were not detected in any samples.

Line 57A

Oxidation Suite Elements

The Cl response along Line 57A is 30% that of Line TX as indicated by the comparisons of means and maximums among the two lines listed in Table 3. The remaining oxidation suite elements were detected at similar levels among both sample lines.

Among the halogens, only iodine shows an apparent halo that brackets the Flora zone. Chlorine forms peaks at 500NW and 1200NW, the former of which occurs near the southern edge of the Flora zone. The area between these two Cl peaks could be a central low as suggested by the consistently low Br values at 800NW-1000NW.

Vanadium is enriched over the Flora zone and like Br, is most concentrated at the southern end of Line 57A, suggesting that a fault could be present in the subsurface at the end or south of the end of Line 57A.

Weak As and Mo peaks occur respectively at and near the northern end of Line 57A, near the edge of the Anomaly "A" conventional soil As-Zn zone. Molybdenum also forms a peak at 600NW that corresponds to the largest Cu, Zn, and Pb peaks on Line 57A. Another Mo peak at 900NW corresponds with the center of the possible Br and Cl central low described above. As described below, Cu, Zn, and particularly Pb appear to form a halo that brackets this Mo high at 900NW, thus suggesting that this Mo feature is an apical high marking a mineralized zone in the subsurface. These relationships are illustrated in the summary plot of halogens and base metals along Line 57A showing superimposed Cl, Br, and I distributions and Cu, Zn, Pb distributions.

Thorium and uranium were only detected in one sample, 1500NW, at or near the detection limits for these samples. These elements do not indicate oxidation halos or apical anomalies.

Metals

As indicated by Table 3, the Mn, Co, and Ni values along Line 57A are only about one half as high as along Line TX. Copper, Zn, Cd, and Pb are much more enriched along Line TX than along Line 57A.

The correspondence of Cu, Zn, and Pb peaks at 600NW, as well as the mapped Flora structural zone, strongly suggests that these peaks are fault controlled apical anomalies. However, other Cu and Pb peaks occur to the north at 1400NW and 1200NW respectively, and are not associated with major mapped structural features such as the Flora zone. The Pb distribution in particular corroborates the Cl and Br oxidation halo centered at 900NW.

Cobalt and manganese are distributed into halos that surround central lows between 500NW and 1000NW. Although apical Co and Mn highs are apparent over the Flora zone at 600NW, the southern edge of these halos seems to be defined by the values at 400NW. Additionally, the Co and Mn peaks on the northern margin of the halo occur at 1100NW and not at 1200NW where the Pb peak is developed. The observed zonation within this anomaly increases the authors' confidence that these features represent an oxidation halo with a central low near 800-900NW.

The Cd, Ni, and Ga distributions are of low contrast near the detection limits of these elements and do not define oxidation halos or apical highs. However, it should be noted that the highest Cd value occurs at 900NW, at the center of the apparent oxidation halo.

Rare Earth Elements

The REE are similarly enriched along both lines.

Lanthanum, praseodymium, and neodymium form halos surrounding a central low the middle of Line 57A. Cerium also forms a halo here, but the northern most Ce spike occurs at the northern end of Line 57A and to the north of the other REE peaks.

Lithophile Elements

Lithium, Rb, Sr, and Cs are slightly more enriched along Line TX. The Ba response along Line TX is about twice as strong as that along Line 57A.

As is true on Line TX, Sr is enriched above the Flora zone and may indicate the presence of altered intrusive materials within this shear zone. This element also appears to be concentrated into an oxidation halo that surrounds a weaker apical high at 900NW. The apical Sr high at 900NW suggests that intrusive rocks could be associated with a potential mineralized zone in the subsurface here.

The Ba distribution is mostly characterized by background variations but a high is indicated at 1400NW.

The Rb distribution shows only background variations.

Lithium and cesium were not detected along Line 57A.

High Field Strength Elements

The average Zr, Y, and Ti responses are roughly the same along both lines, but the maximum values are about 1.5 to 3.5 times higher along Line TX.

Zirconium and yttrium show similar patterns in which halos surround central lows that contain apical highs at 800-900NW. The Zr distribution is particularly interesting as two nested halos may be present with an apical high in the center. The innermost Zr halo is indicated by peaks at 600NW and 1100NW while the outer Zr halo occurs at 300NW and 1500NW. A fault may lay at the center of these halos as indicated by the Zr high at 800-900NW.

Titanium shows a pattern that is similar to that of Zr, with two apparently nested halos surrounding an apical high. The inner Ti halo is quite asymmetrical.

Niobium was only detected in one sample near the detection limit.

Precious Metals

No precious metals were detected along Line 57A.

Discussion and Conclusions

The responses of many important elements including Cl and the base metals are significantly higher along Line TX than along Line 57A. A moderate contrast oxidation halo containing significant Pb, Zn, and Cu values surrounds the large quartz-sericite-pyrite alteration zone suggesting that this feature is enriched in these metals. The Flora shear zone appears to be indicated as an apical high where it crosses beneath Line 57A. The signature of the Flora zone is also strong on Line TX but the relationship between this feature and the Enzyme LeachSM data is less clear on this traverse. This is because samples were not collected above the shear zone along Line TX, and the Flora zone coincides with the edge of the quartz-sericite-pyrite alteration zone here. While a strong oxidation halo brackets a central low between samples TX-18 to TX-20, it is not known if the base metals form apical anomalies above the Flora zone here, as they do on Line 57A. Nonetheless, these data suggest that an important mineralized zone could occur in the subsurface adjacent to the Flora zone, beneath samples TX-18 to TX-20. The subsurface beneath TX-18 to TX-20 is an interesting target that should be pursued farther.

To the north, a broader oxidation halo is defined by Cl, Co, Mn, Cu, Pb, and Zn as shown in a Summary Figure of many of these elements along Line TX in which all values are normalized to their medians. This process allows for profiles of all of these elements to be plotted together and also illustrates the levels of contrast shown by each element. There appears to be a zonation among these elements where successively wider Co-Mn, Pb, and Cl halos bracket an apical Zn high. Copper and Zn are concentrated into a weak halo that is marked by small highs on the margins of consistently low, below background Cu values. The central lows of all of the elements shown in this plot coincide from TX-8 to TX-12. This, along with the coincident Zn high at TX-11 suggests that the subsurface beneath TX-8 to TX-12, and particularly beneath TX-11 is prospective. As noted above, TX-11 also coincides with a photo linear which likely represents a mineralized fault or post-mineral fault that cuts a mineralized body in the subsurface. This potential mineralized structural zone is ranked as the highest priority drill target within the sampled area.

A summary Figure plotting normalized halogen and metals values along Line 57A is also included with this report. This Figure shows that an oxidation halo is present and brackets a central low 600NW to 900NW. A Zr high coincides with this central low and may mark a structural zone in the subsurface. Strong highs are consistently developed among the metals at 600NW. This sample was collected above the Flora shear zone which forms an apical anomaly. This apical high appears to occur within the central low near the edge of the oxidation halo as indicated by Cl and Br peaks at 500NW, Co and Mn peaks at 400NW, and La and Zr peaks at 300NW. The halo is also zoned on the north. However, zonation within this halo does not appear to be symmetrical as is the case within the halo centered above TX-8 to TX-12. The oxidation halo along Line 57A also lacks apical highs, other than Zr within the central low at 800NW. In addition, the base metals are much less enriched in this halo than they are in the halo on Line TX. Therefore, the subsurface below 700NW to 900NW should be considered as a drill target, but should be given lower priority than the subsurface beneath TX-8 to TX-12.

These data indicate that oxidation halos and apical anomalies are present within the study area. Furthermore, many of the Enzyme LeachSM anomalies identified in this study correspond with known features such as the Flora shear zone, the quartz-sericite-pyrite alteration zone, and the identified photo linear that crosses Line TX. Additional Enzyme LeachSM sampling would likely further define the extents of these oxidation halos and apical anomalies.

Table 2. Simple statistics generated from all Enzyme LeachSM (ICP-MS) data, Lines TX and 57A. n/a - not applicable due to too few or no detected values. Statistics calculated after ½ detection limit values substituted for not detected values.

Element	Li	Be	Cl	Sc	Ti	V	Mn	Co	Ni	Cu	Zn
Det. Limit (ppb)	10	20	3000	100	100	5	10	1	5	5	10
Maximum	15	n/a	331064	n/a	1150	69	24606	113	71	139	689
Mean	n/a	n/a	62563.7	n/a	284.0	27.4	5161.7	24.4	12.6	33.4	182.7
Std. Dev.	n/a	n/a	68978.3	n/a	231.0	16.3	5642.6	25.4	13.3	24.3	153.4
Std. Dev.+Mean	n/a	n/a	131542.0	n/a	515.0	43.7	10804.3	49.8	25.9	57.7	336.1

Element	Ga	Ge	As	Se	Br	Rb	Sr	Y	Zr	Nb	Mo	Ru	Pd
Det. Limit (ppb)	1	1	5	30	30	1	1	1	1	1	1	1	1
Maximum	4	3	14	n/a	1058	178	269	32	25	2	7	n/a	n/a
Mean	1.5	n/a	5.3	n/a	409.1	96.9	86.6	9.1	3.8	n/a	1.8	n/a	n/a
Std. Dev.	1.0	n/a	3.2	n/a	229.7	32.8	66.6	6.2	4.2	n/a	1.5	n/a	n/a
Std. Dev.+Mean	2.5	n/a	8.5	n/a	638.8	129.7	153.2	15.3	8.0	n/a	3.3	n/a	n/a

Element	Ag	Cd	In	Sn	Sb	Te	I	Cs	Ba	La	Ce	Pr	Nd	Sm
Det. Limit (ppb)	0.2	0.2	0.2	1	1	1	10	1	1	1	1	1	1	1
Maximum	n/a	18.7	n/a	n/a	2	n/a	506	4	907	30	26	6	24	5
Mean	n/a	5.26	n/a	n/a	n/a	n/a	192.0	n/a	286.9	6.9	10.2	1.7	7.5	1.6
Std. Dev.	n/a	4.94	n/a	n/a	n/a	n/a	121.5	n/a	211.8	5.2	5.6	1.1	4.3	0.9
Std. Dev.+Mean	n/a	10.20	n/a	n/a	n/a	n/a	313.5	n/a	498.7	12.1	15.8	2.8	11.8	2.5

Element	Eu	Gd	Tb	Dy	Ho	Er	Tm	Yb	Lu	Hf	Ta	W
Det. Limit (ppb)	1	1	1	1	1	1	1	1	1	1	1	1
Maximum	1	4	n/a	4	n/a	2	1	2	n/a	n/a	n/a	n/a
Mean	n/a	1.6	n/a	1.5	n/a	n/a	n/a	n/a	n/a	n/a	n/a	n/a
Std. Dev.	n/a	0.9	n/a	0.9	n/a	n/a	n/a	n/a	n/a	n/a	n/a	n/a
Std. Dev.+Mean	n/a	2.5	n/a	2.4	n/a	n/a	n/a	n/a	n/a	n/a	n/a	n/a

Element	Re	Os	Pt	Au	Hg	Tl	Pb	Bi	Th	U
Det. Limit (ppb)	0.1	1	1	0.1	1	1	1	1	1	1
Maximum	n/a	n/a	n/a	n/a	n/a	3	571	1	2	1
Mean	n/a	n/a	n/a	n/a	n/a	n/a	61.4	n/a	n/a	n/a
Std. Dev.	n/a	n/a	n/a	n/a	n/a	n/a	127.2	n/a	n/a	n/a
Std. Dev.+Mean	n/a	n/a	n/a	n/a	n/a	n/a	188.6	n/a	n/a	n/a

Table 3. Means and maximums for Lines TX and 57A. n/a - not applicable due to too few or no detected values. Statistics calculated after ½ detection limit values substituted for not detected values.

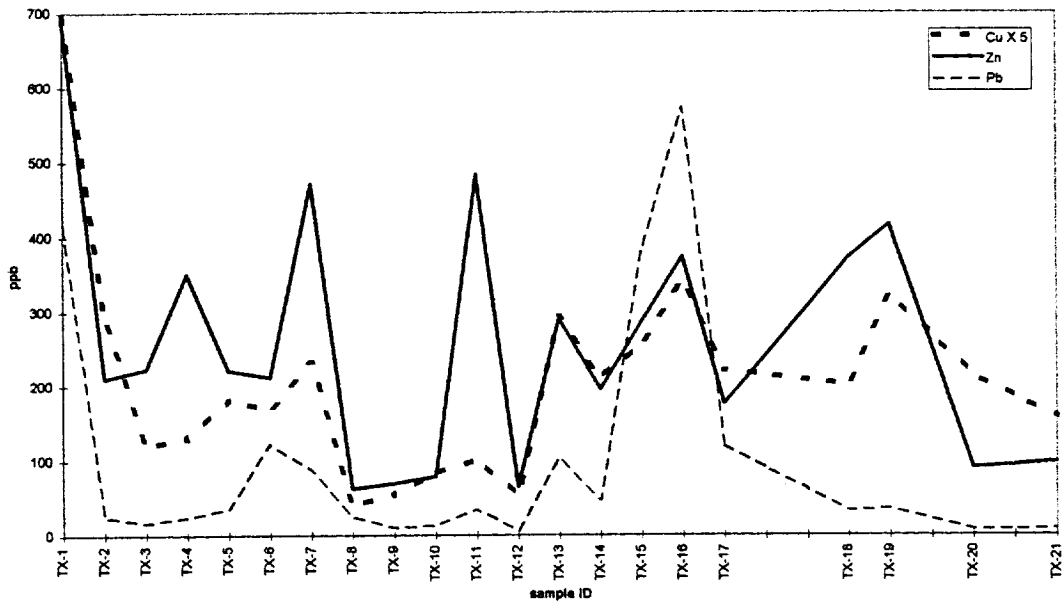
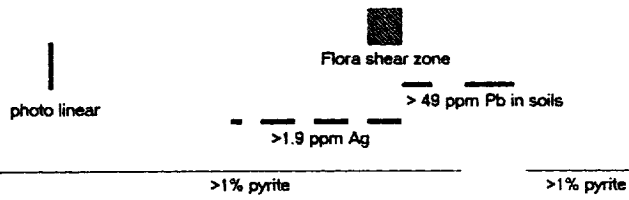
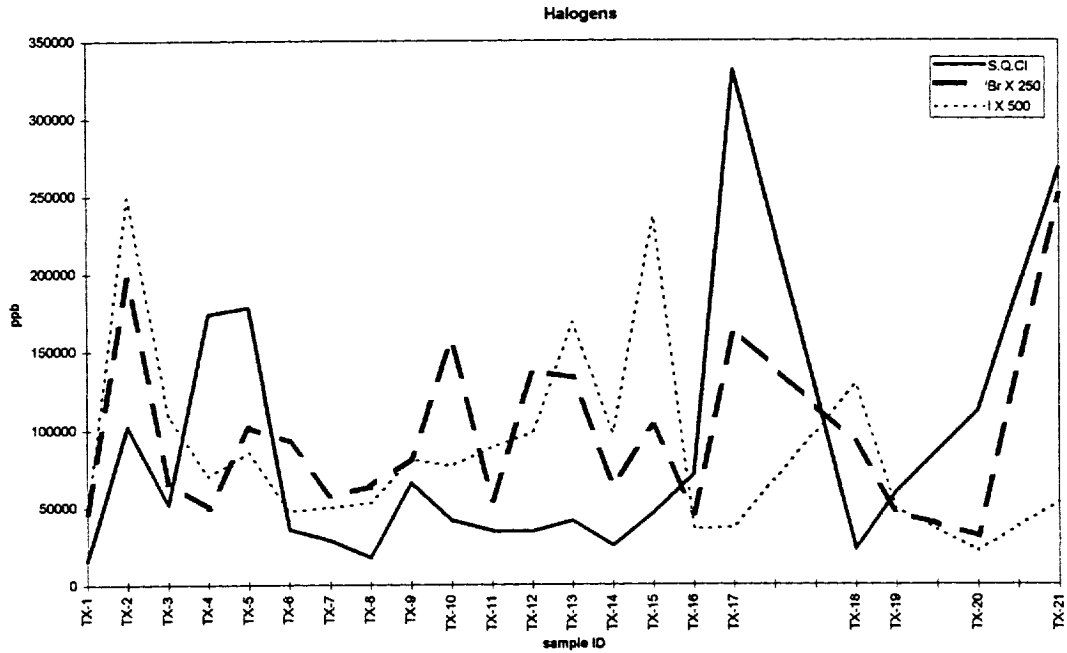
Element	Li	Be	Cl	Sc	Ti	V	Mn	Co	Ni	Cu	Zn
Mean Line TX	5.7	n/a	95424.6	n/a	274.8	21.9	6964.5	30.9	16.1	42.0	253.0
Max. Line TX	15	n/a	331064	n/a	1150	51	24606	113	71	139	689
Mean Line 57A	n/a	n/a	34907.3	n/a	273.8	34.0	2706.5	15.3	7.1	22.7	83.1
Max. Line 57A	n/a	n/a	79233	n/a	755	69	11804	50	18	46	147

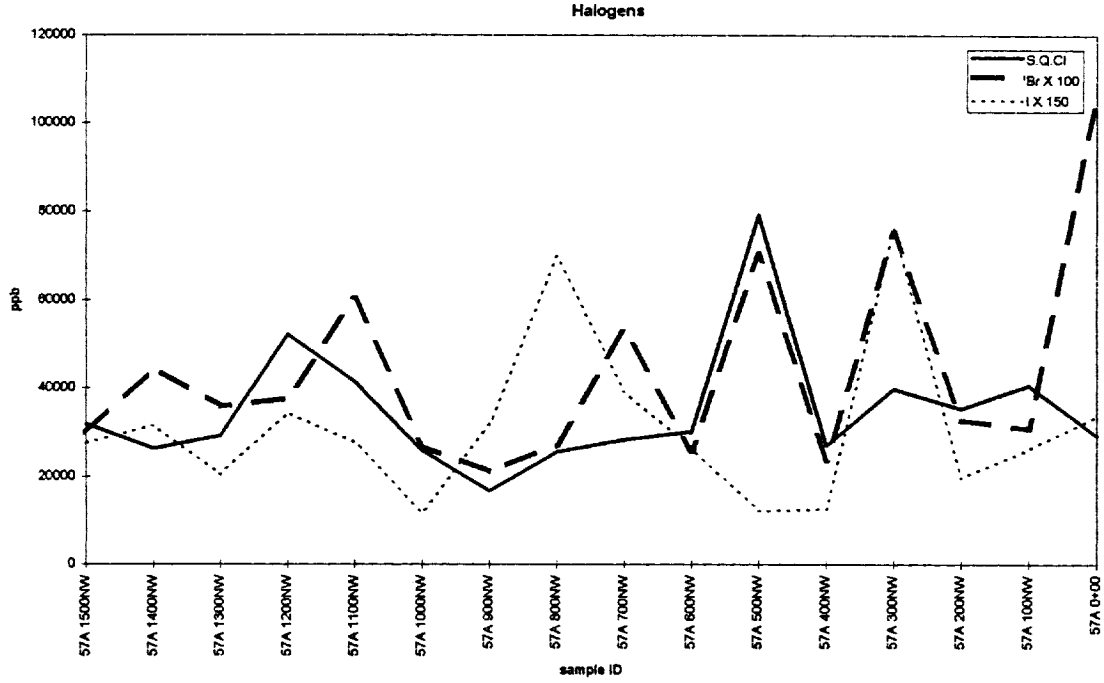
Element	Ga	Ge	As	Se	Br	Rb	Sr	Y	Zr	Nb	Mo	Ru	Pd
Mean Line TX	1.4	n/a	6.2	n/a	394.4	114.1	96.3	8.9	3.7	n/a	2.1	n/a	n/a
Max. Line TX	4	3	12	16	1001	178	269	32	25	2	5	n/a	n/a
Mean Line 57A	1.6	n/a	3.7	n/a	438.0	72.3	83.0	9.0	3.3	0 n/a	1.6	n/a	n/a
Max. Line 57A	4	n/a	14	n/a	1058	100	246	24	7	2	7	n/a	n/a

Element	Ag	Cd	In	Sn	Sb	Te	I	Cs	Ba	La	Ce	Pr	Nd	Sm
Mean Line TX	n/a	8.1	n/a	n/a	n/a	n/a	169.6	0.7	381.1	7	11.8	1.8	7.9	1.7
Max. Line TX	n/a	18.7	n/a	n/a	2	n/a	498	4	907	30	26	6	24	5
Mean Line 57A	n/a	1.62	n/a	n/a	n/a	n/a	208.7	n/a	199.9	6.4	7.6	1.4	6.6	1.4
Max. Line 57A	n/a	2.7	n/a	n/a	n/a	n/a	506	n/a	446	19	17	4	15	4

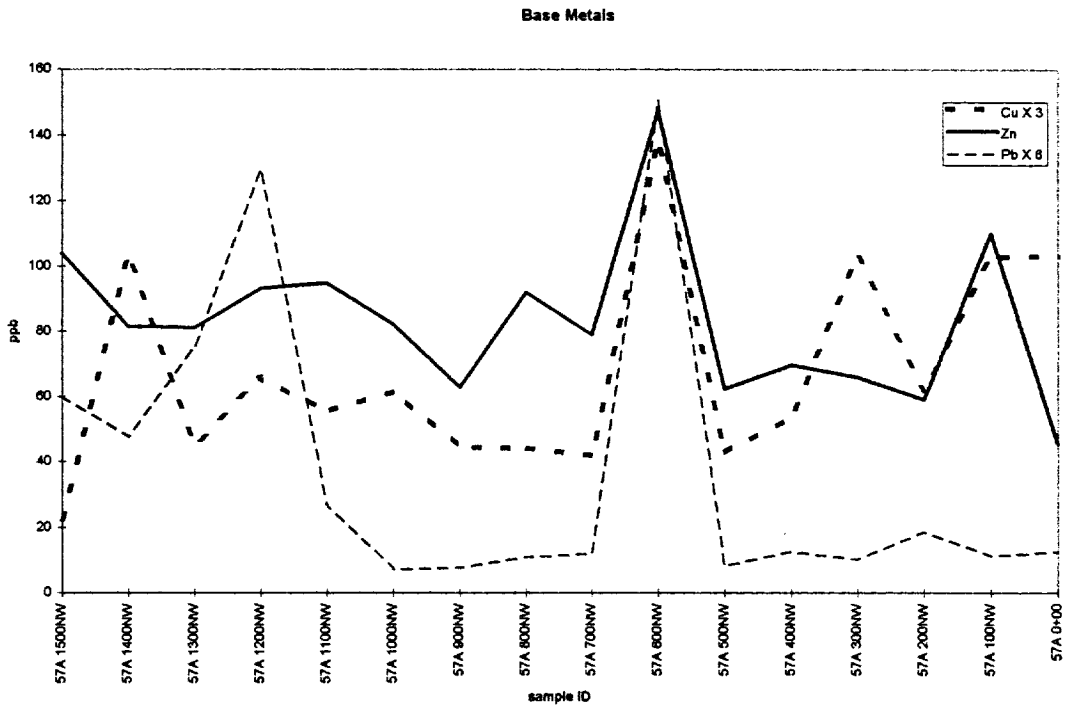
Element	Eu	Gd	Tb	Dy	Ho	Er	Tm	Yb	Lu	Hf	Ta	W
Mean Line TX	n/a	1.7	n/a	1.5	n/a	n/a	n/a	n/a	n/a	n/a	n/a	n/a
Max. Line TX	1	4	n/a	4	n/a	2	n/a	2	n/a	n/a	n/a	n/a
Mean Line 57A	n/a	1.4	n/a	1.4	n/a	n/a	n/a	n/a	n/a	n/a	n/a	n/a
Max. Line 57A	n/a	3	n/a	3	n/a	2	n/a	1	n/a	n/a	n/a	n/a

Element	Re	Os	Pt	Au	Hg	Tl	Pb	Bi	Th	U
Mean Line TX	n/a	n/a	n/a	n/a	n/a	n/a	91.9	n/a	n/a	n/a
Max. Line TX	n/a	n/a	n/a	0.70	n/a	3	571	1	n/a	n/a
Mean Line 57A	n/a	n/a	n/a	n/a	n/a	n/a	6.2	n/a	n/a	n/a
Max. Line 57A	n/a	n/a	n/a	n/a	n/a	n/a	25	n/a	2	1

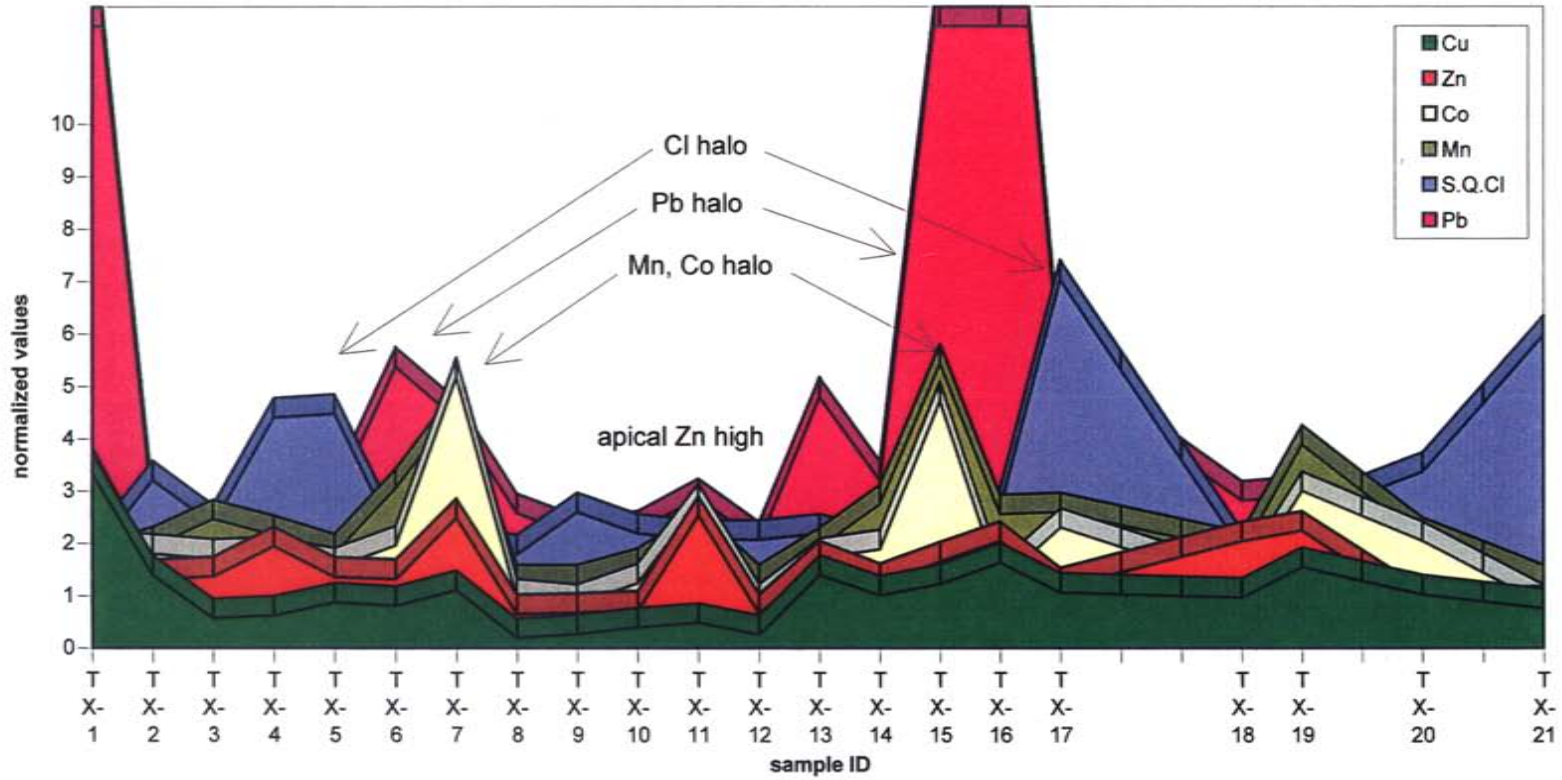




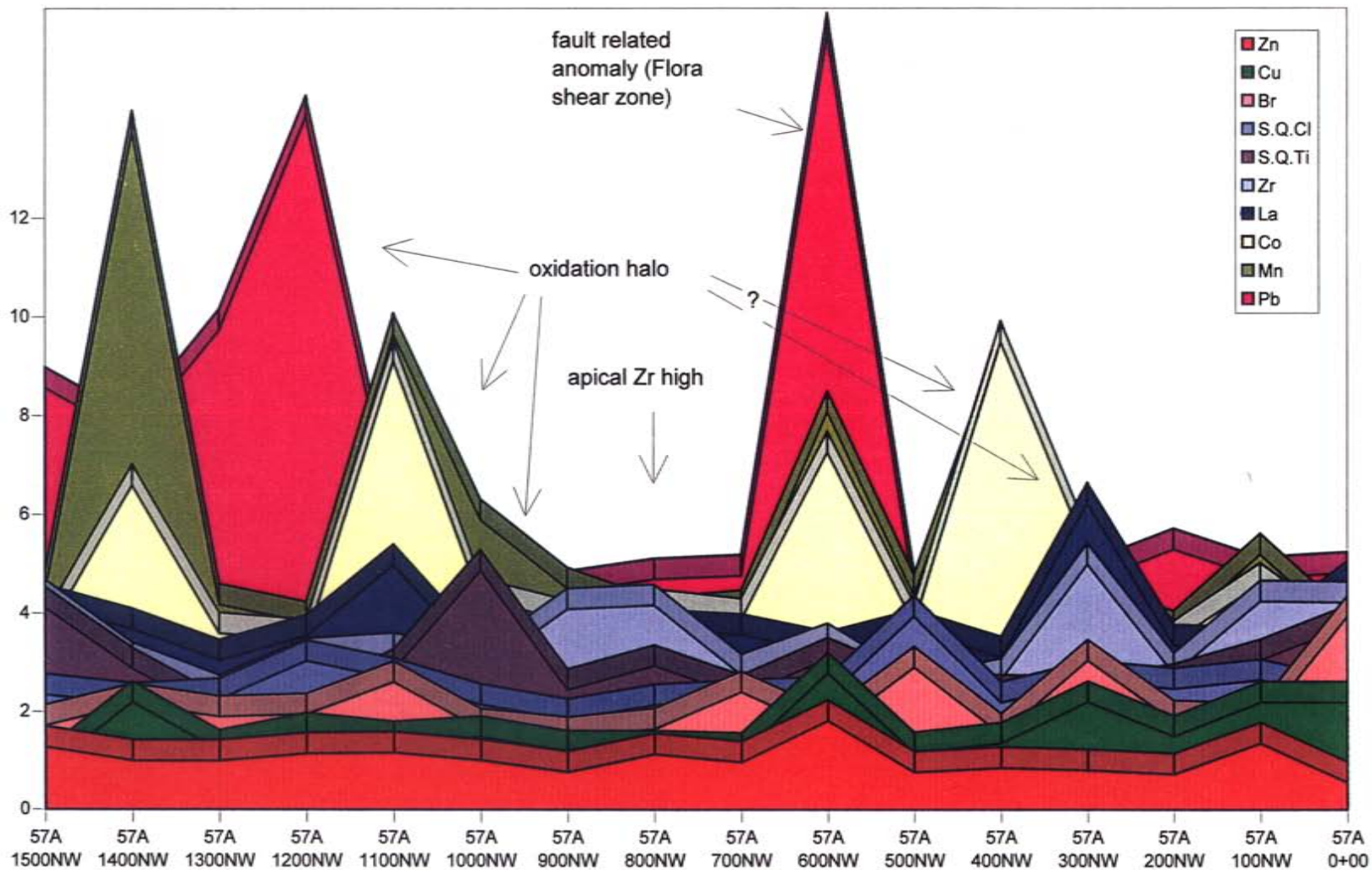
conventional soil Anomaly "A" (Minfile 092C-119, Fig. 4)
Elevated As to 99 ppm, and Zn to 317 ppm



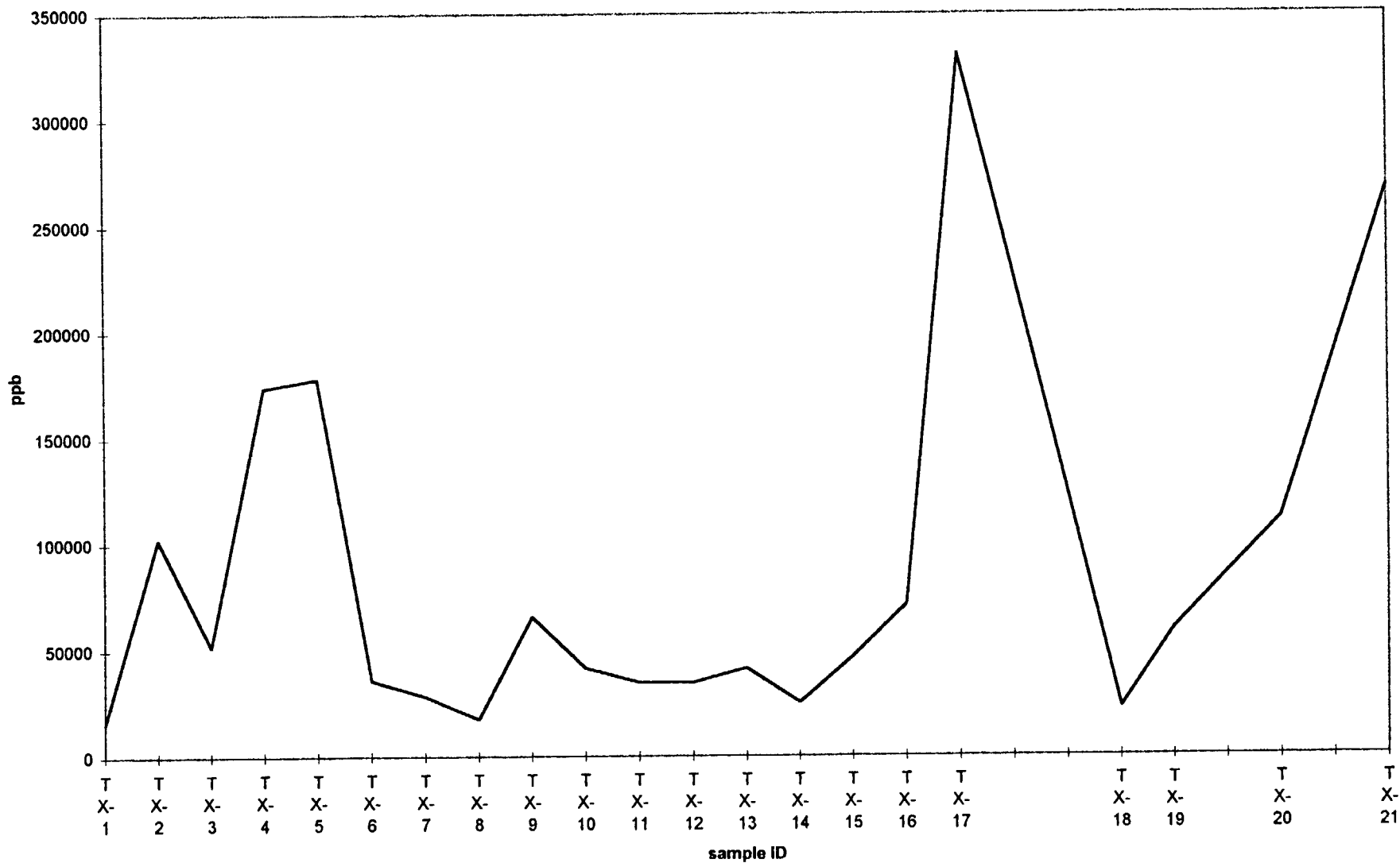
Summary Figure Line TX
all values normalized to medians



Summary Figure Line 57A
all values normalized to medians

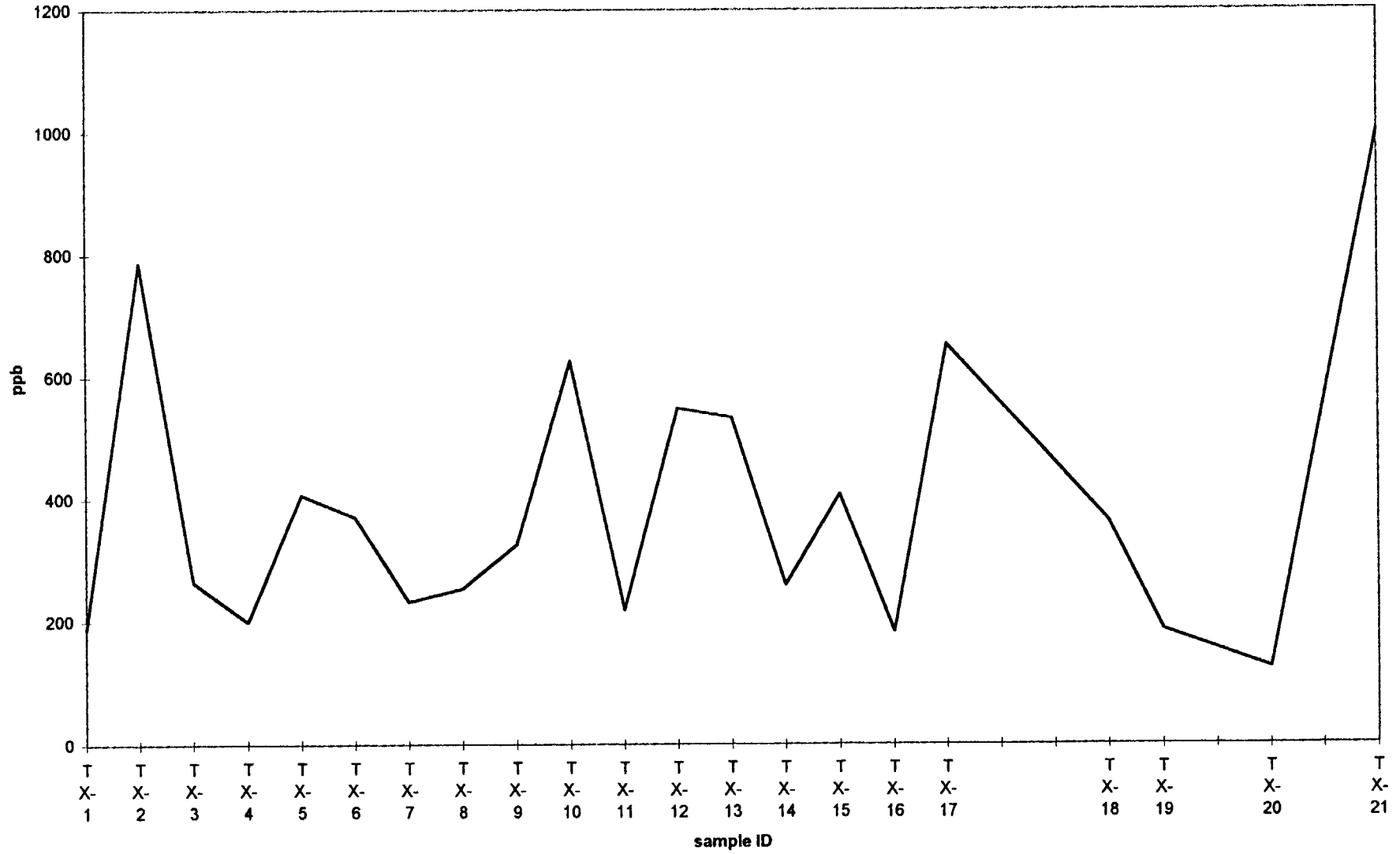


S.Q.C.I



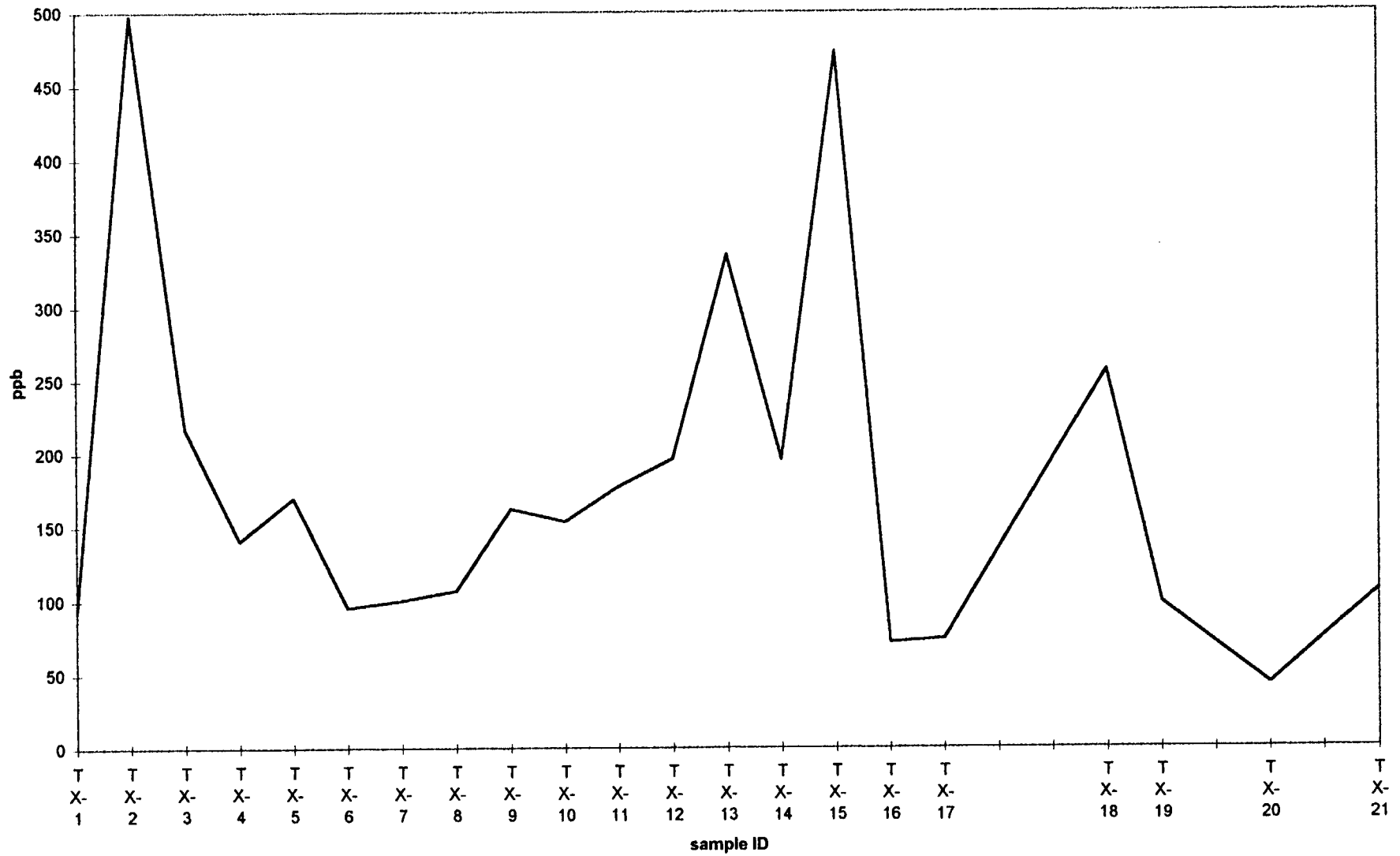
TUZEX CLAIMS Enzyme Leach (SM) data

Br



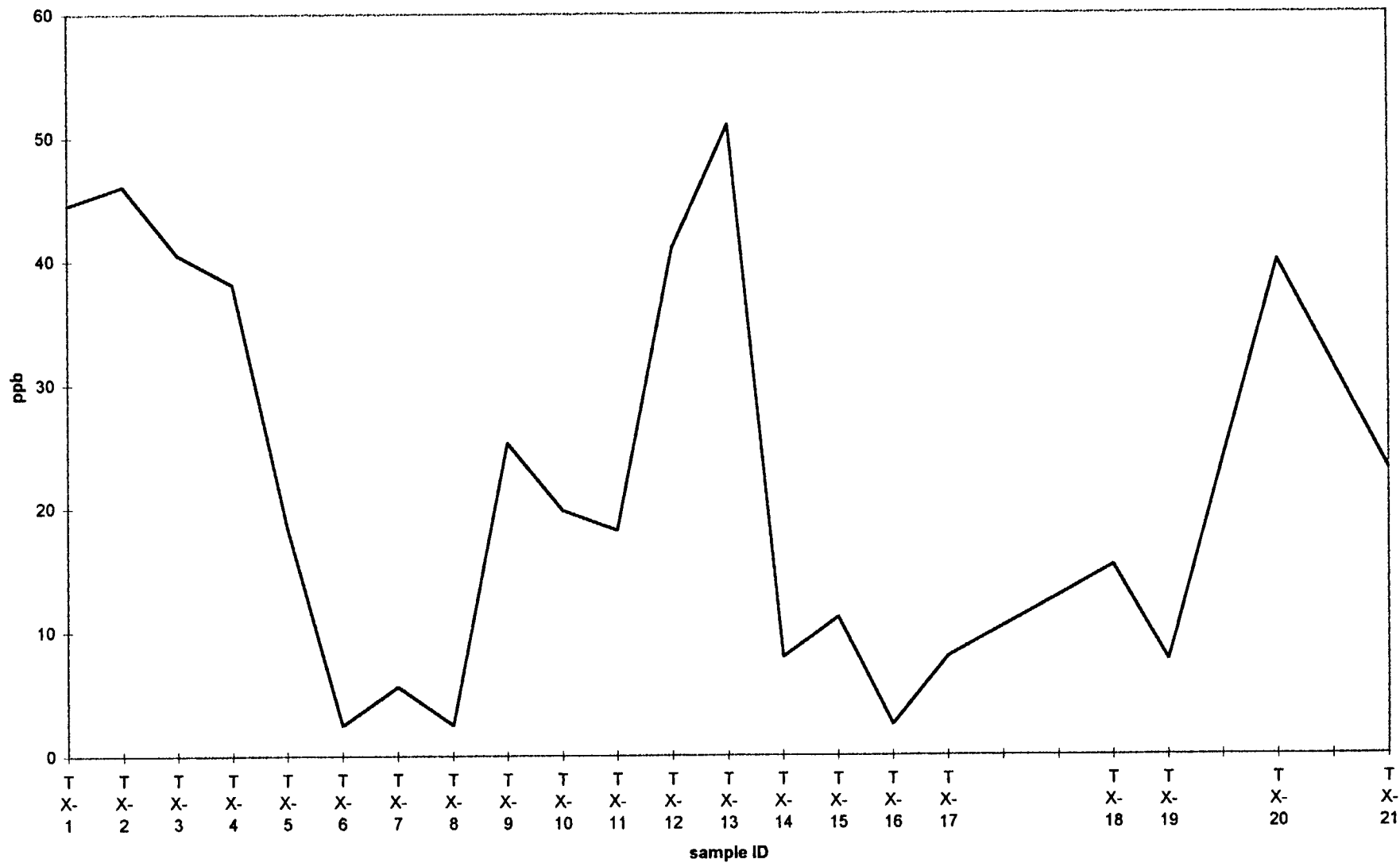
TUZEX CLAIMS Enzyme Leach (SM) data

1



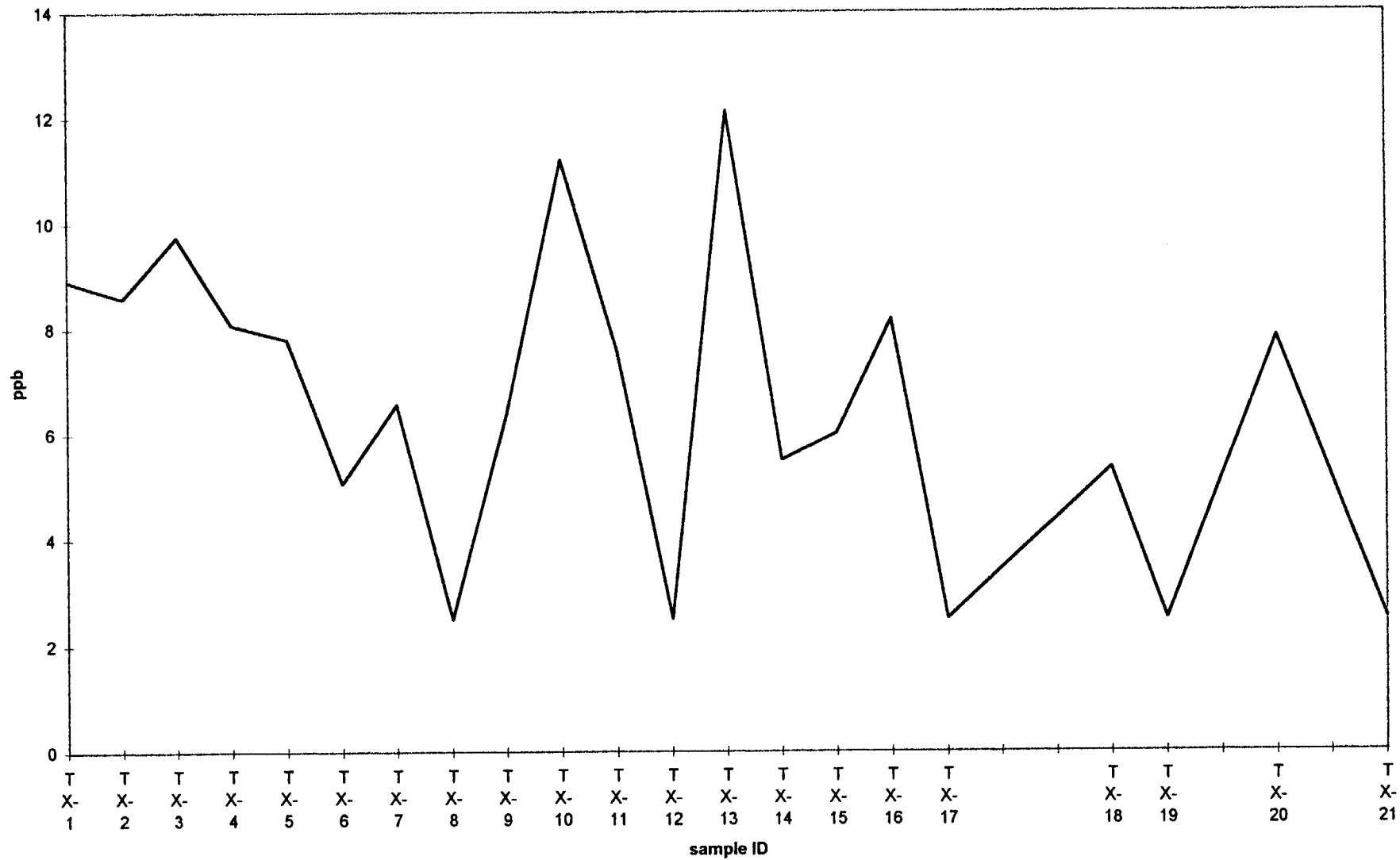
TUZEX CLAIMS Enzyme Leach (SM) data

v



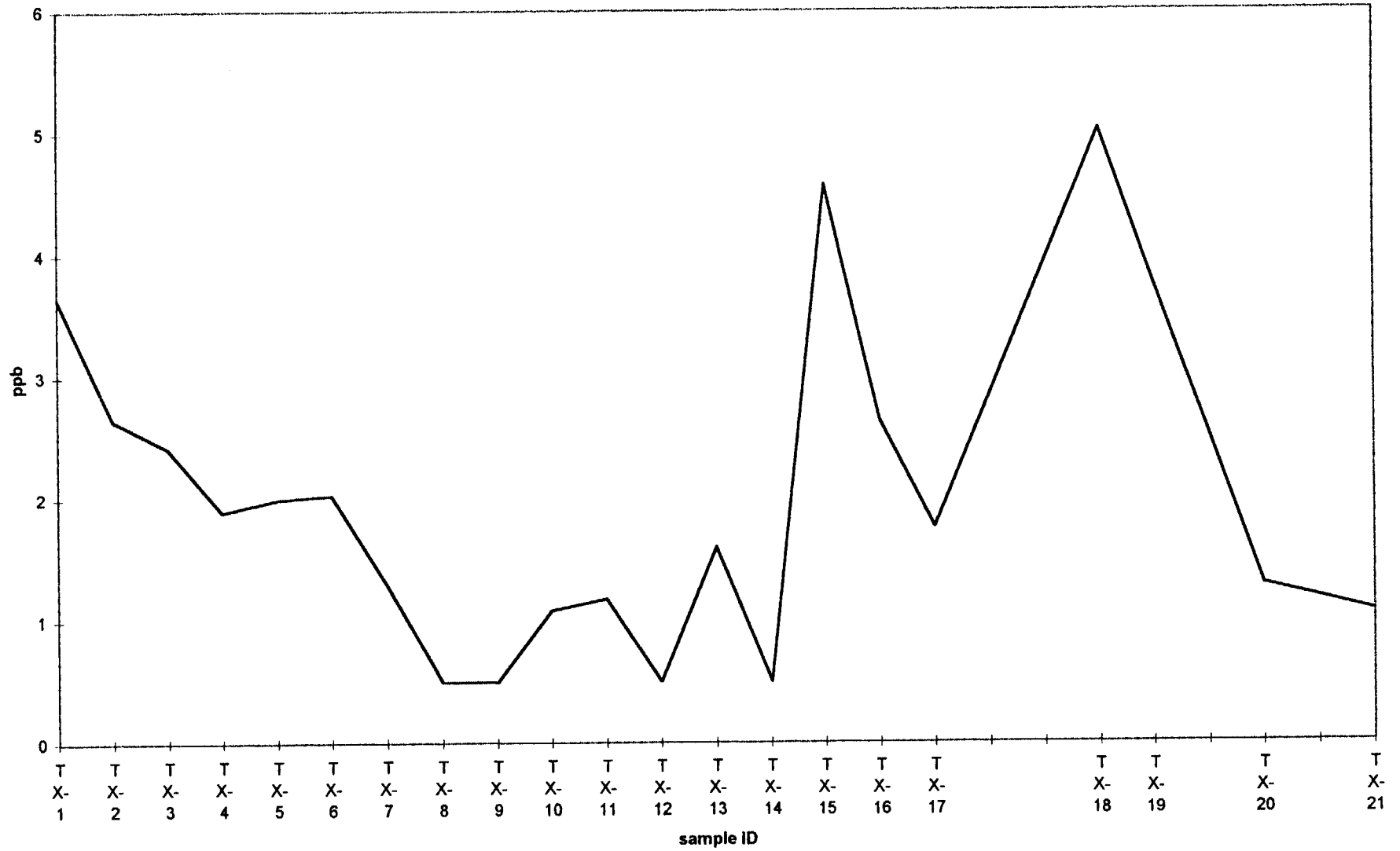
TUZEX CLAIMS Enzyme Leach (SM) data

As



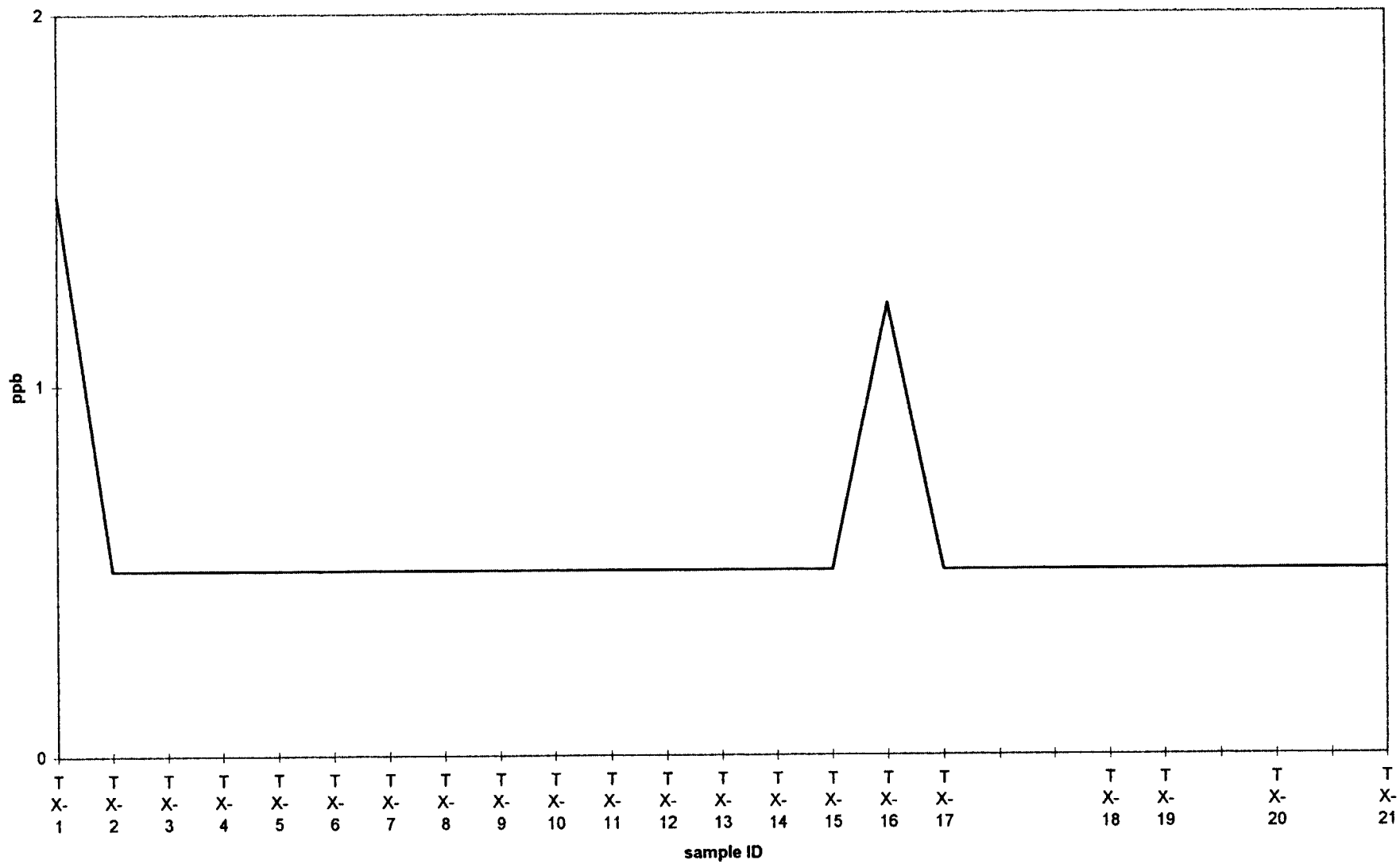
TUZEX CLAIMS Enzyme Leach (SM) data

Mo



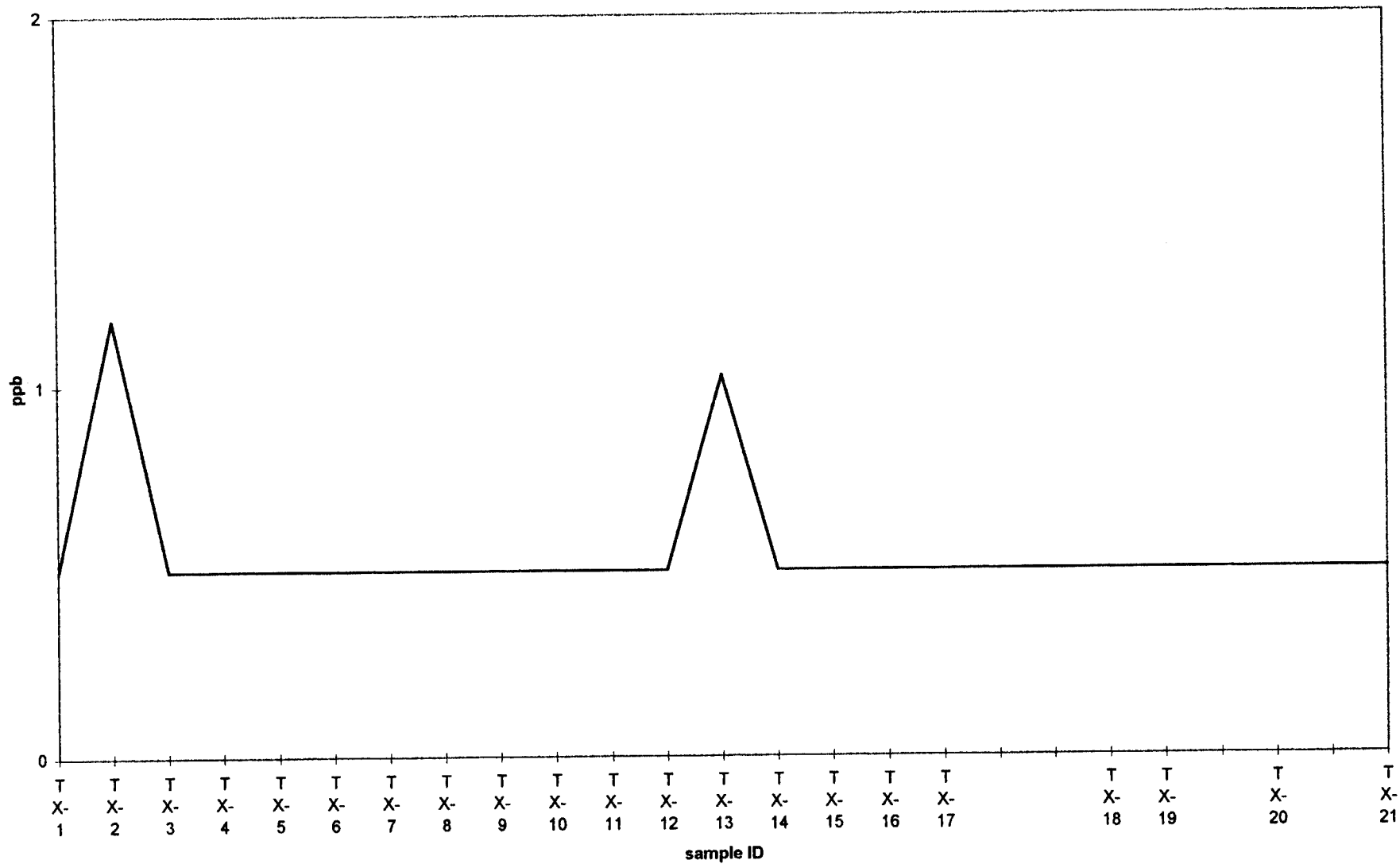
TUZEX CLAIMS Enzyme Leach (SM) data

Sb



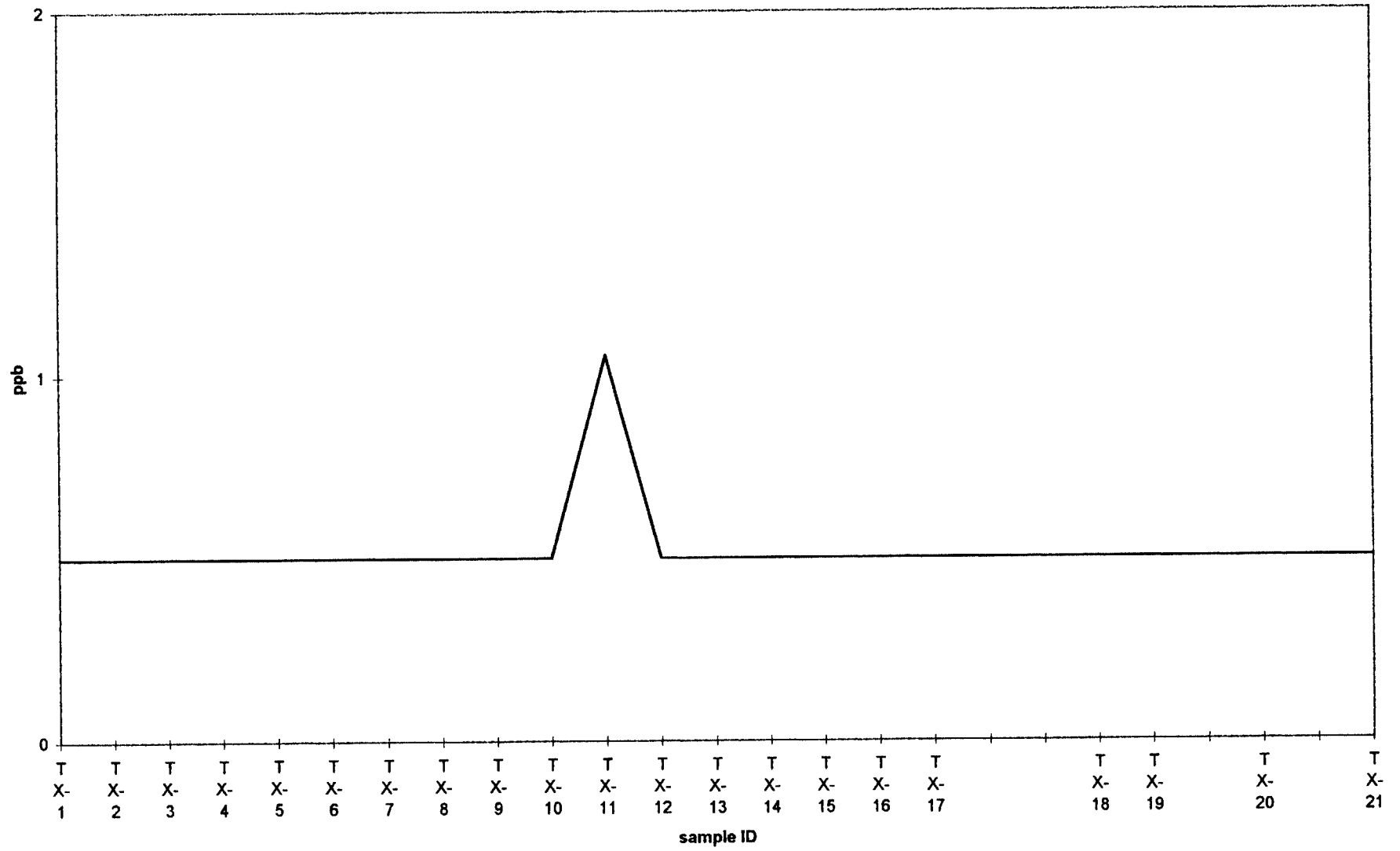
TUZEX CLAIMS Enzyme Leach (SM) data

Th



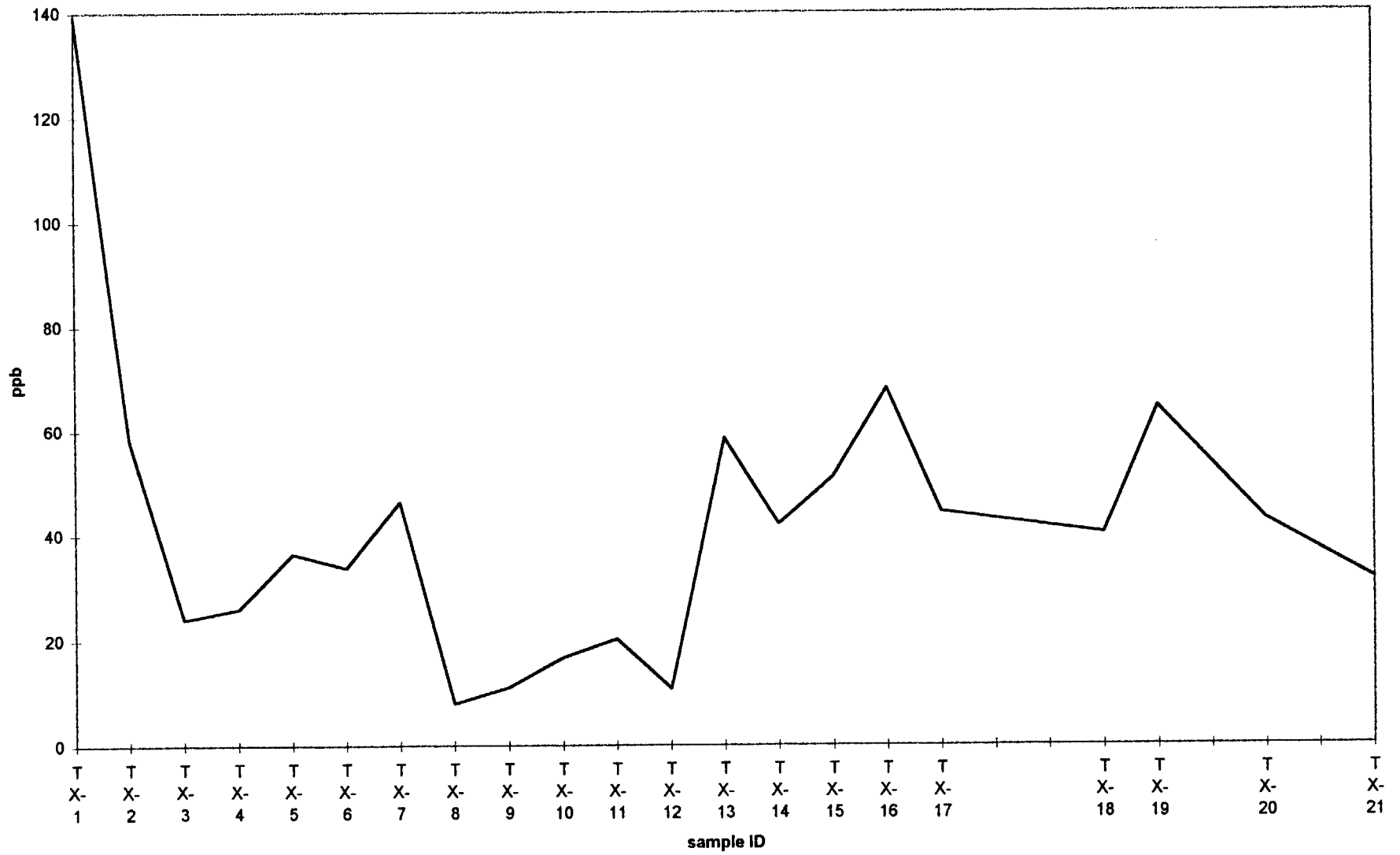
TUZEX CLAIMS Enzyme Leach (SM) data

U



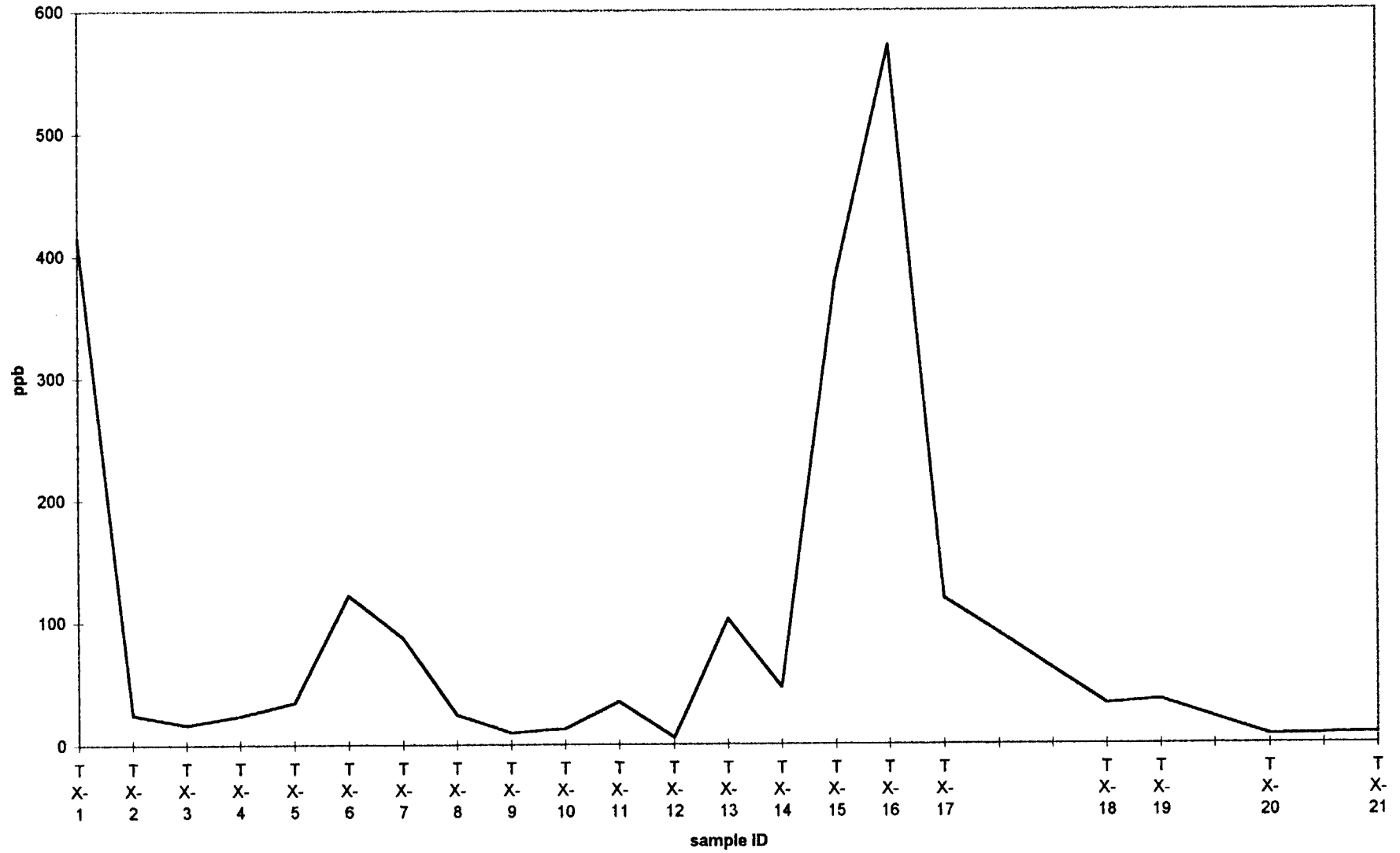
TUZEX CLAIMS Enzyme Leach (SM) data

Cu



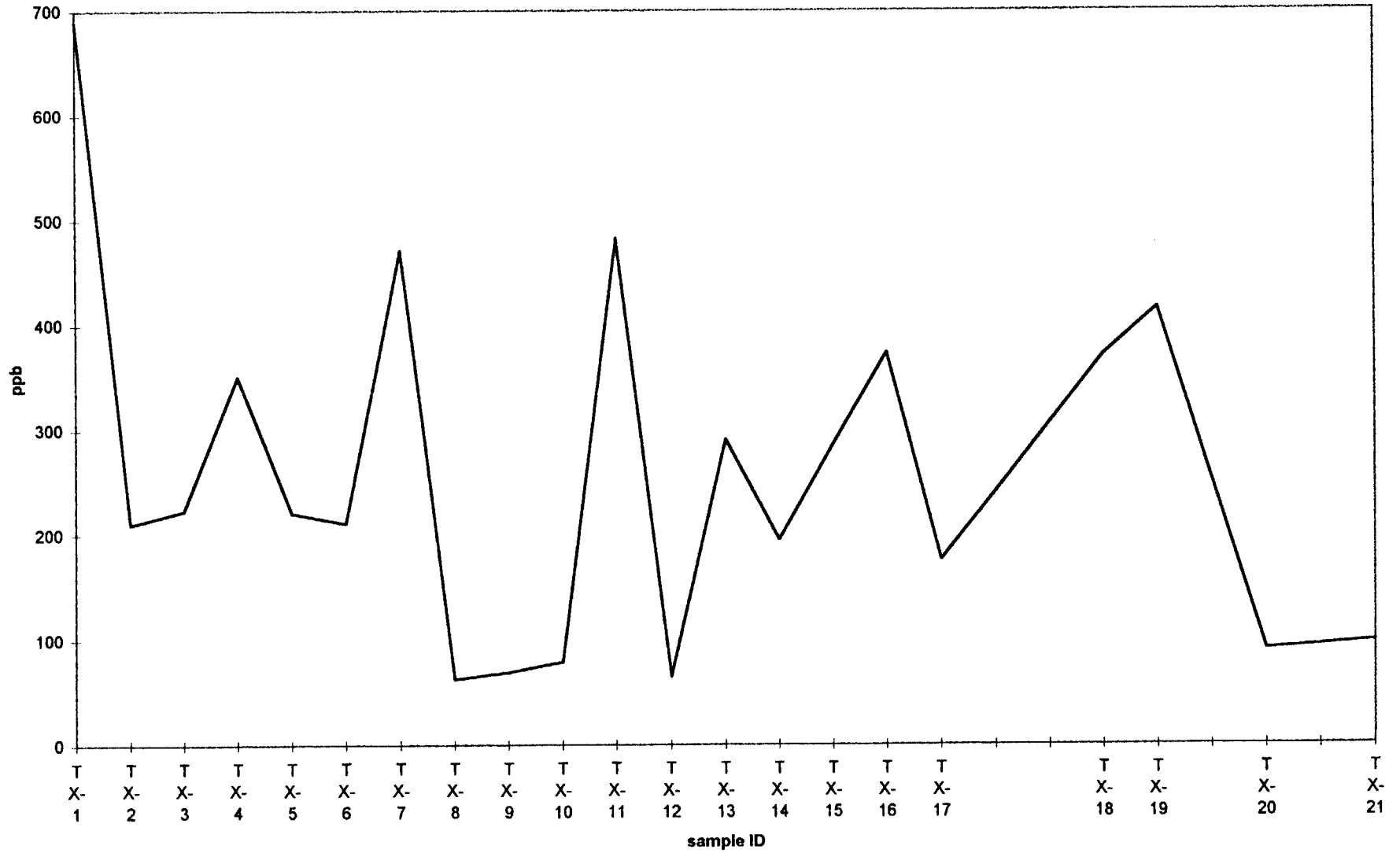
TUZEX CLAIMS Enzyme Leach (SM) data

Pb



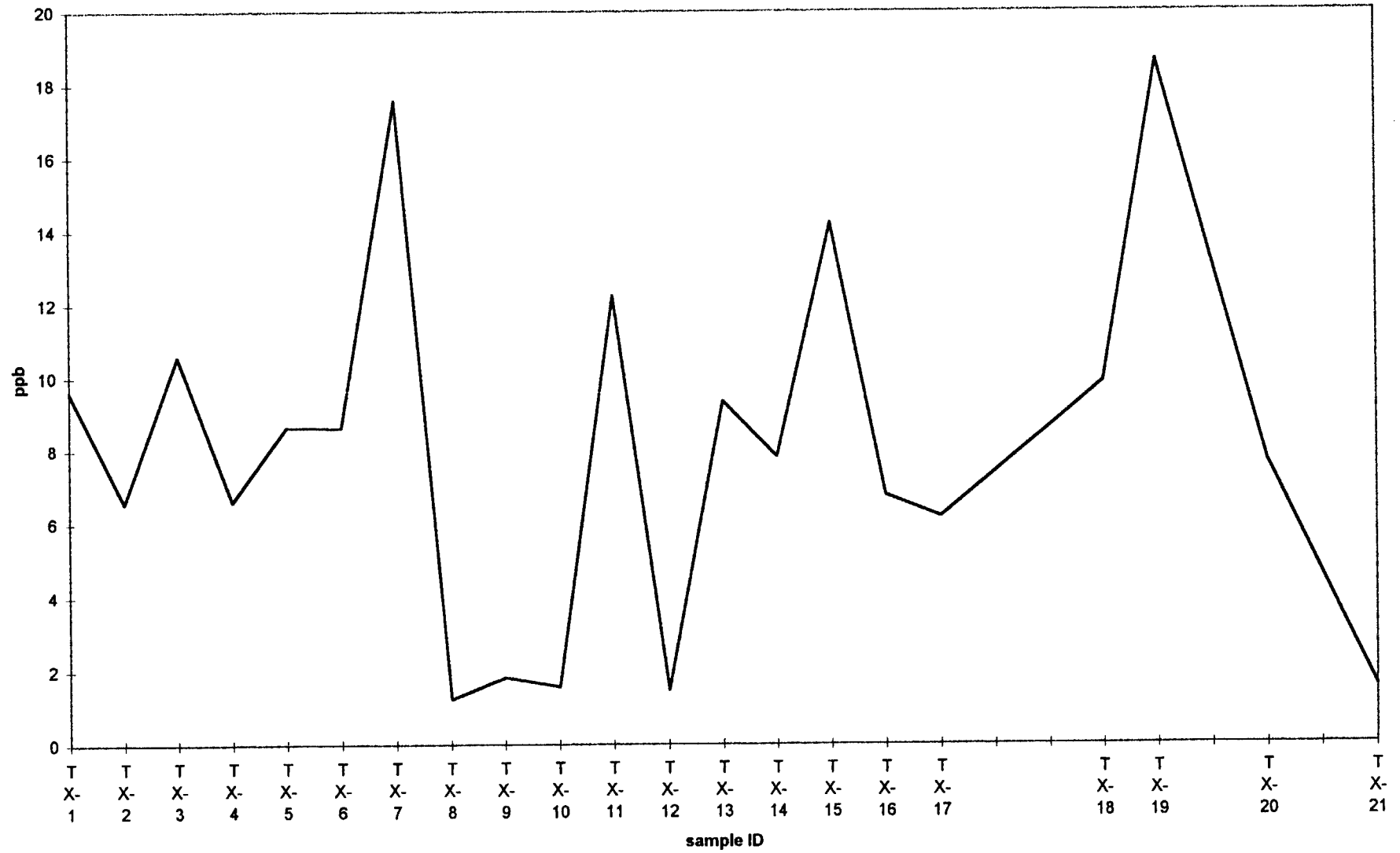
TUZEX CLAIMS Enzyme Leach (SM) data

Zn



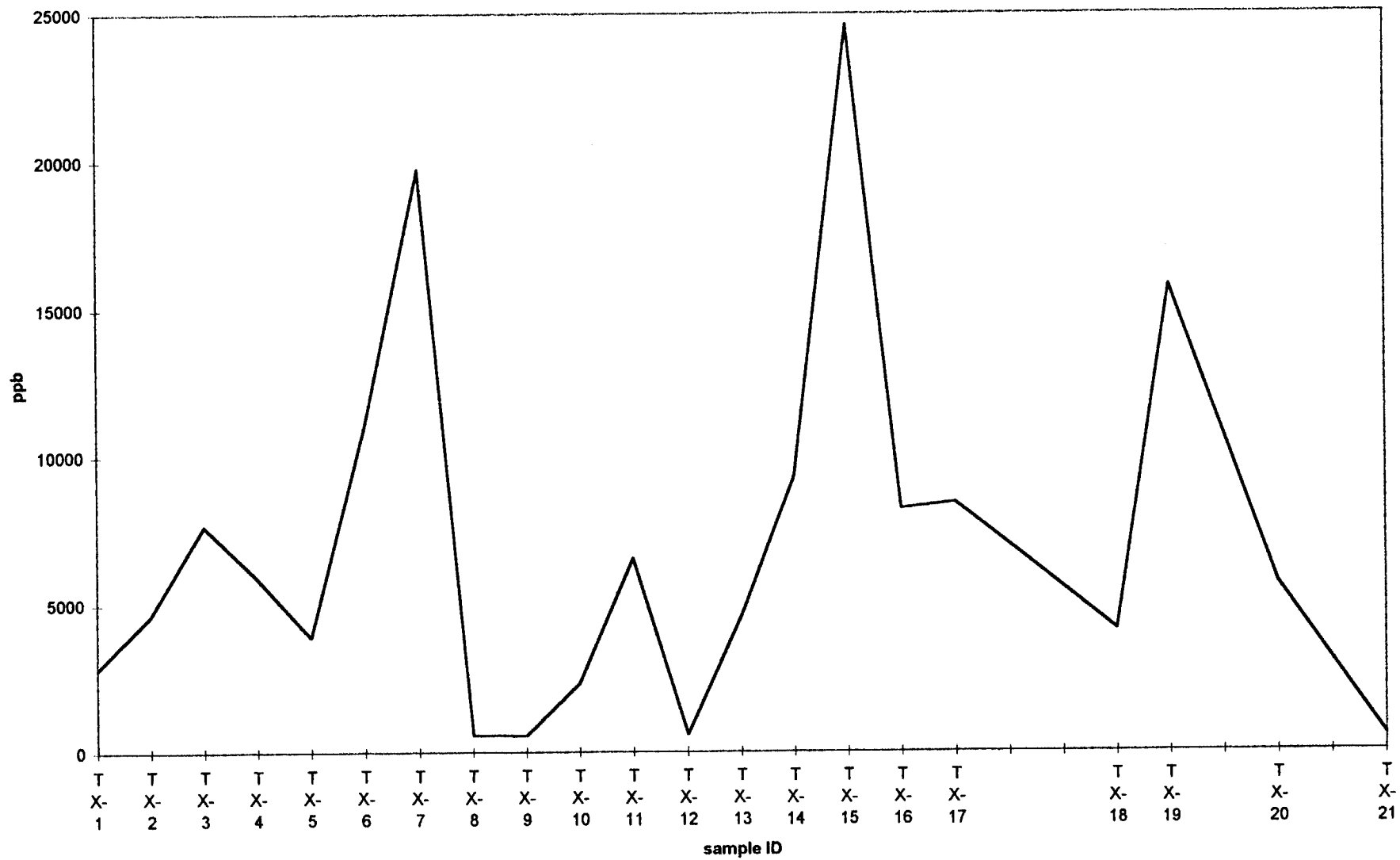
TUZEX CLAIMS Enzyme Leach (SM) data

Cd



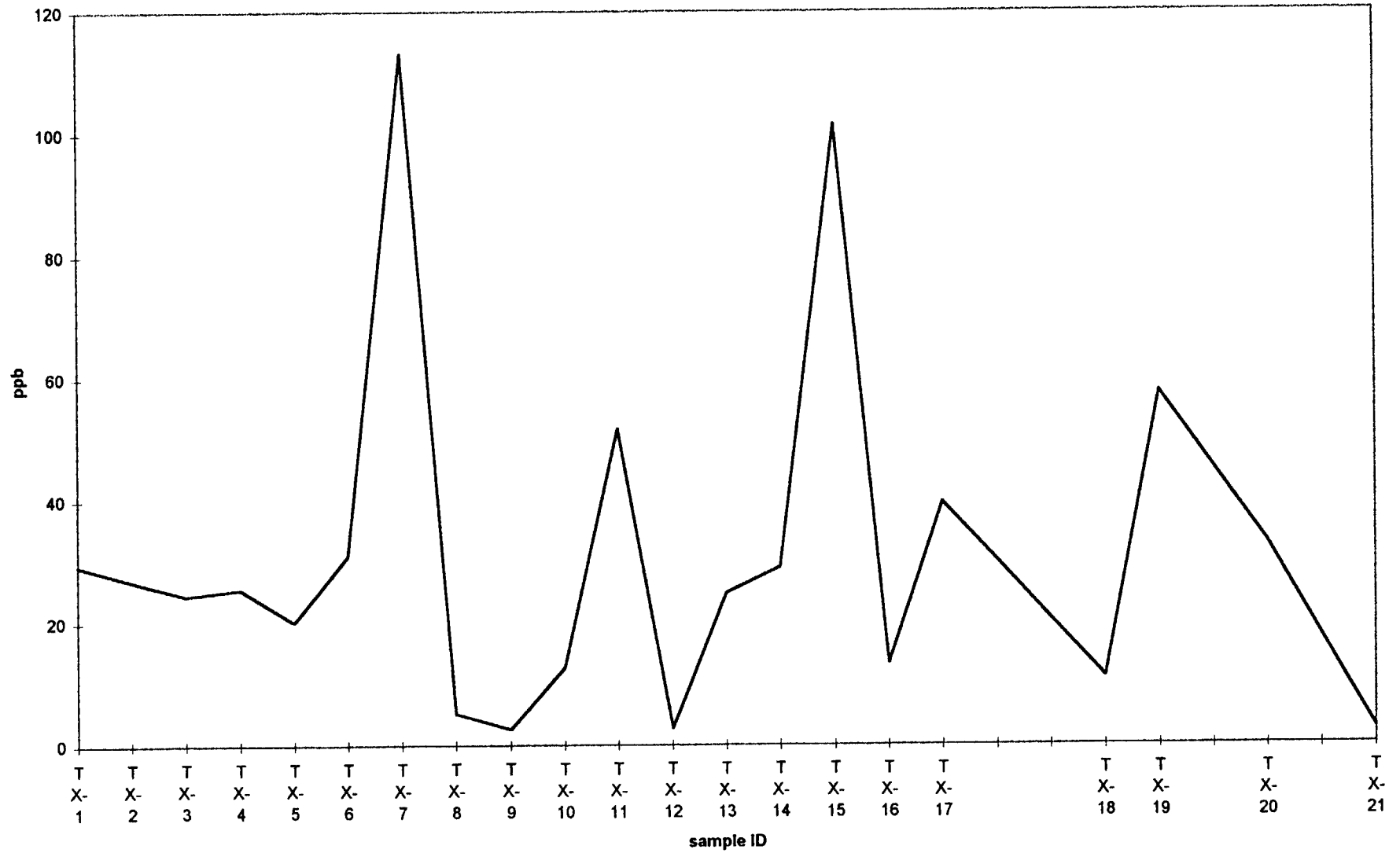
TUZEX CLAIMS Enzyme Leach (SM) data

Mn



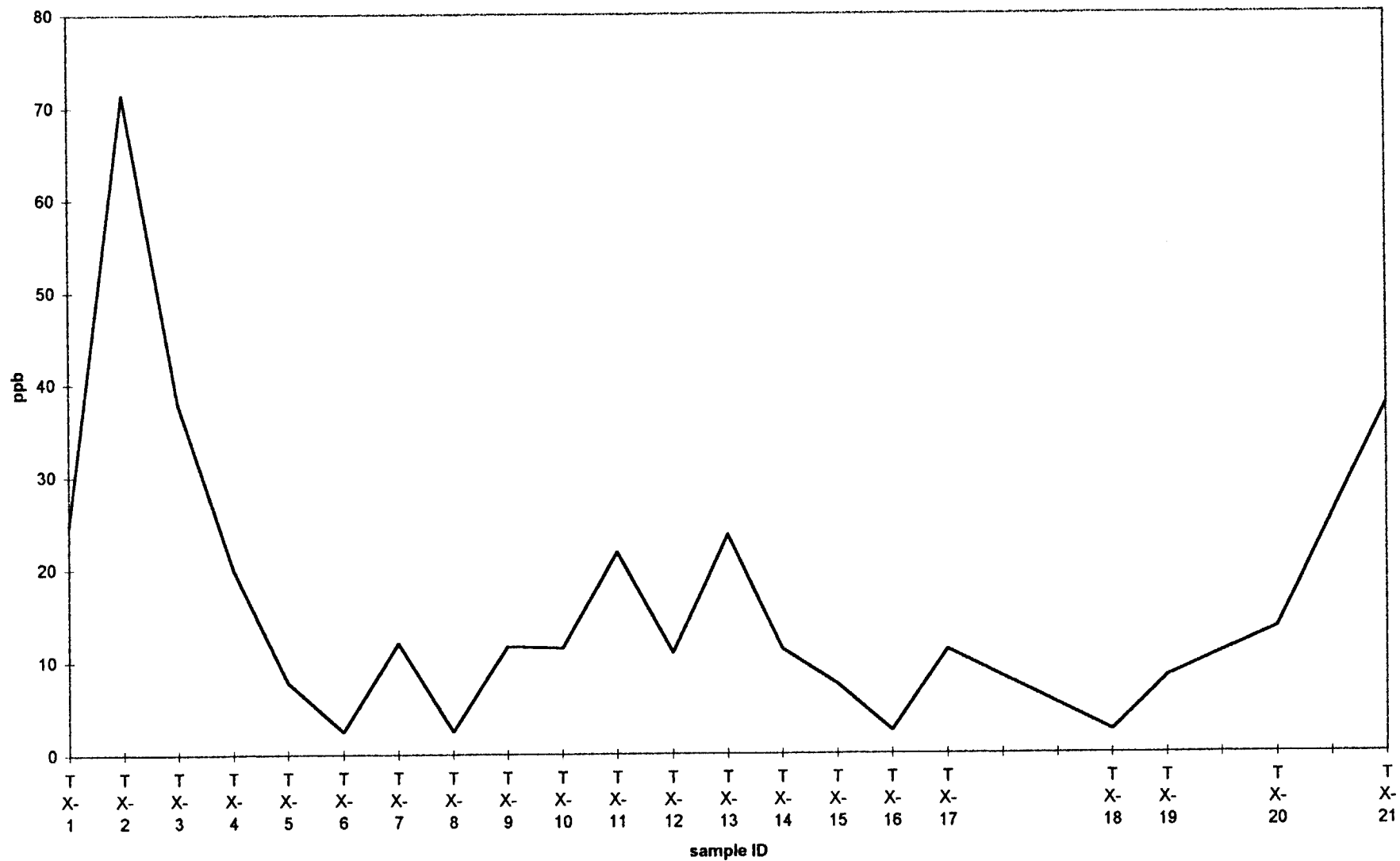
TUZEX CLAIMS Enzyme Leach (SM) data

Co



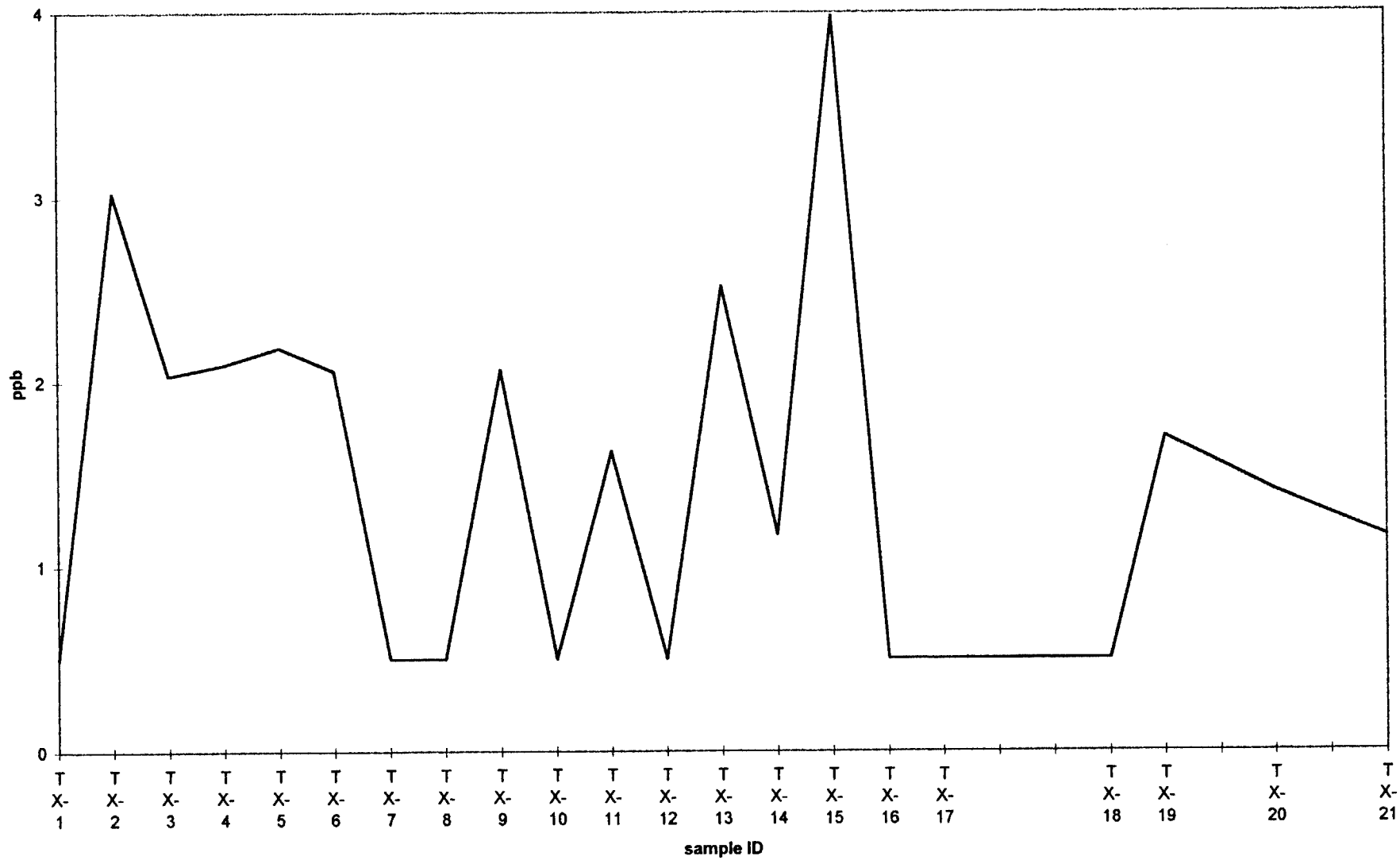
TUZEX CLAIMS Enzyme Leach (SM) data

Ni



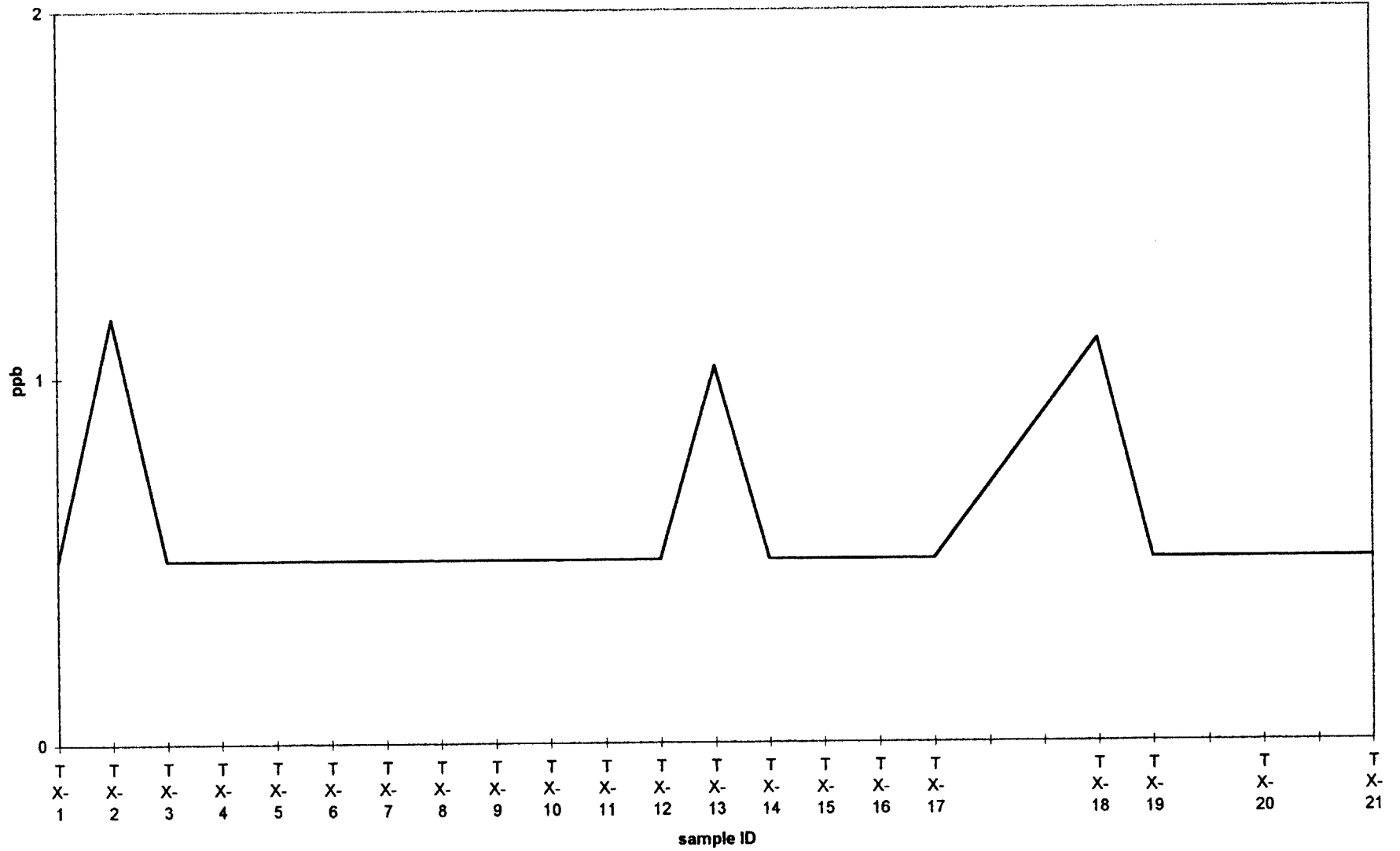
TUZEX CLAIMS Enzyme Leach (SM) data

Ga



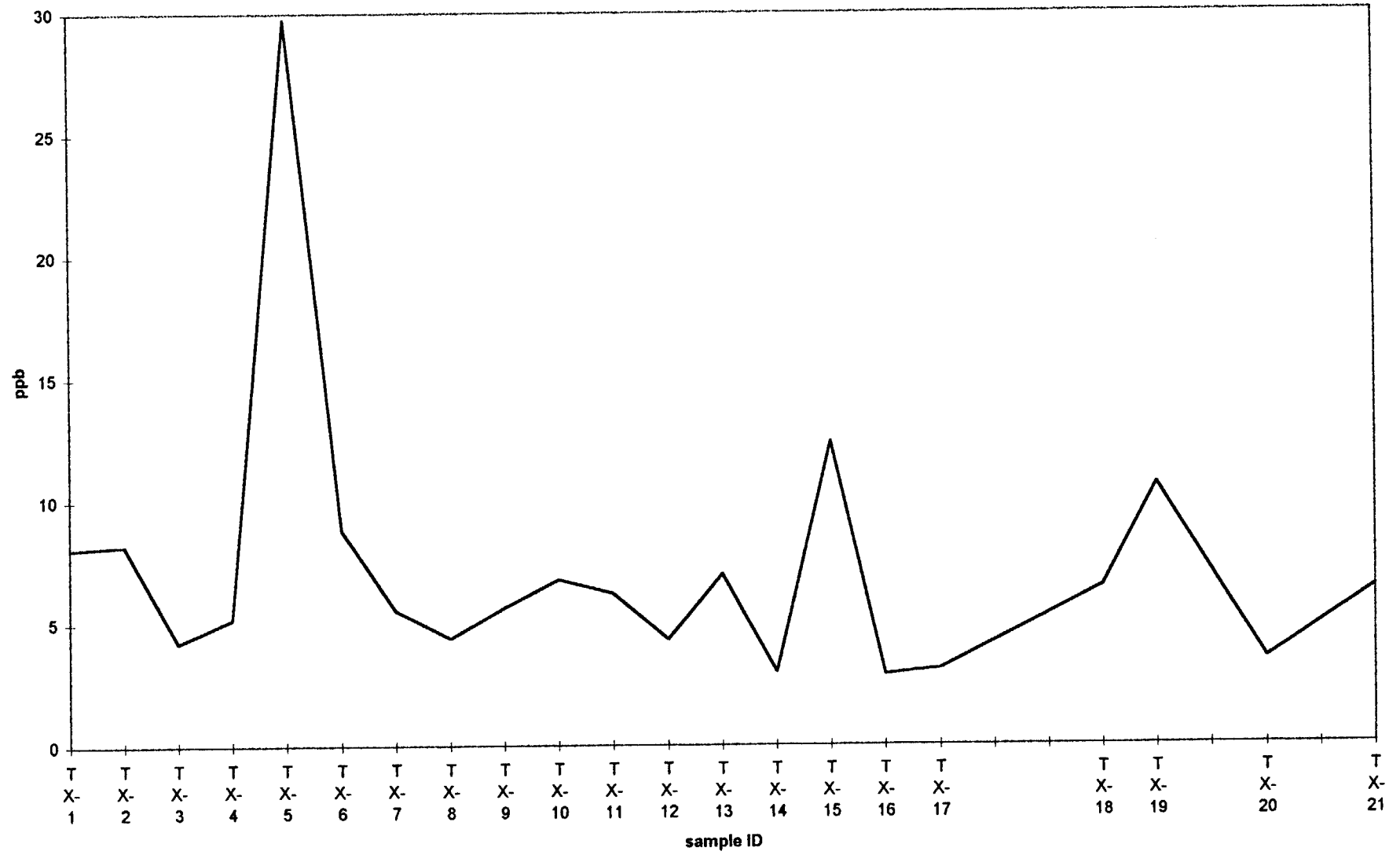
TUZEX CLAIMS Enzyme Leach (SM) data

Bi



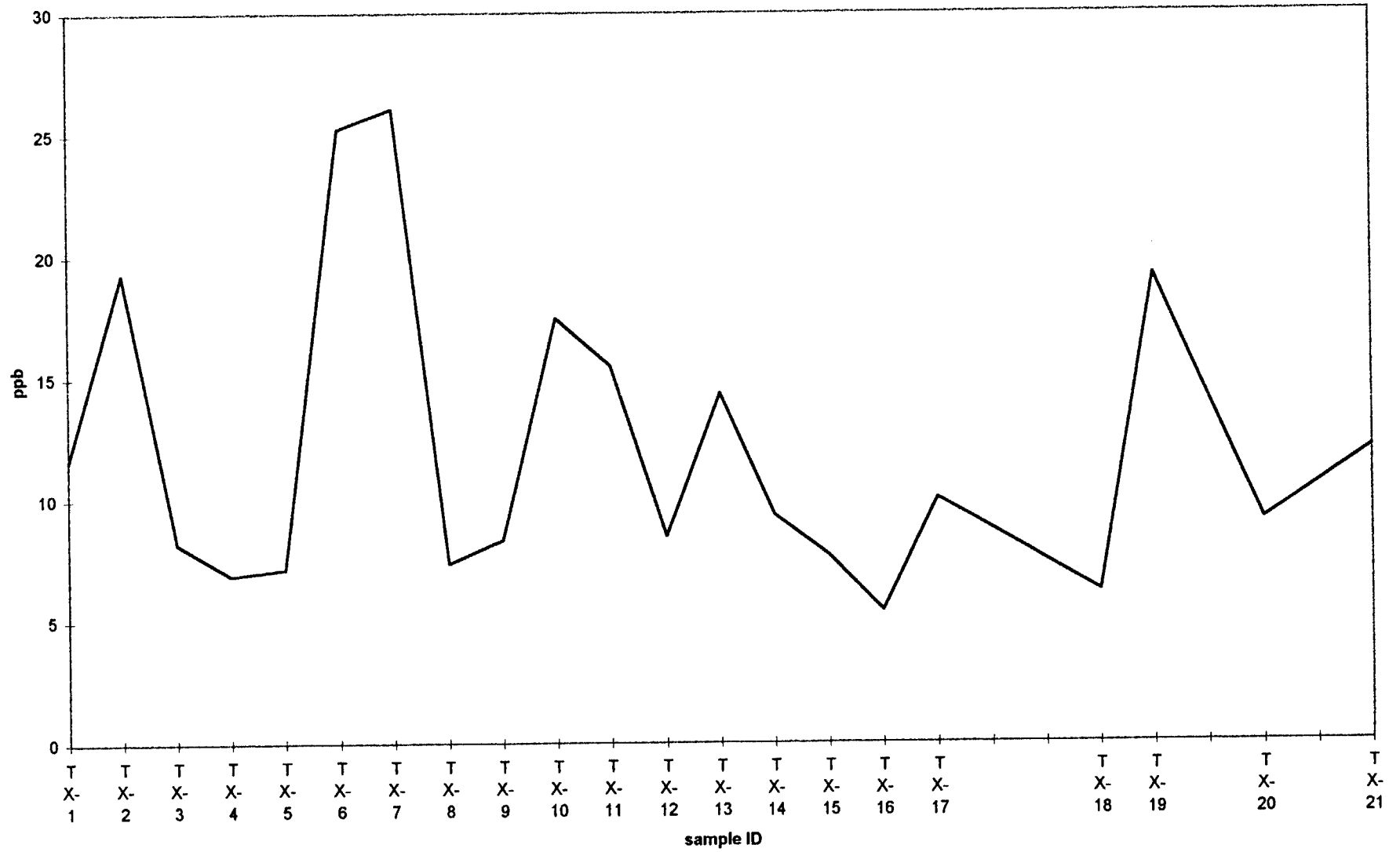
TUZEX CLAIMS Enzyme Leach (SM) data

La



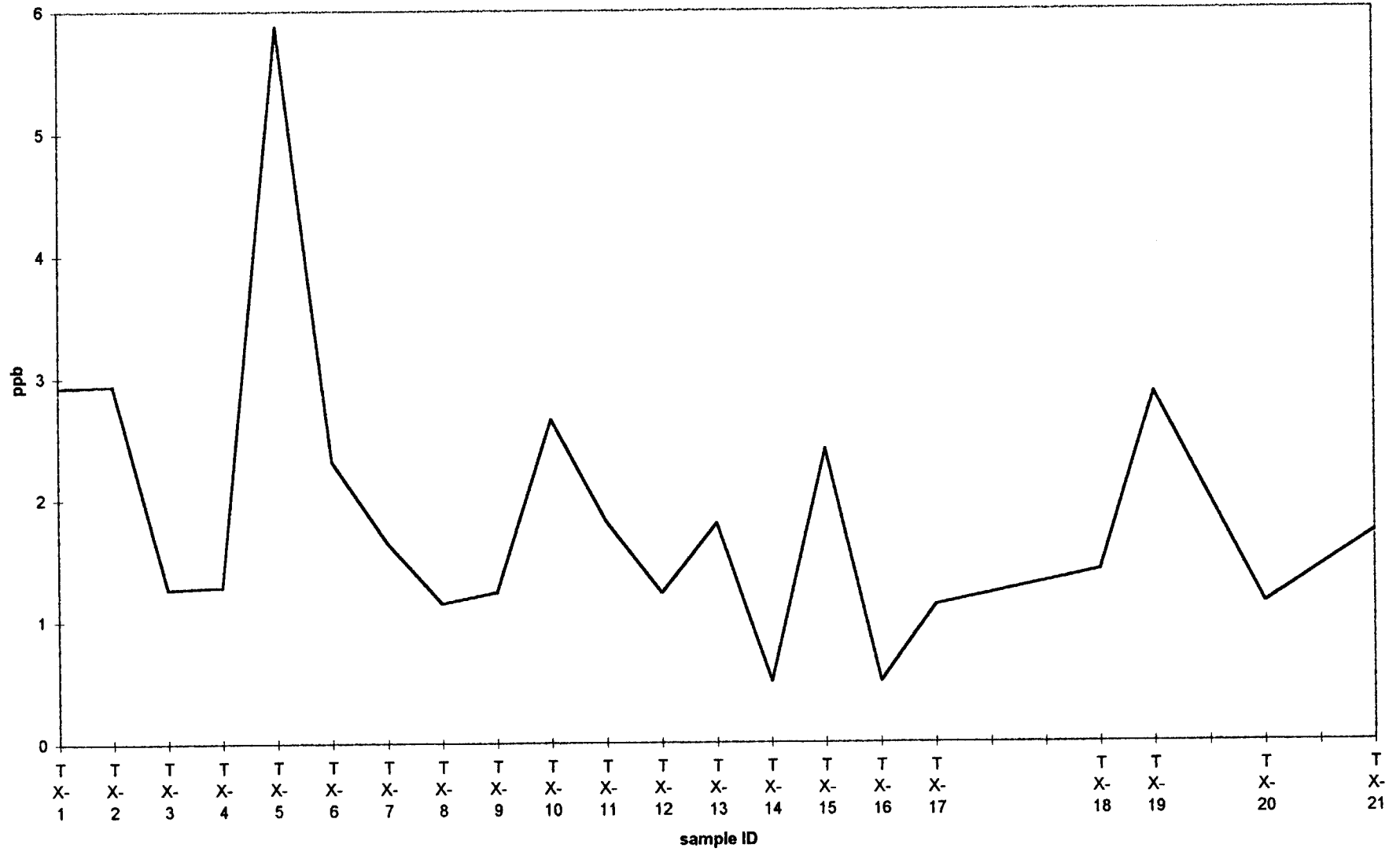
TUZEX CLAIMS Enzyme Leach (SM) data

Ce



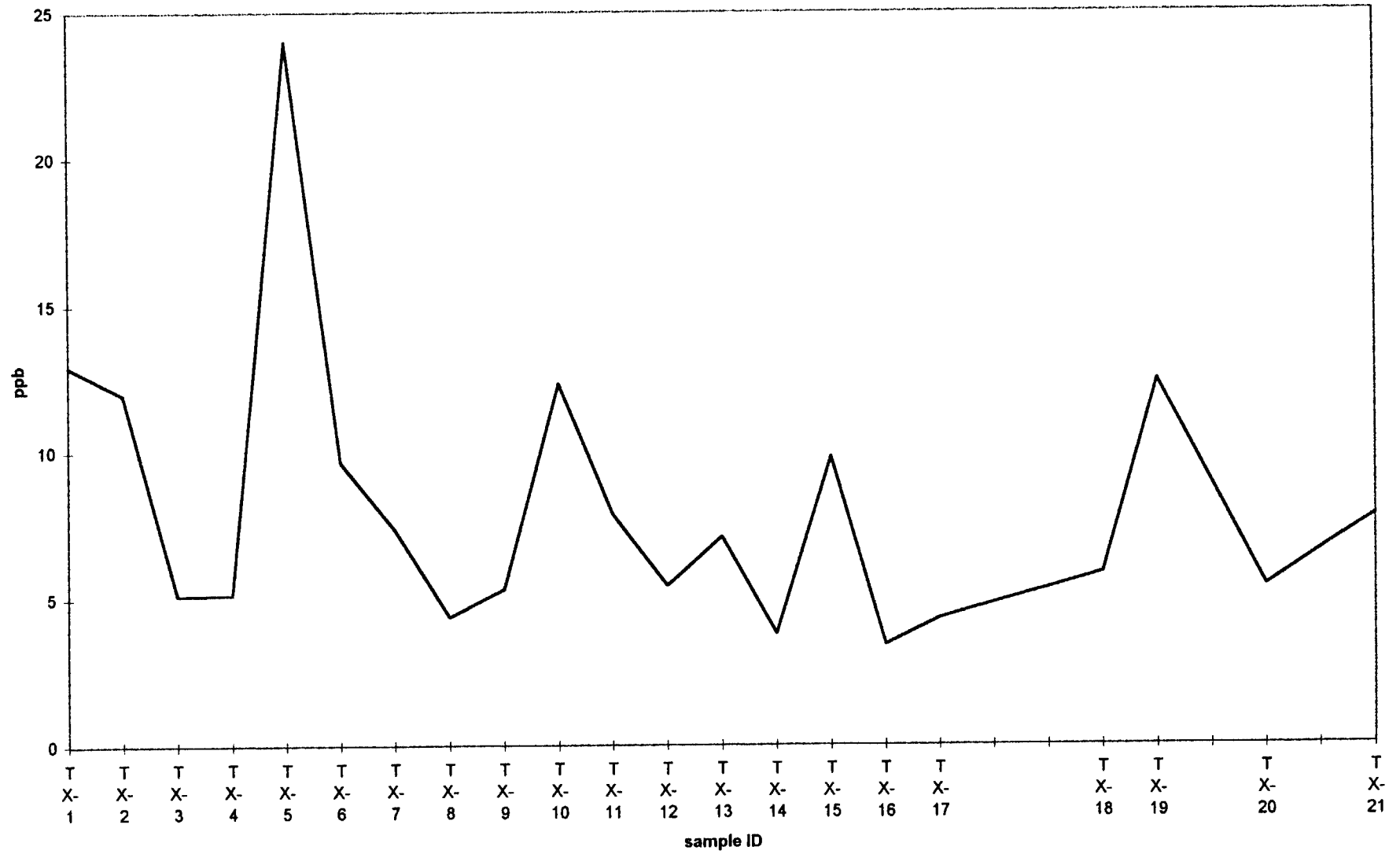
TUZEX CLAIMS Enzyme Leach (SM) data

Pr



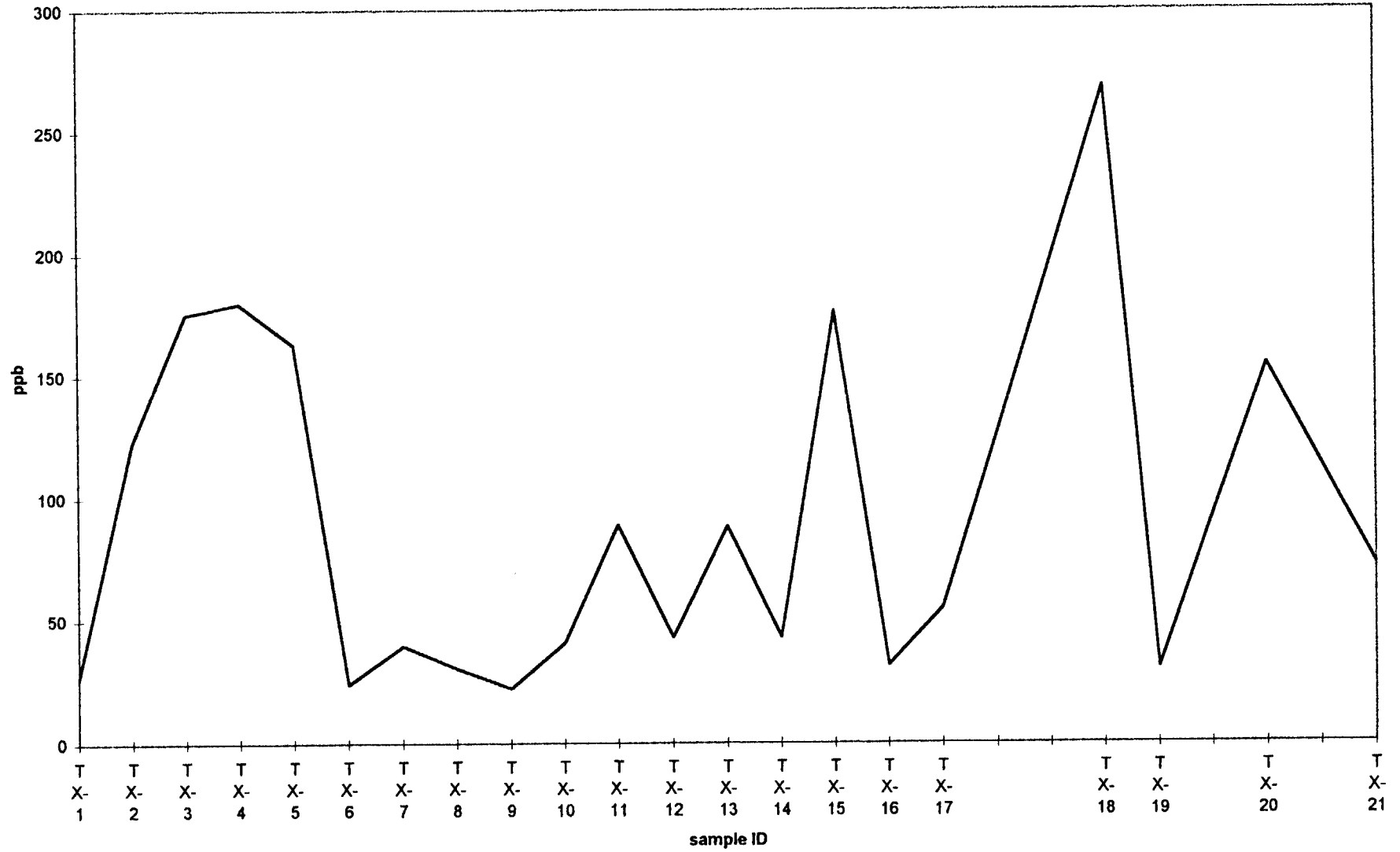
TUZEX CLAIMS Enzyme Leach (SM) data

Nd



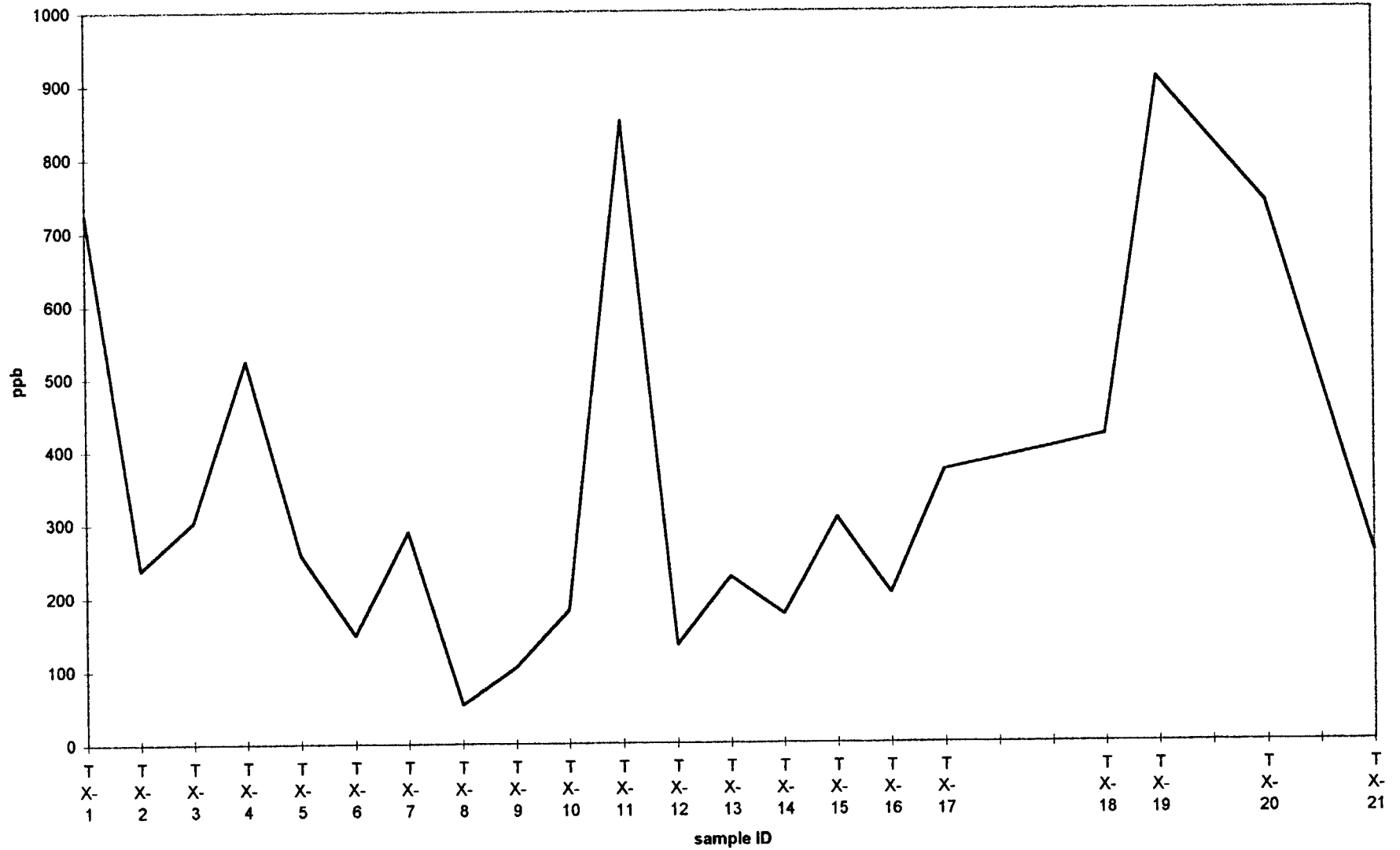
TUZEX CLAIMS Enzyme Leach (SM) data

Sr



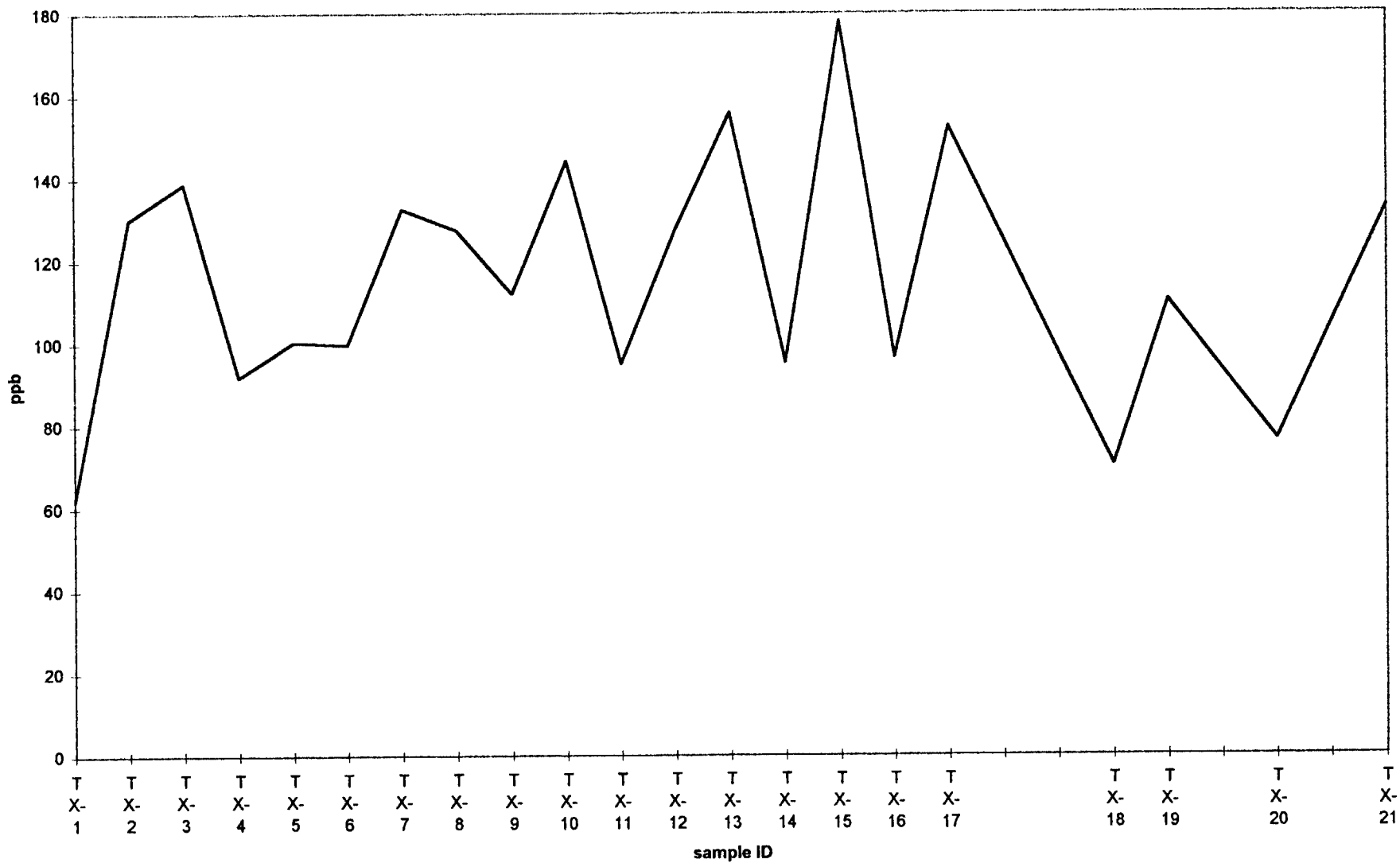
TUZEX CLAIMS Enzyme Leach (SM) data

Ba



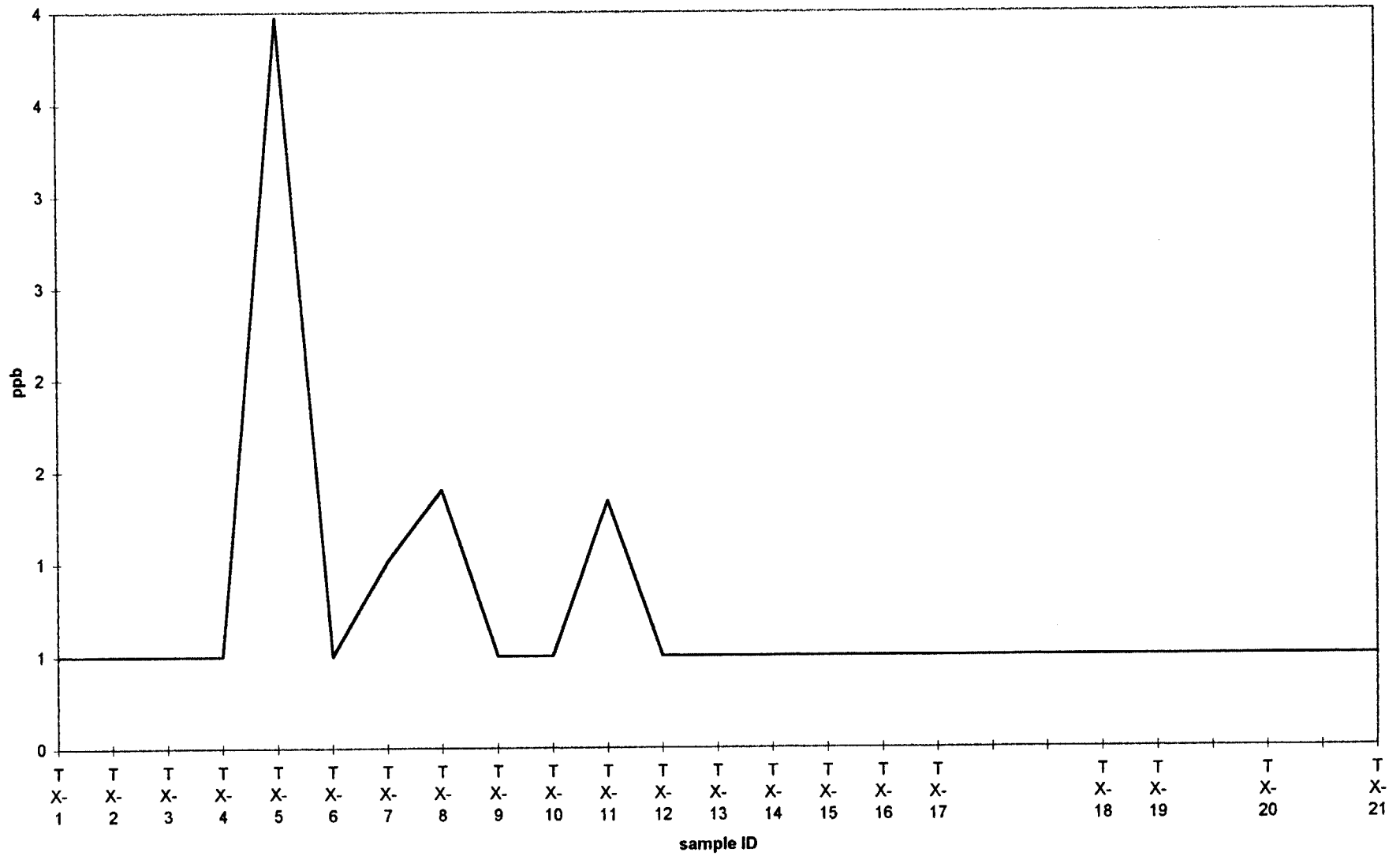
TUZEX CLAIMS Enzyme Leach (SM) data

Rb



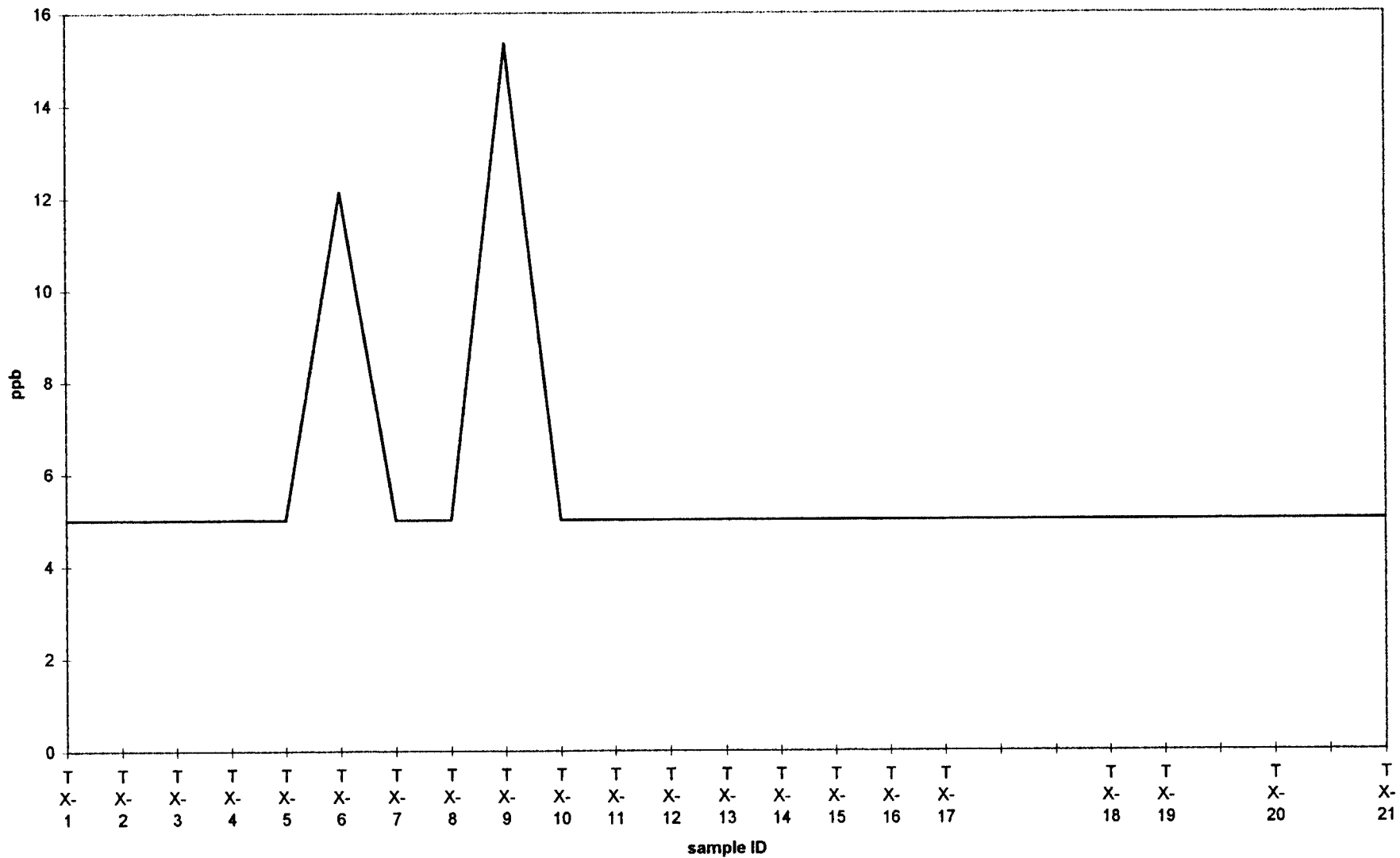
TUZEX CLAIMS Enzyme Leach (SM) data

Cs



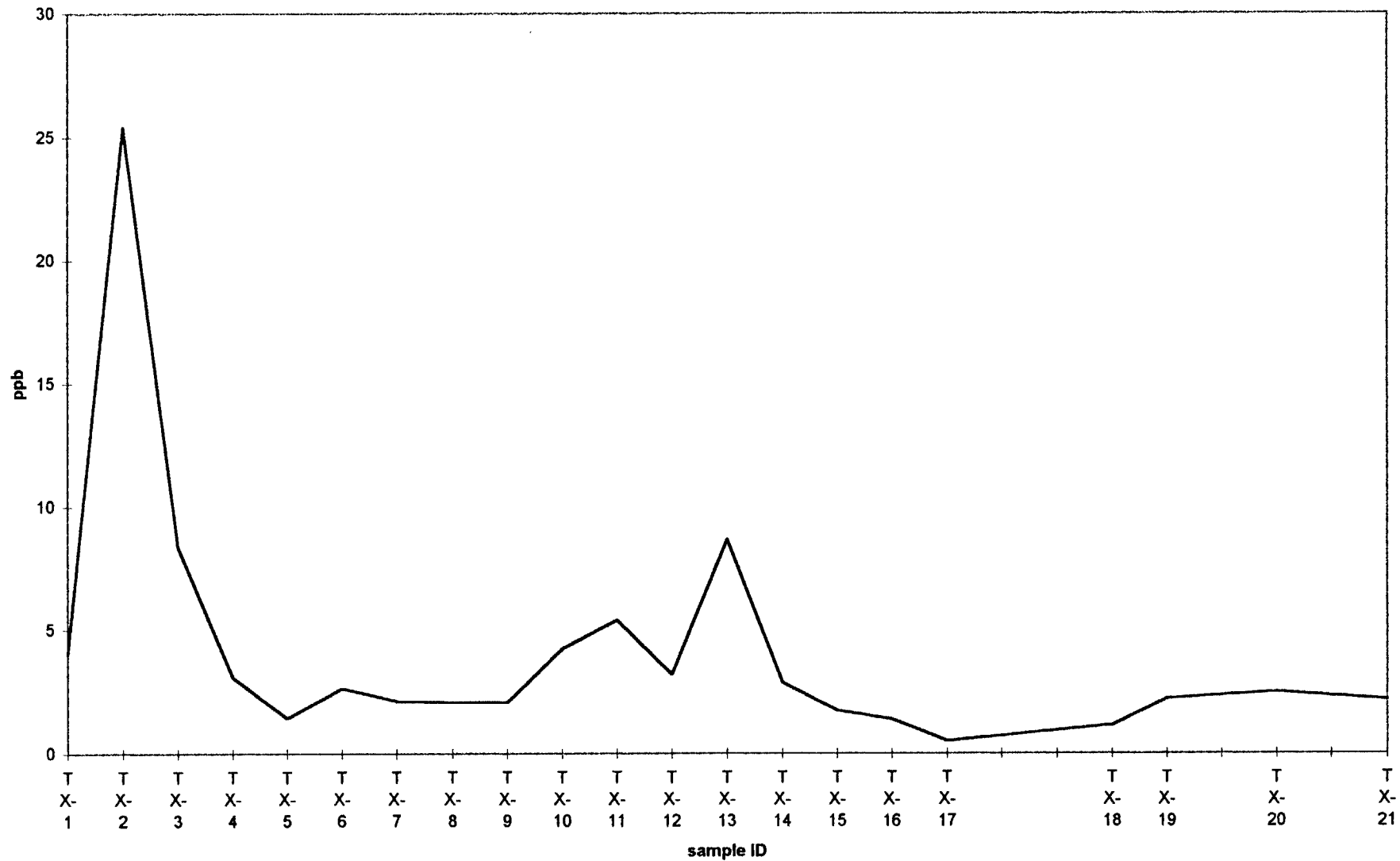
TUZEX CLAIMS Enzyme Leach (SM) data

S.Q.Li



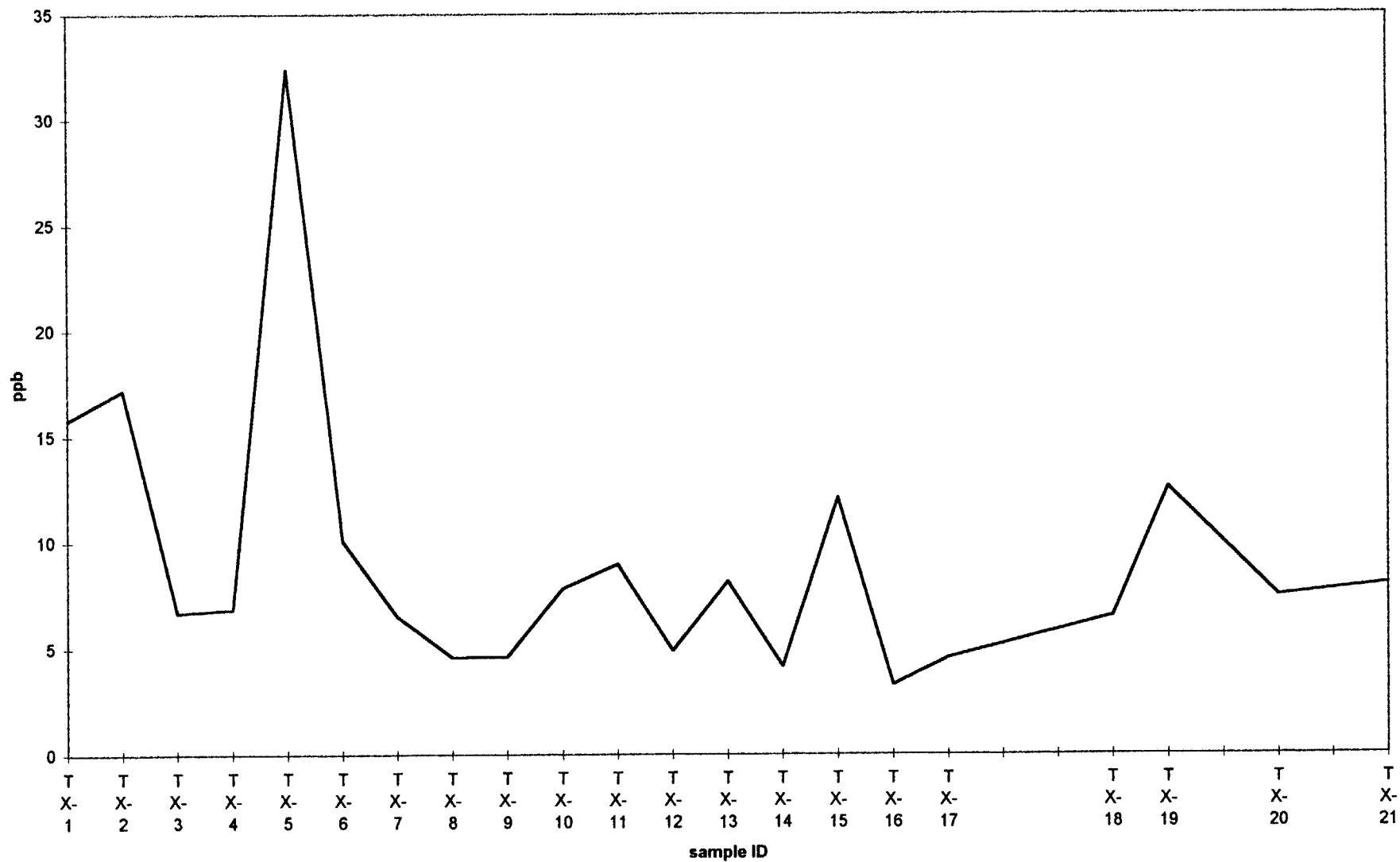
TUZEX CLAIMS Enzyme Leach (SM) data

Zr



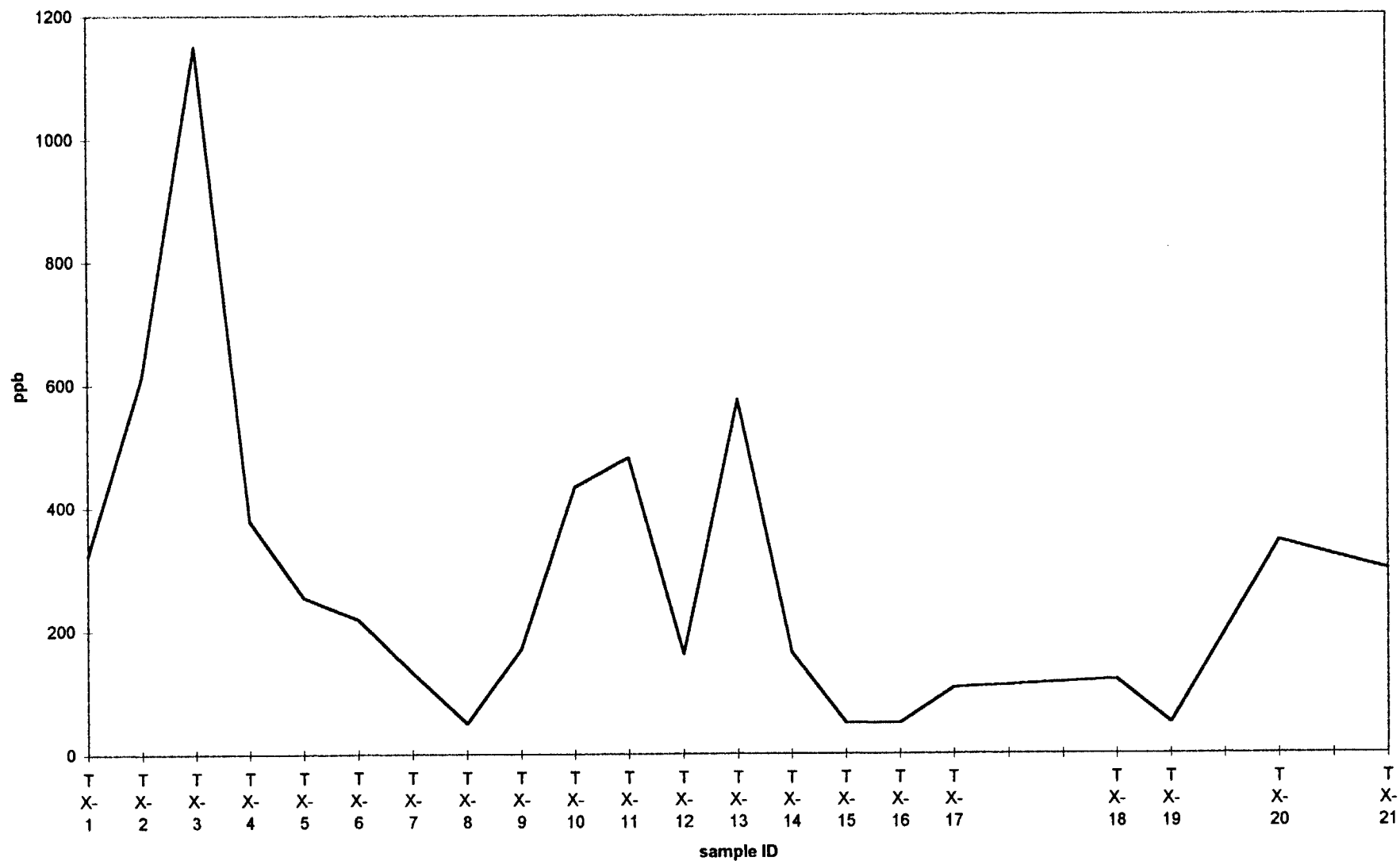
TUZEX CLAIMS Enzyme Leach (SM) data

Y



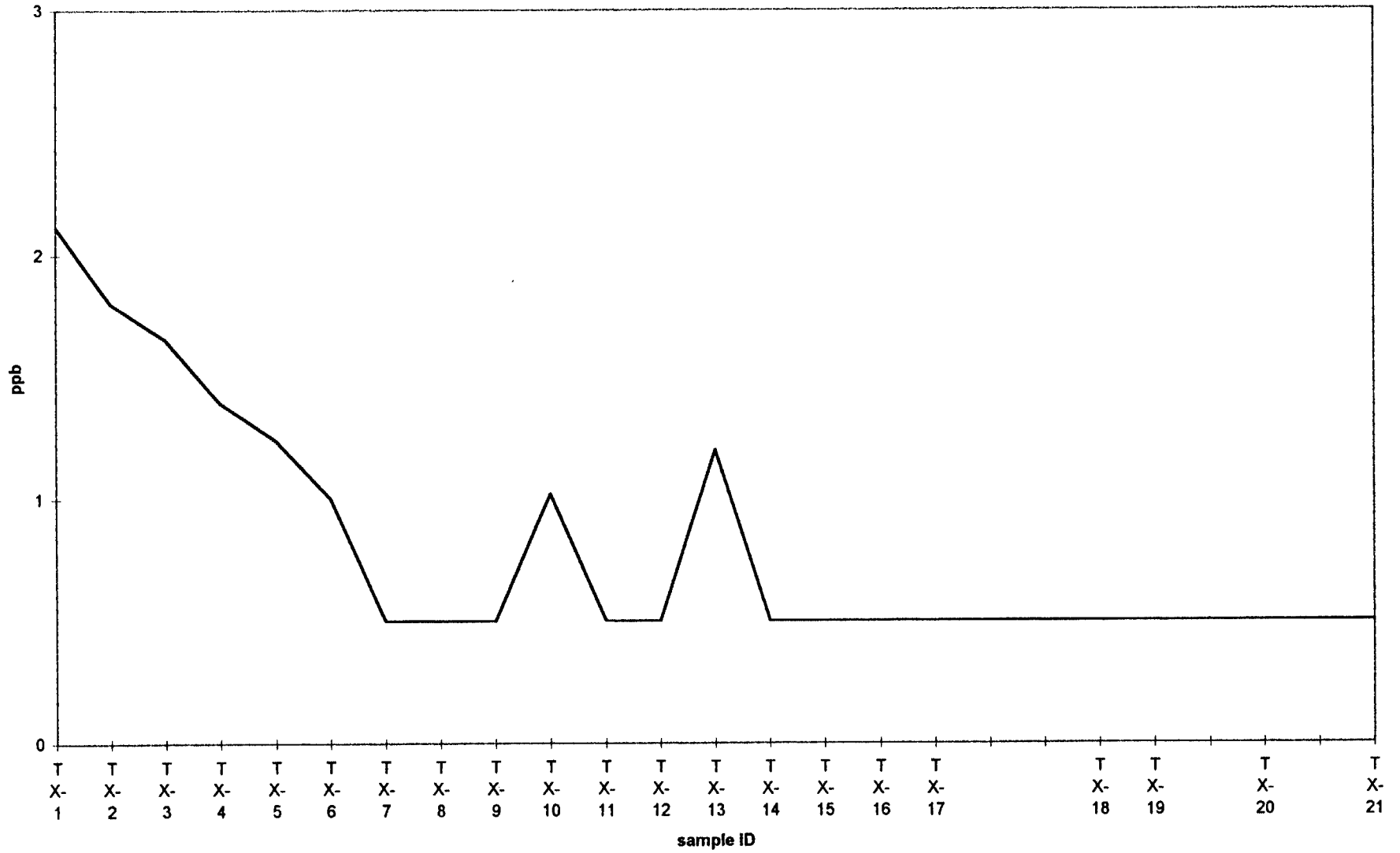
TUZEX CLAIMS Enzyme Leach (SM) data

S.Q.TI



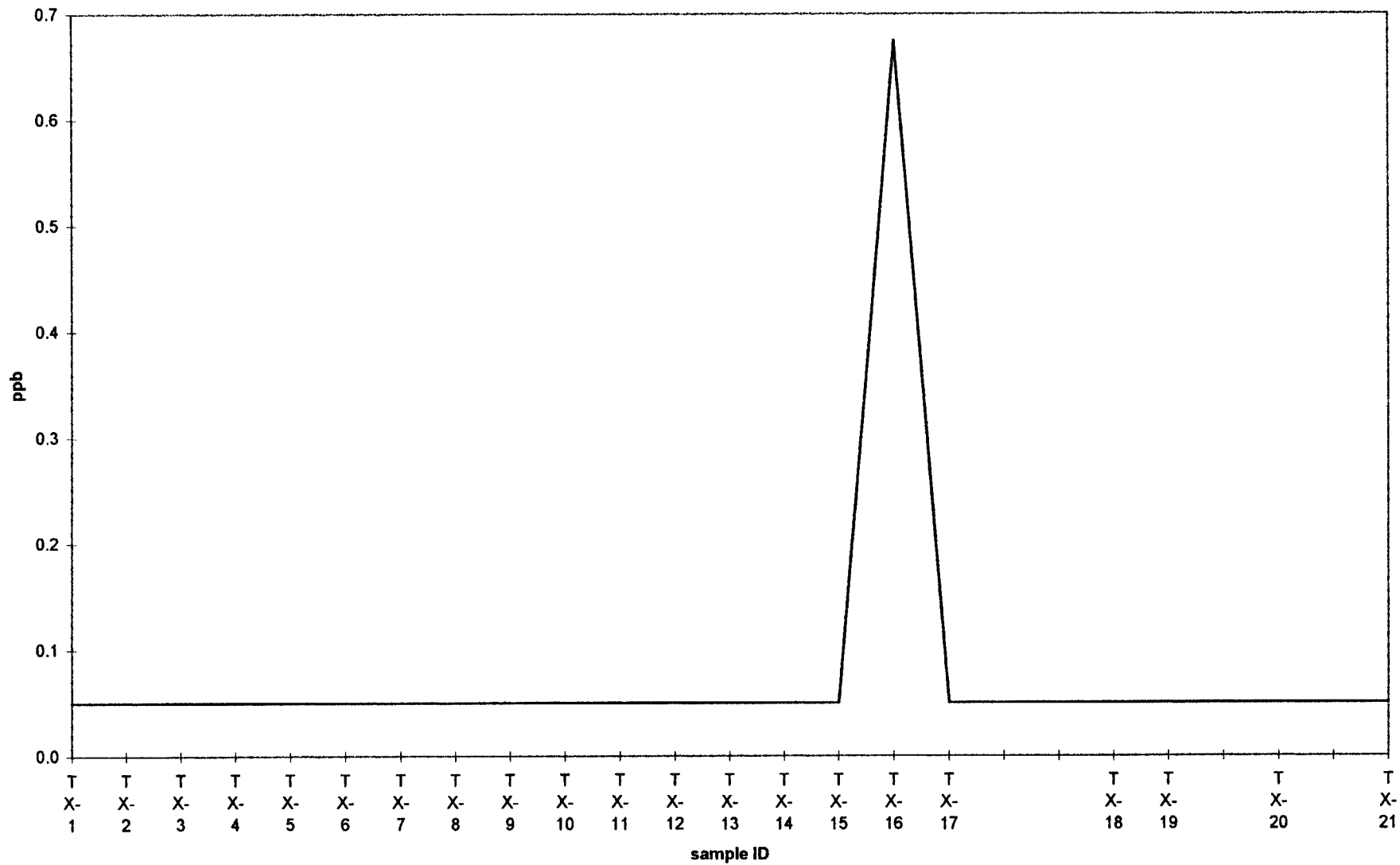
TUZEX CLAIMS Enzyme Leach (SM) data

Nb

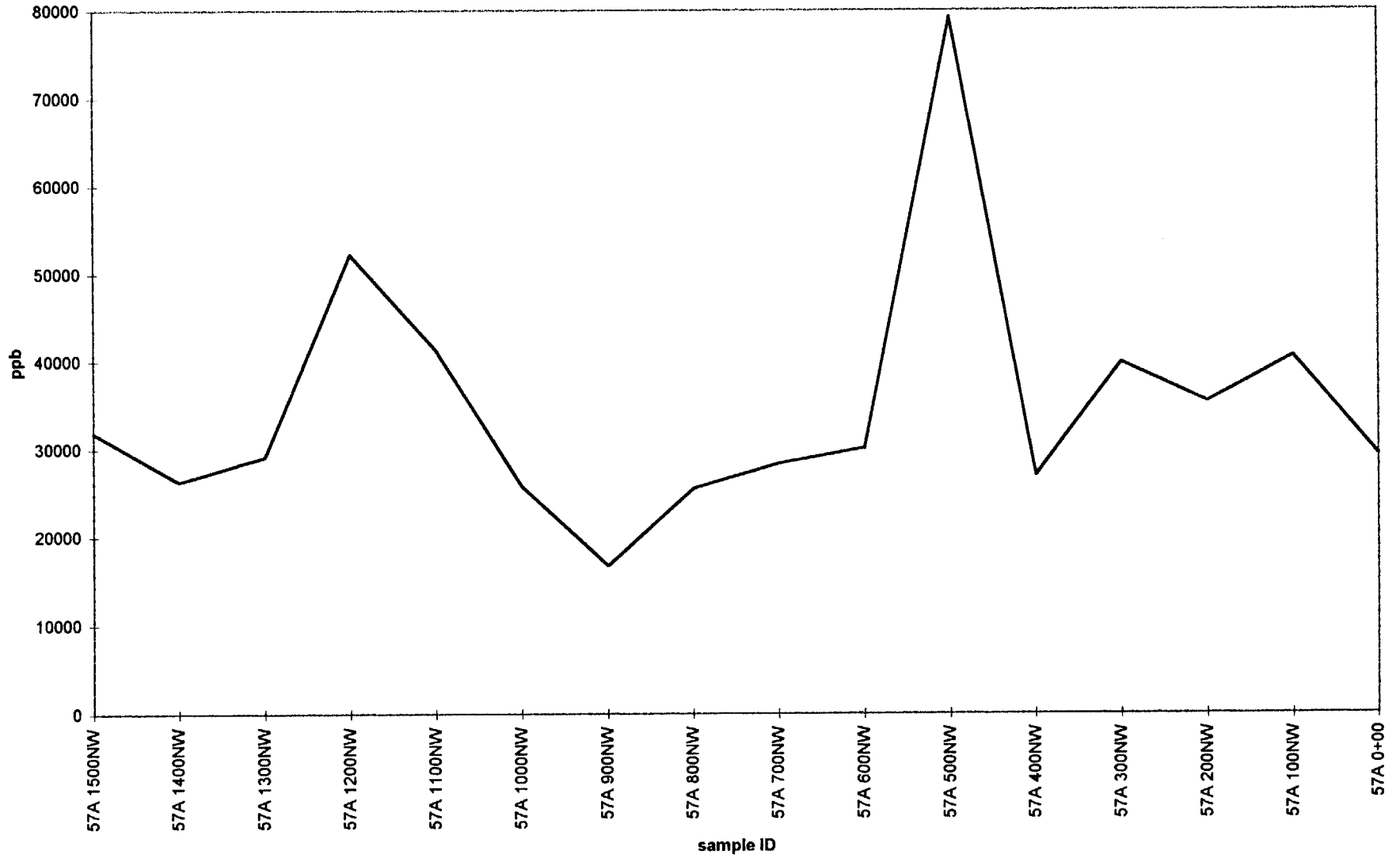


TUZEX CLAIMS Enzyme Leach (SM) data

Au

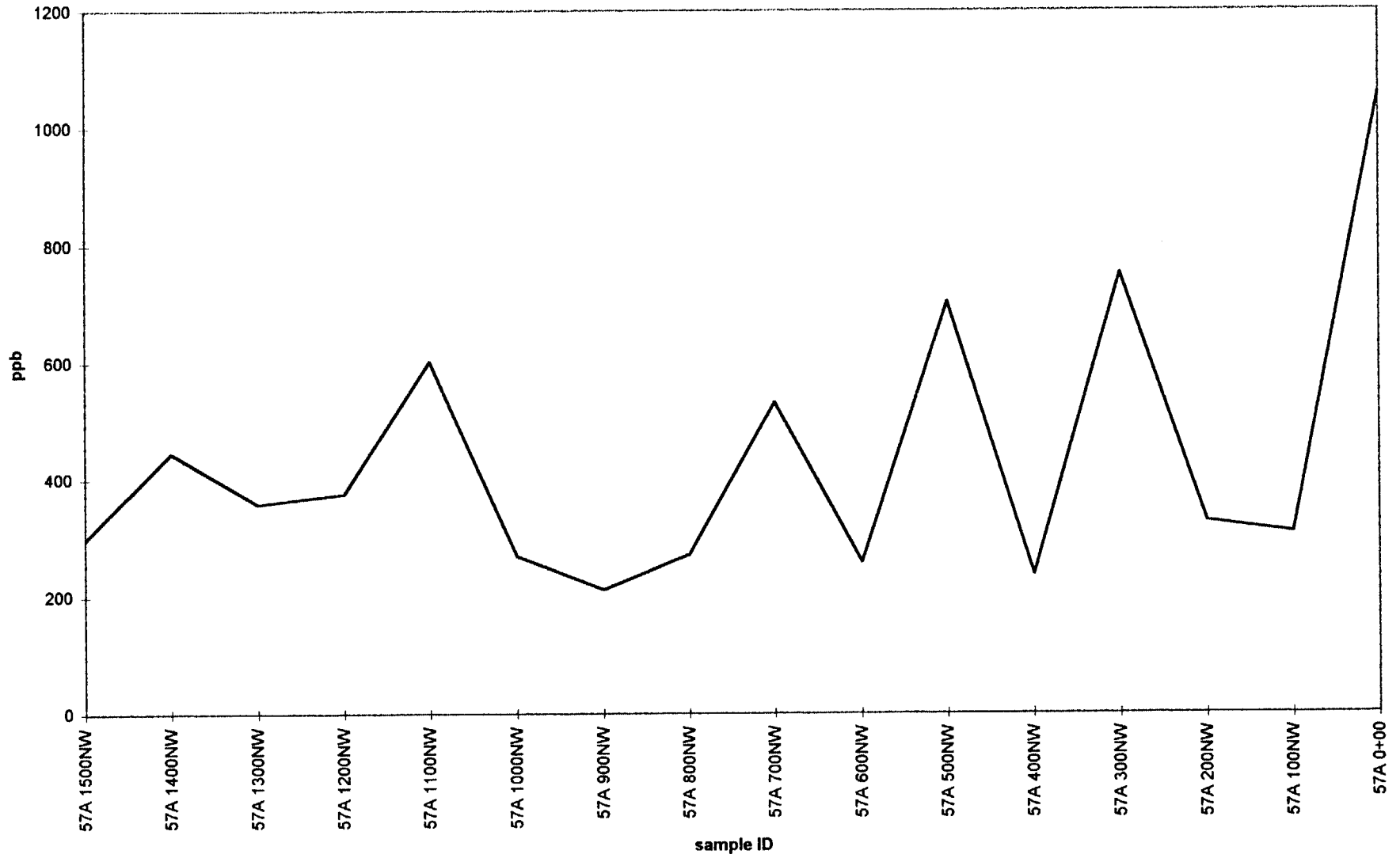


S.Q.Cl

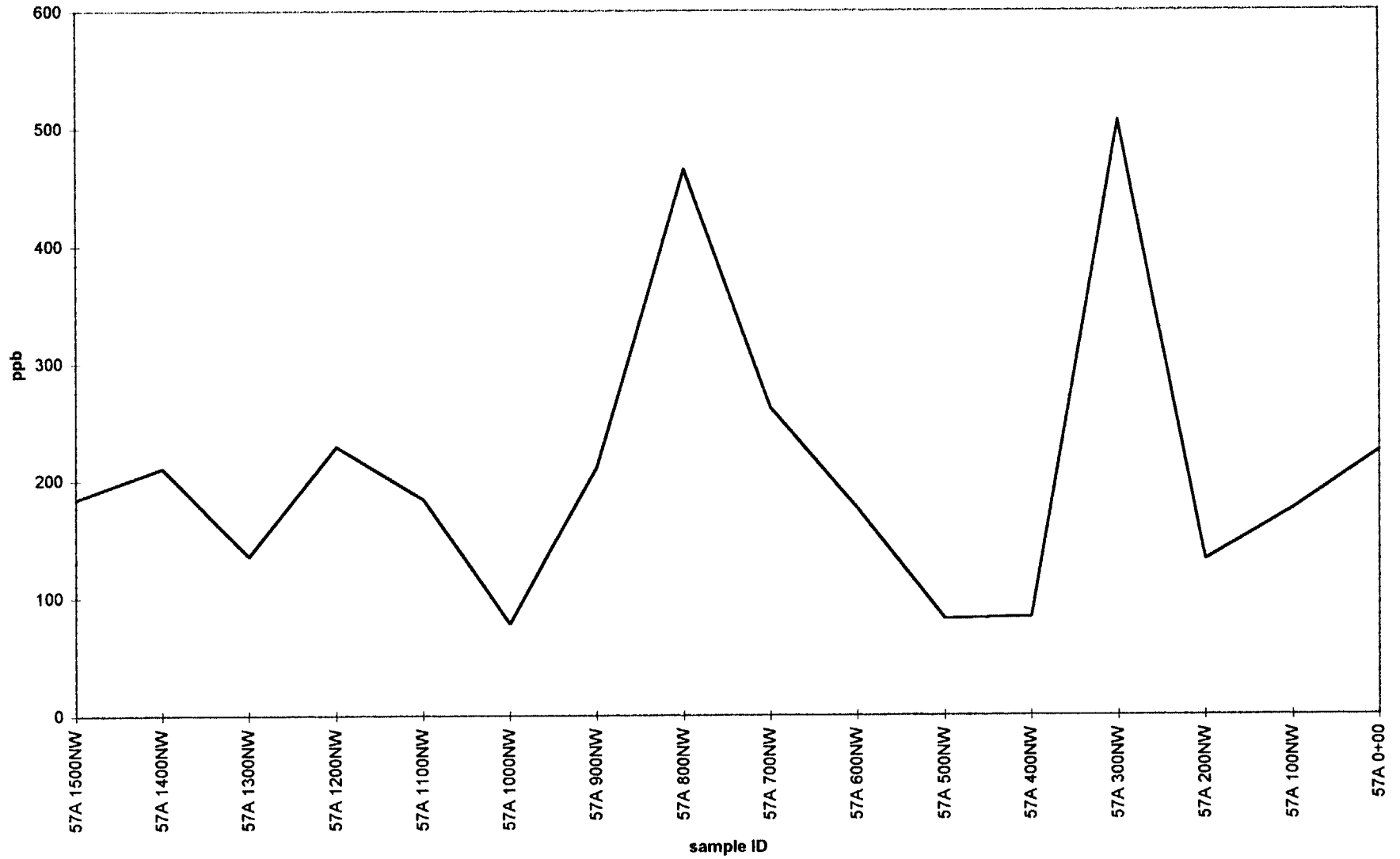


TUZEX CLAIMS Enzyme Leach (SM) data

Br

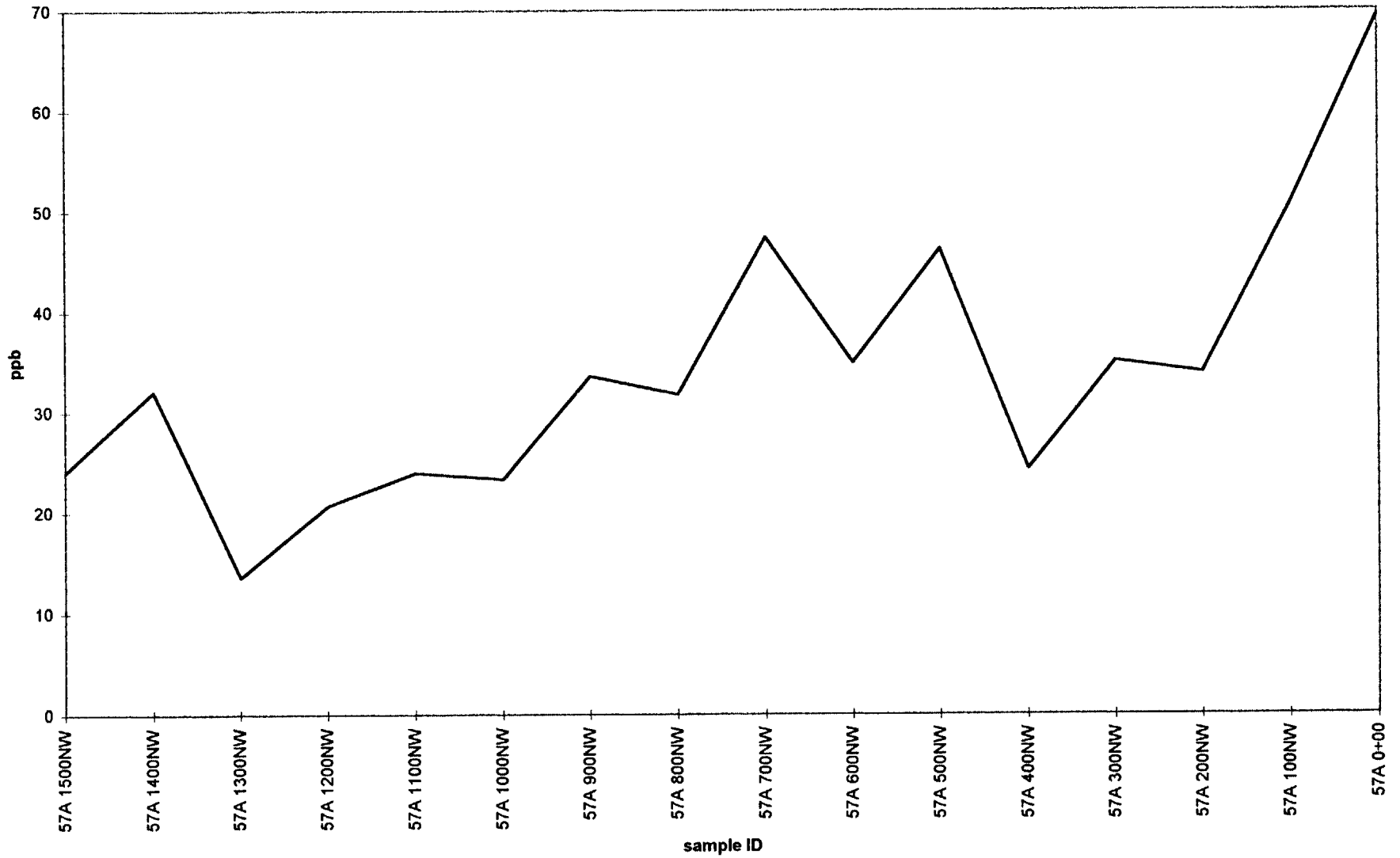


TUZEX CLAIMS Enzyme Leach (SM) data



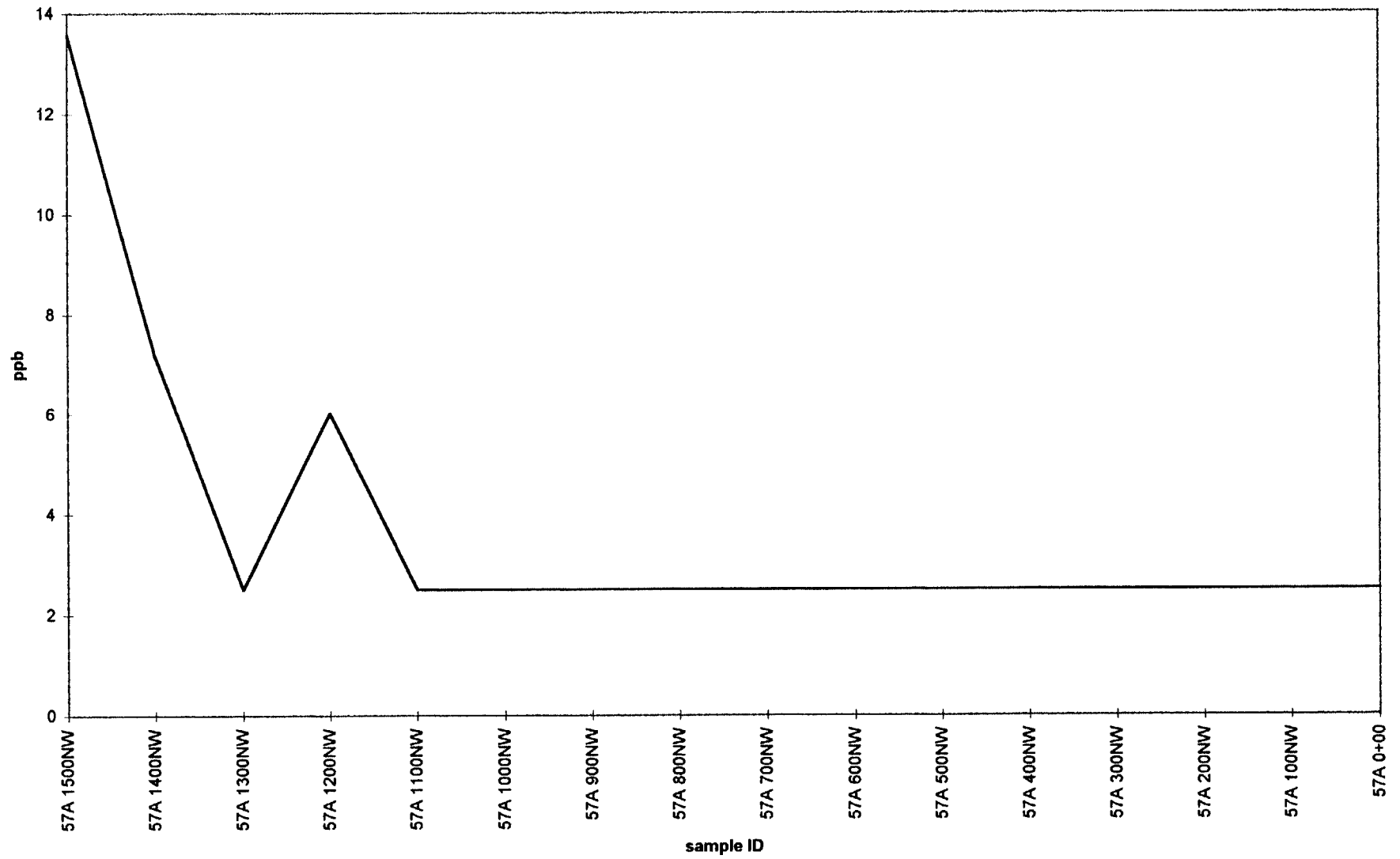
TUZEX CLAIMS Enzyme Leach (SM) data

v

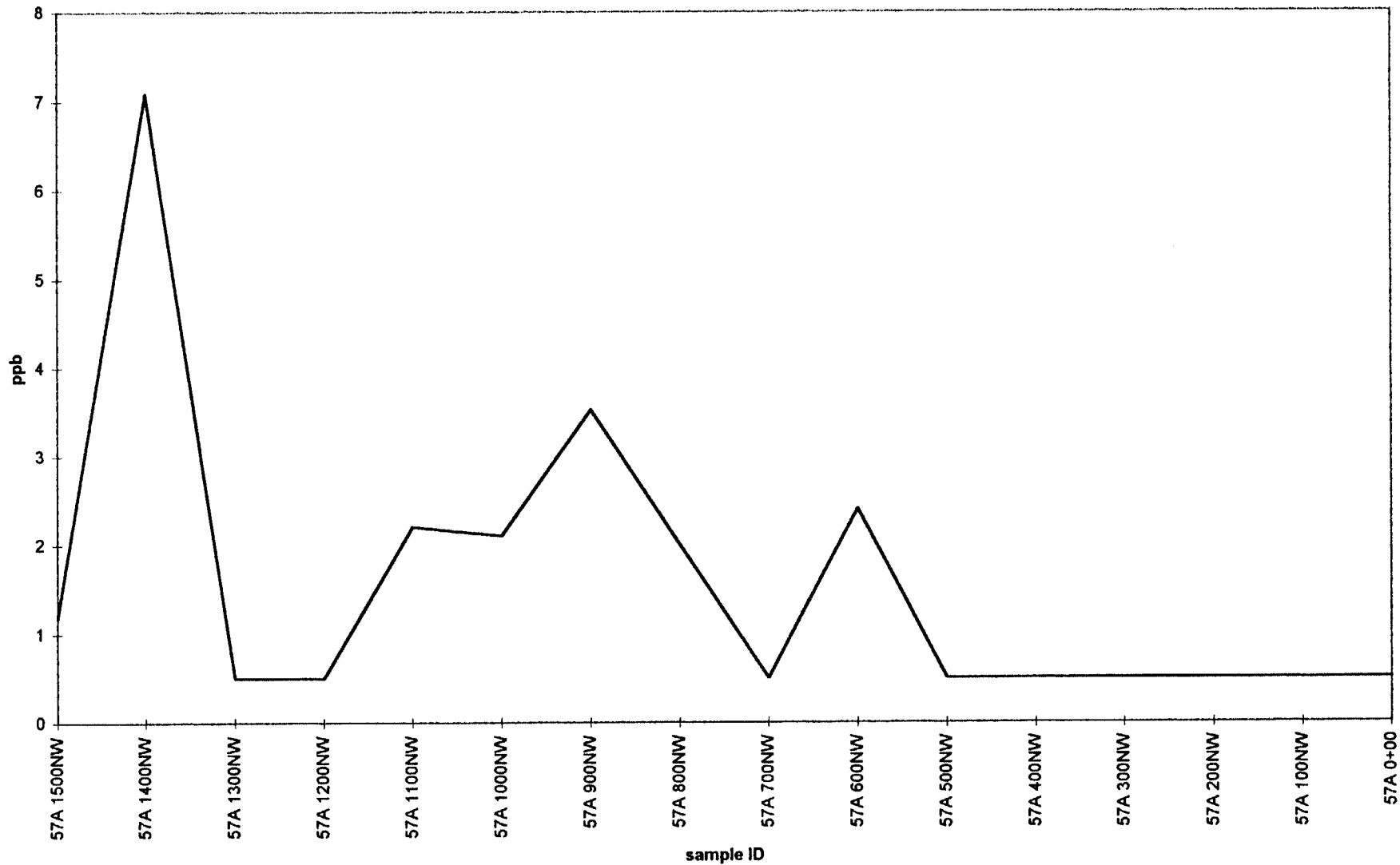


TUZEX CLAIMS Enzyme Leach (SM) data

As

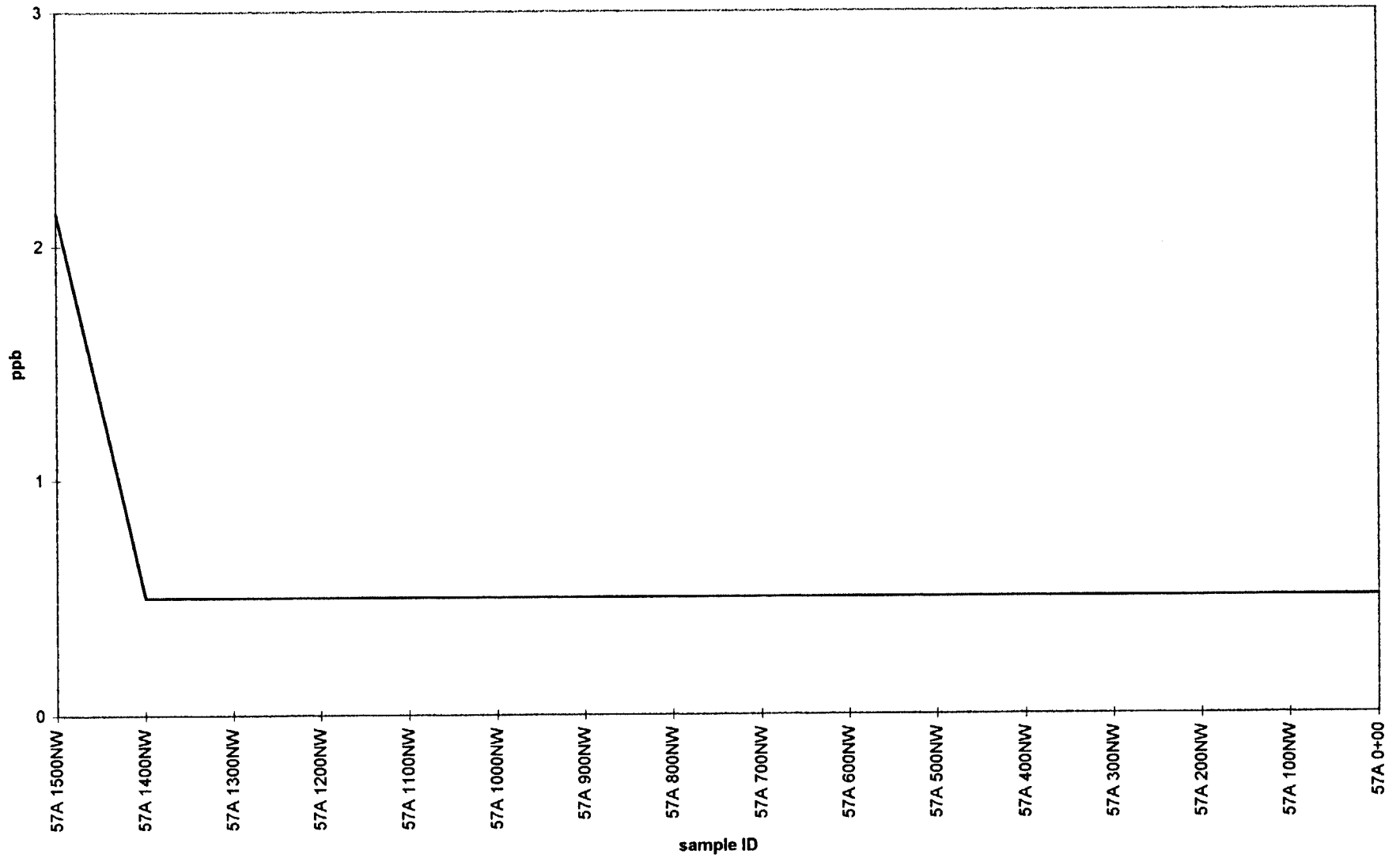


Mo



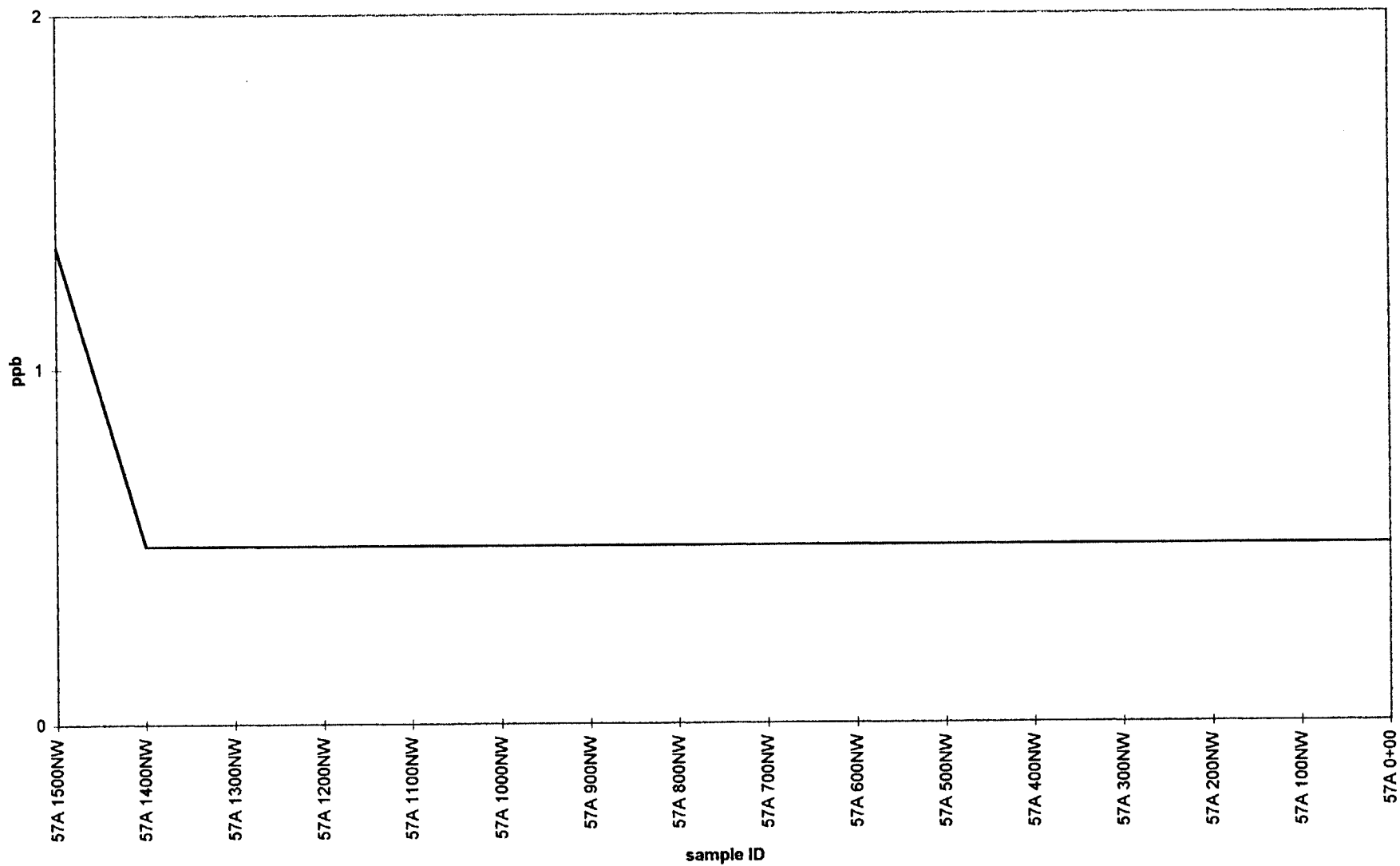
TUZEX CLAIMS Enzyme Leach (SM) data

Th



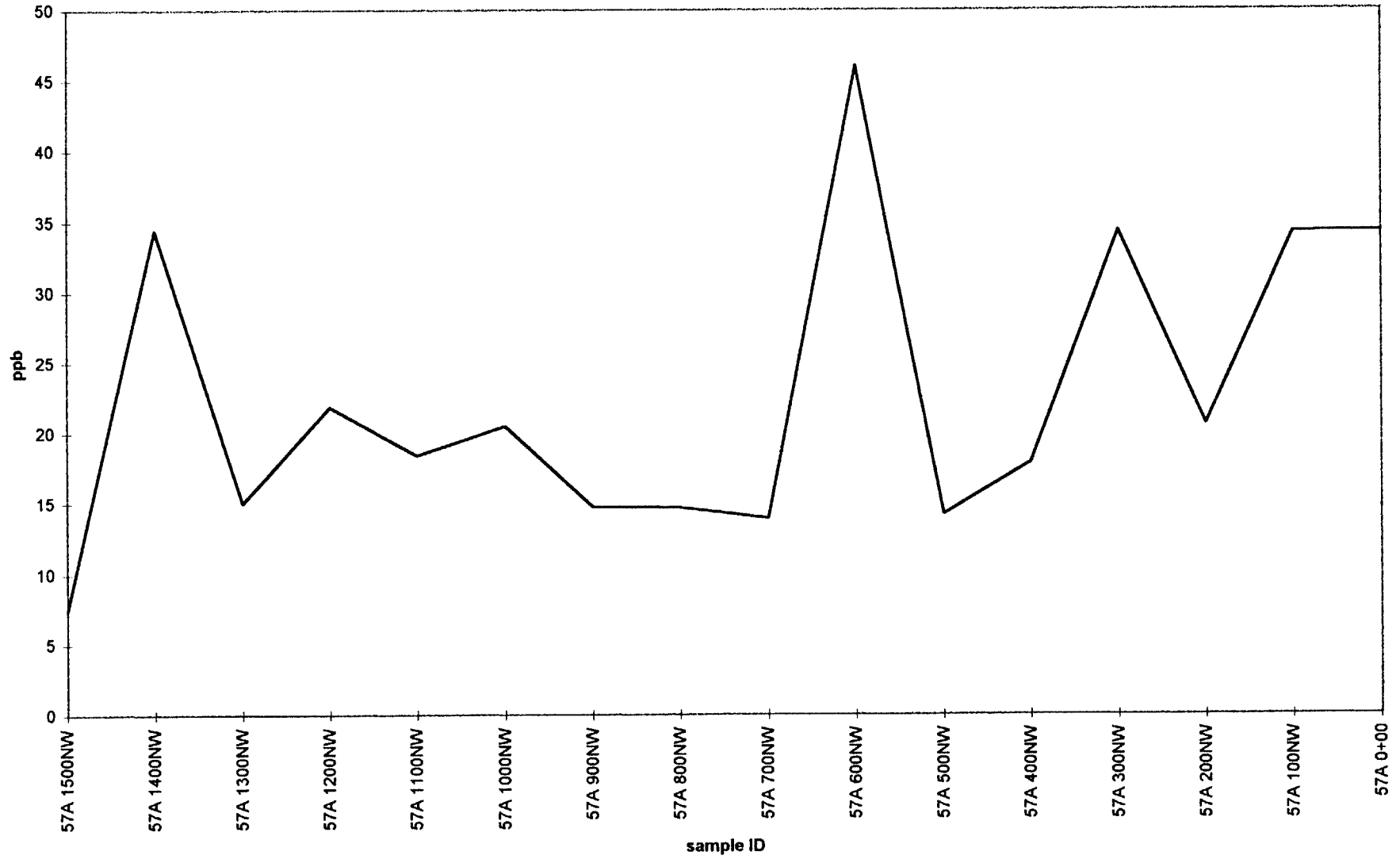
TUZEX CLAIMS Enzyme Leach (SM) data

U



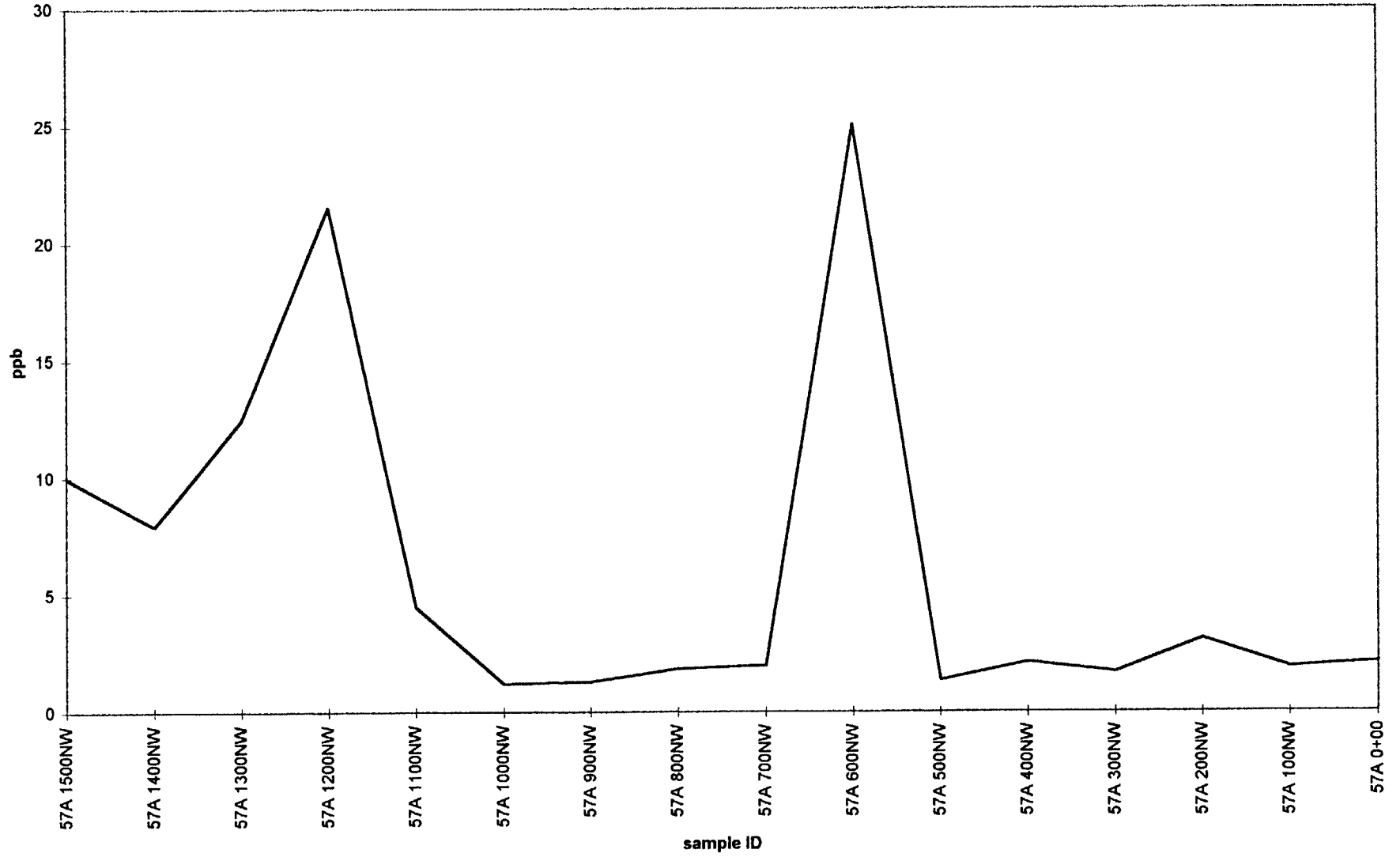
TUZEX CLAIMS Enzyme Leach (SM) data

Cu



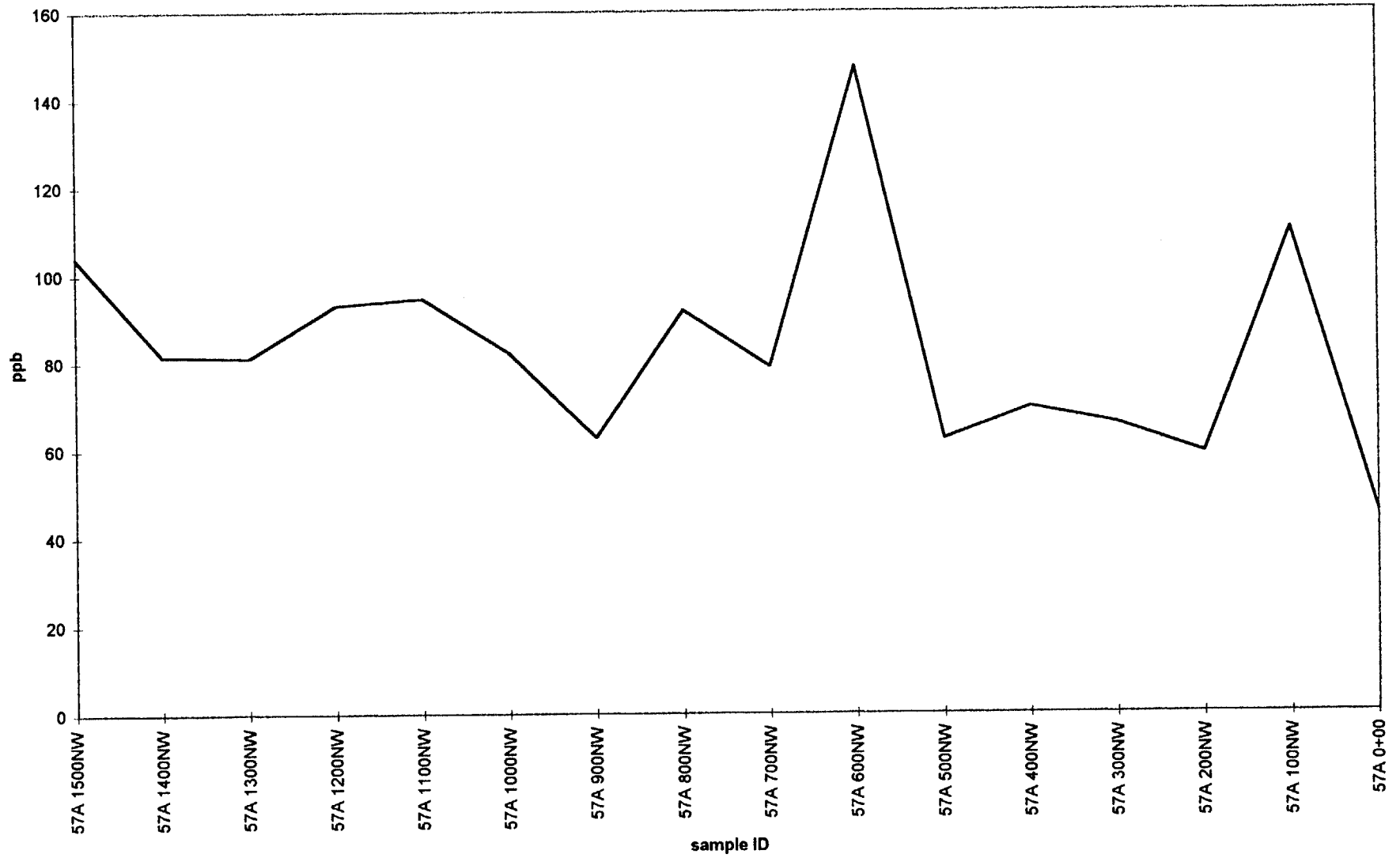
TUZEX CLAIMS Enzyme Leach (SM) data

Pb



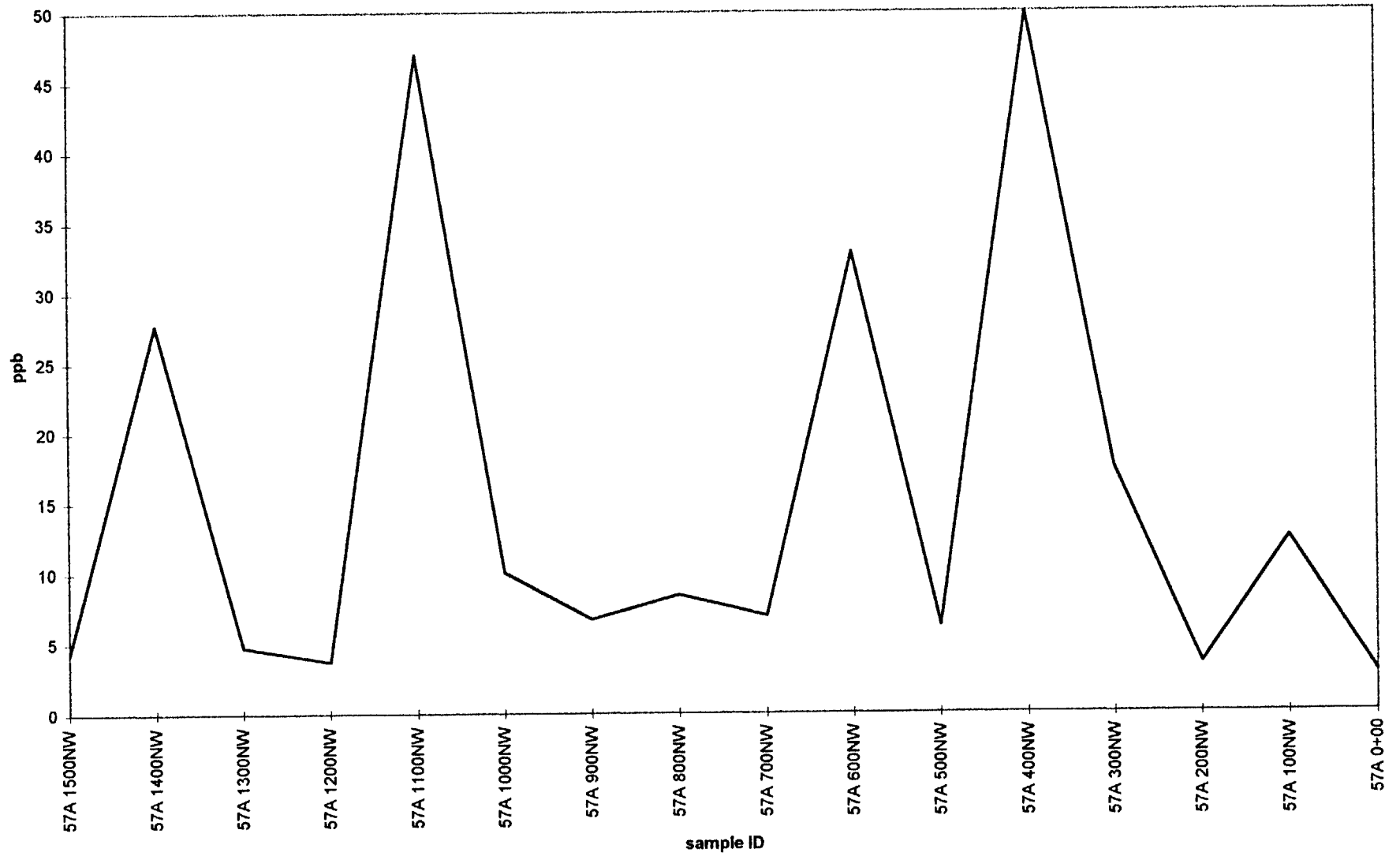
TUZEX CLAIMS Enzyme Leach (SM) data

Zn



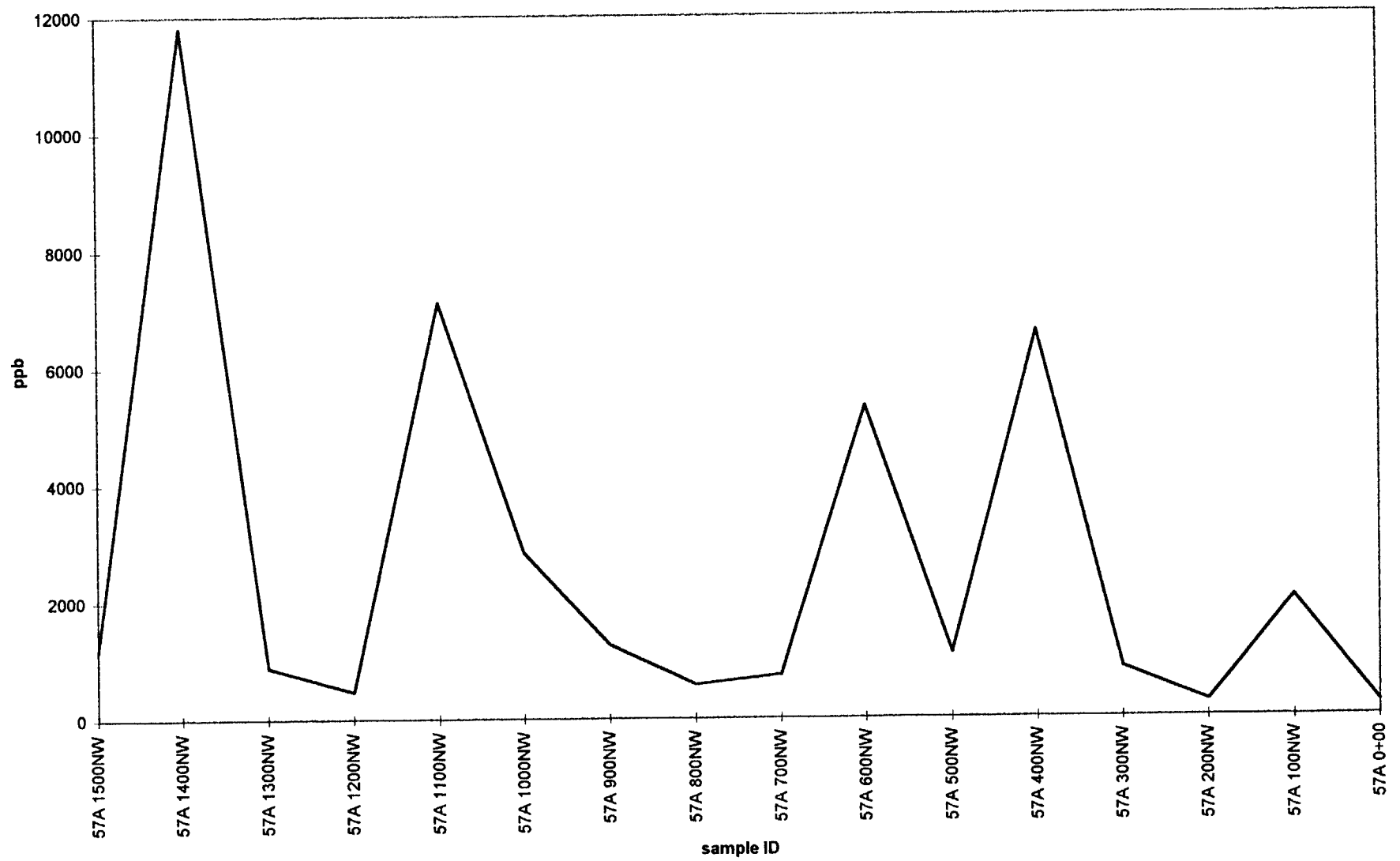
TUZEX CLAIMS Enzyme Leach (SM) data

Co

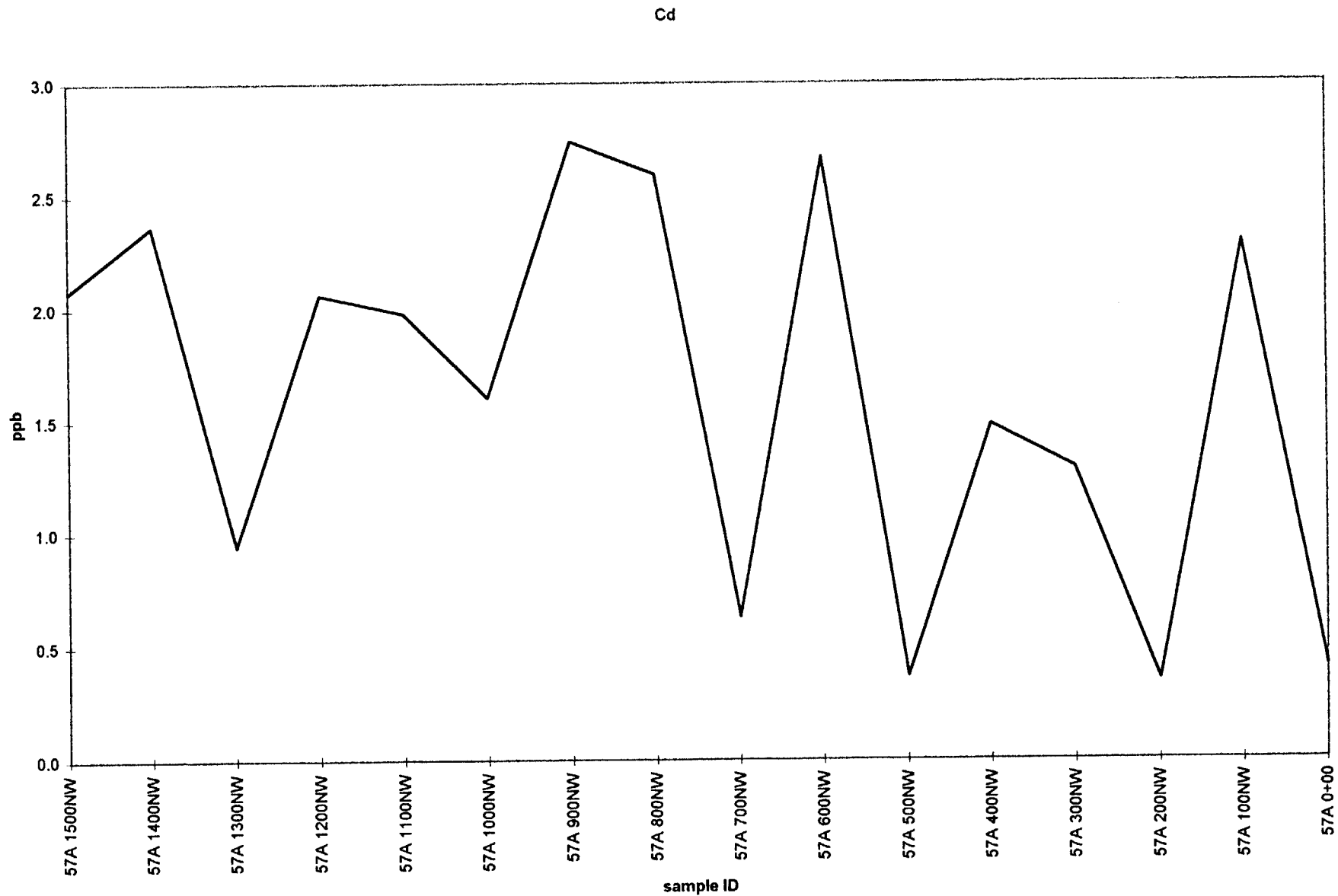


TUZEX CLAIMS Enzyme Leach (SM) data

Mn

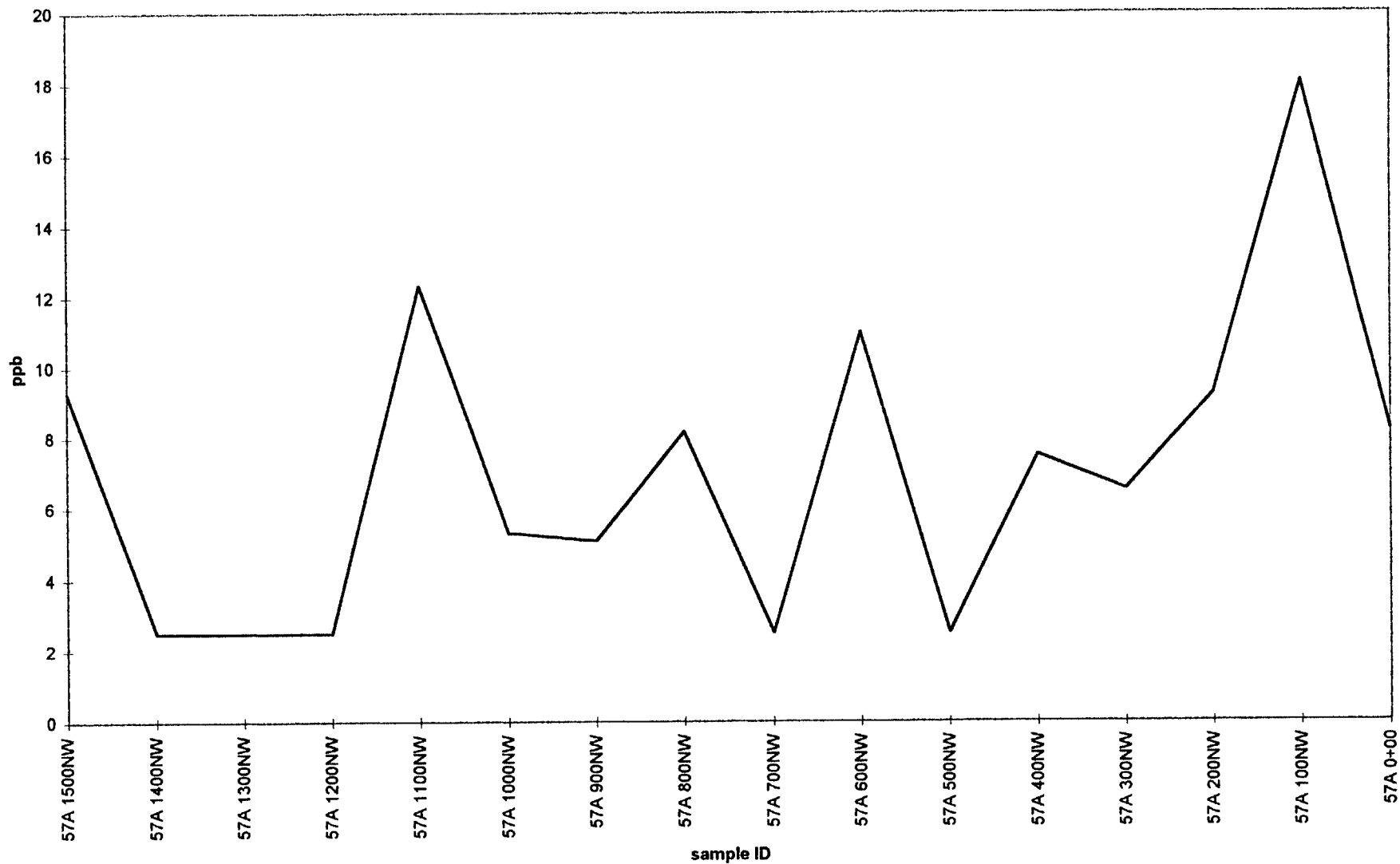


TUZEX CLAIMS Enzyme Leach (SM) data



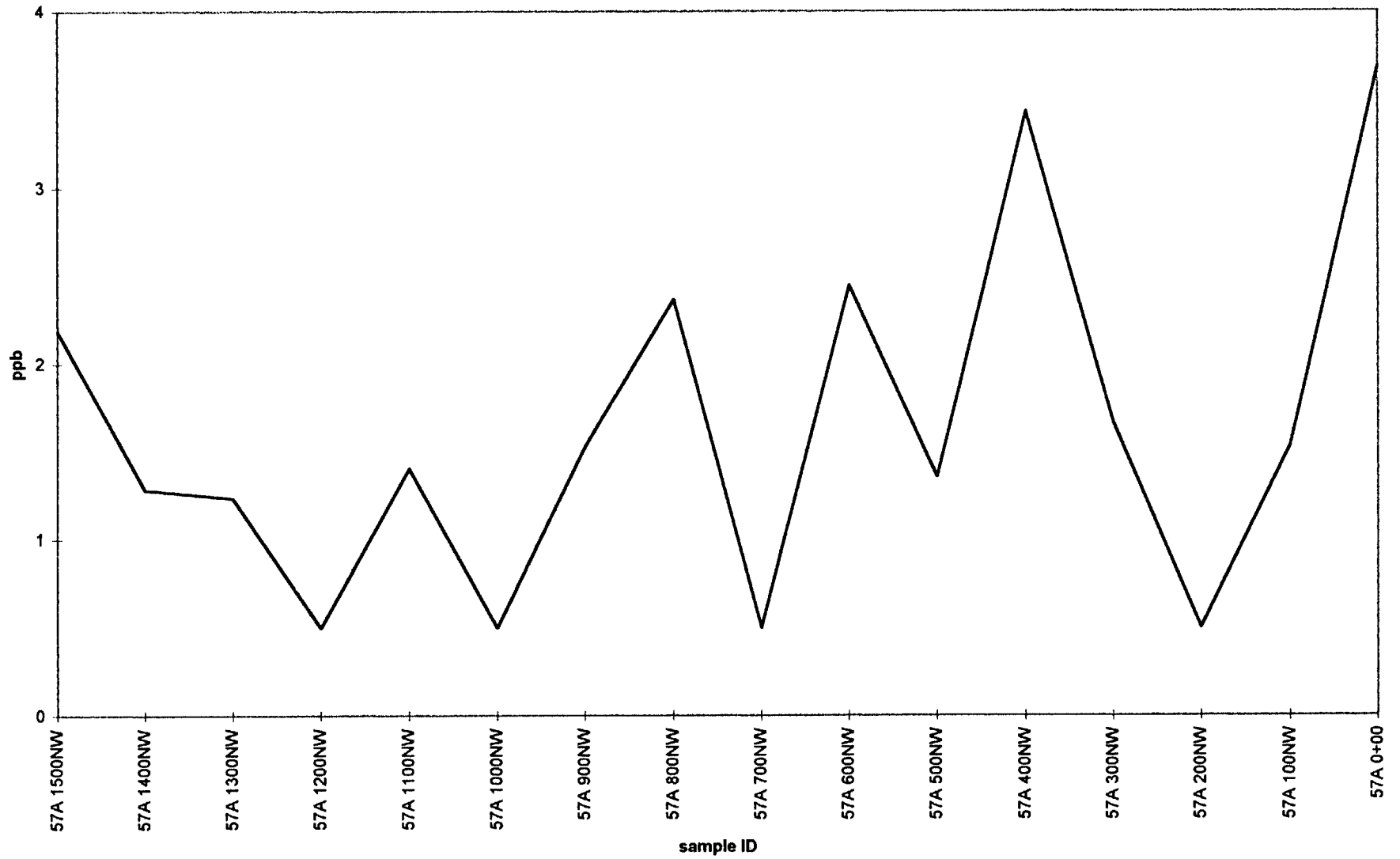
TUZEX CLAIMS Enzyme Leach (SM) data

Ni



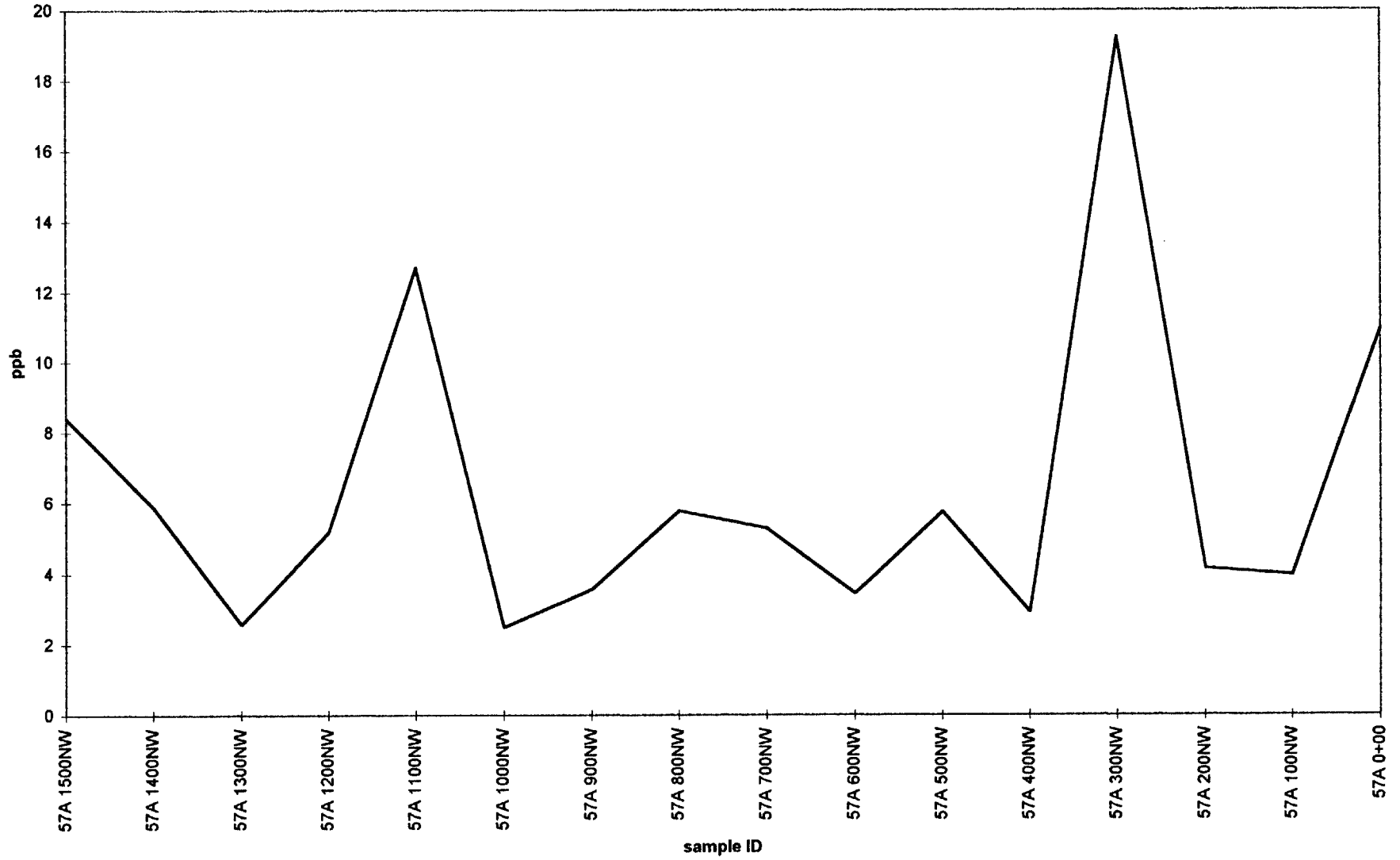
TUZEX CLAIMS Enzyme Leach (SM) data

Ga



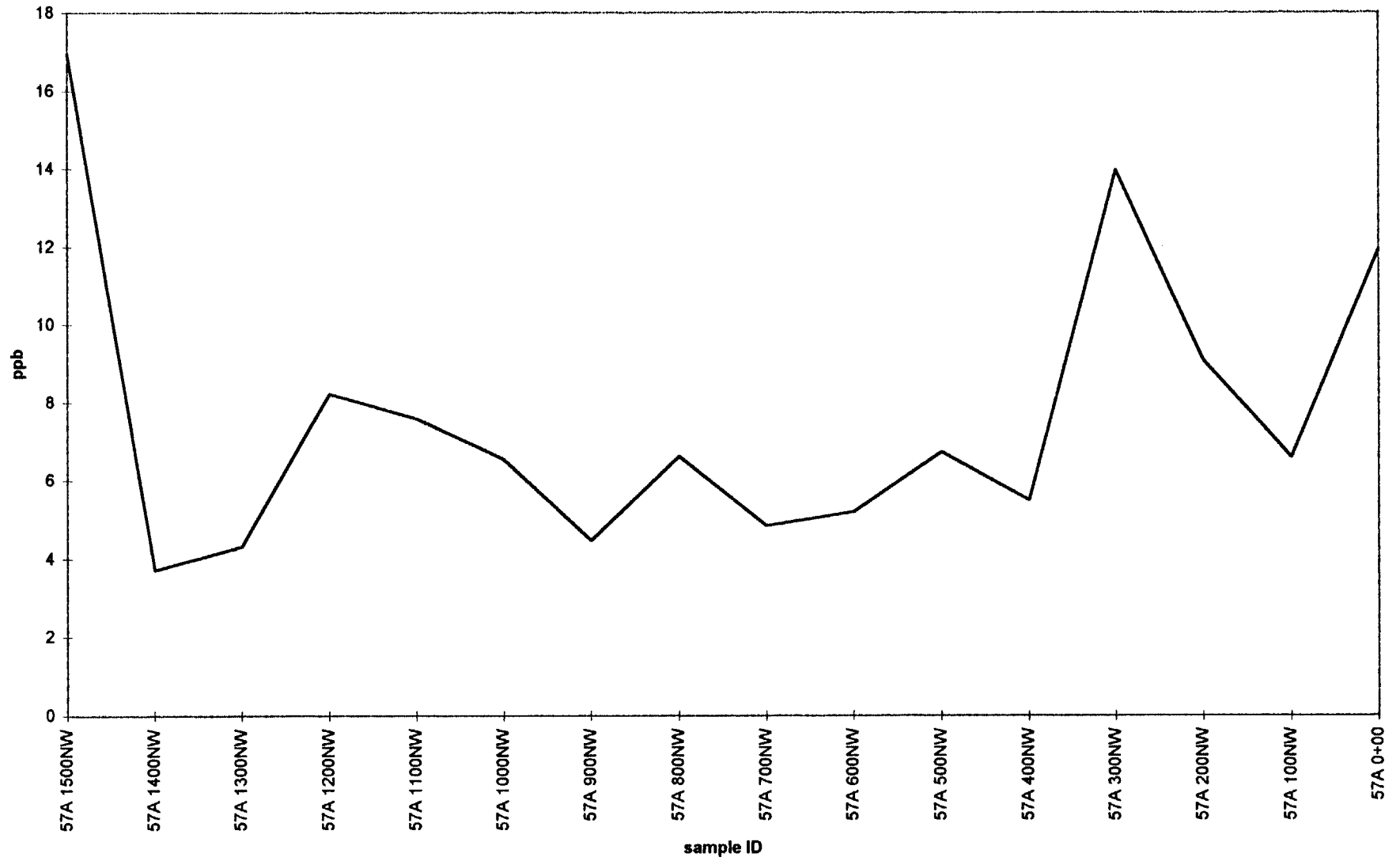
TUZEX CLAIMS Enzyme Leach (SM) data

La



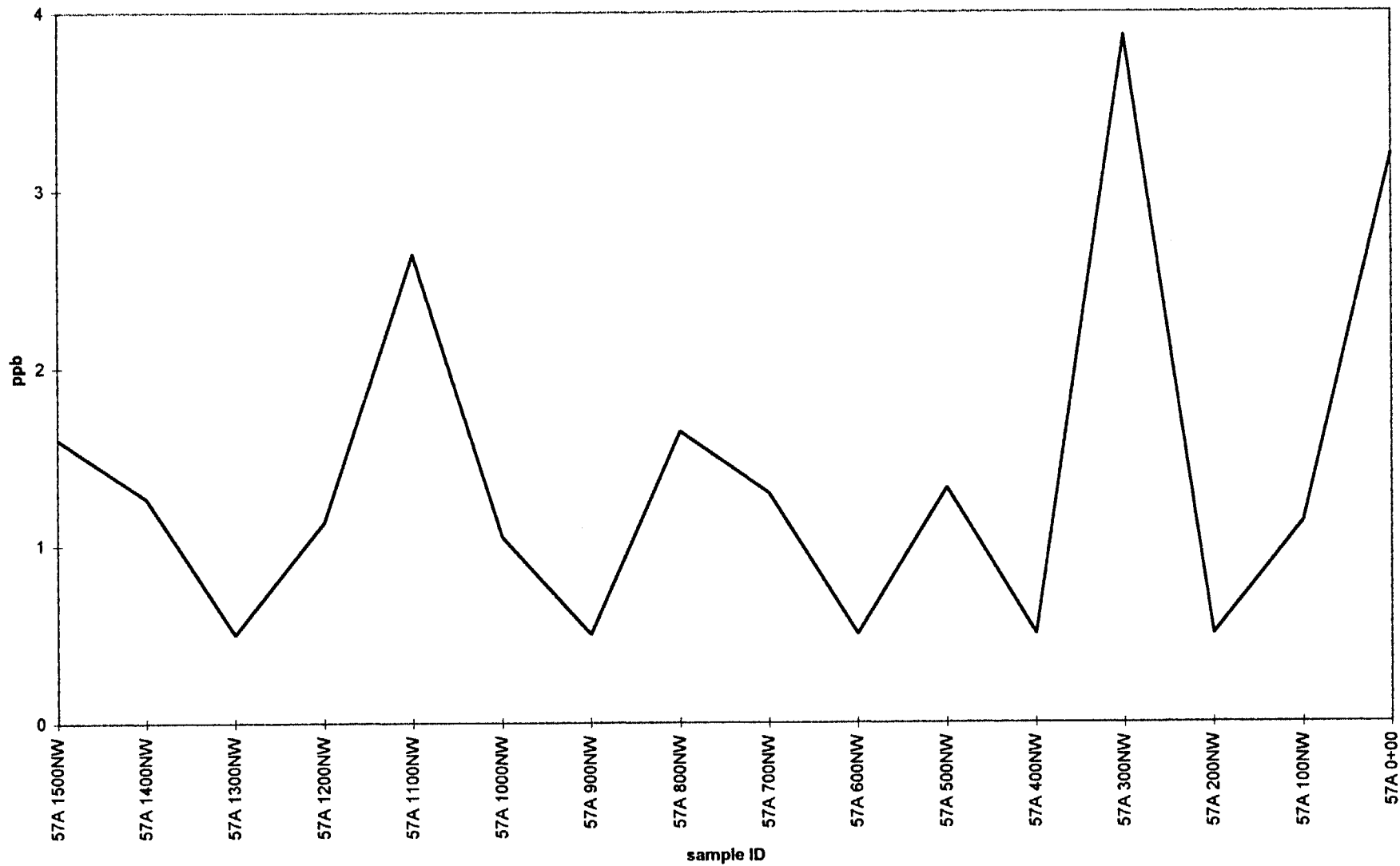
TUZEX CLAIMS Enzyme Leach (SM) data

Ce



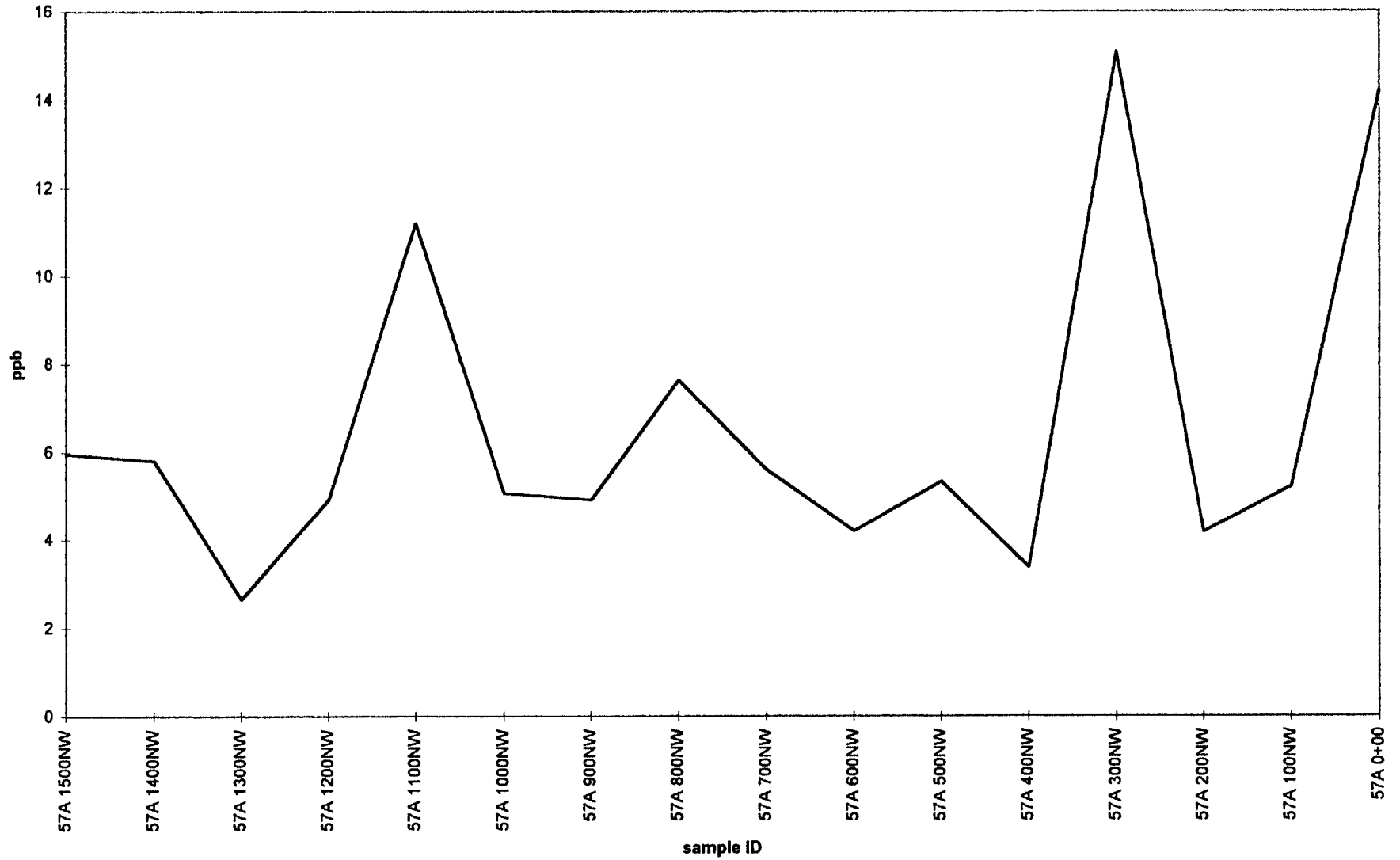
TUZEX CLAIMS Enzyme Leach (SM) data

Pr



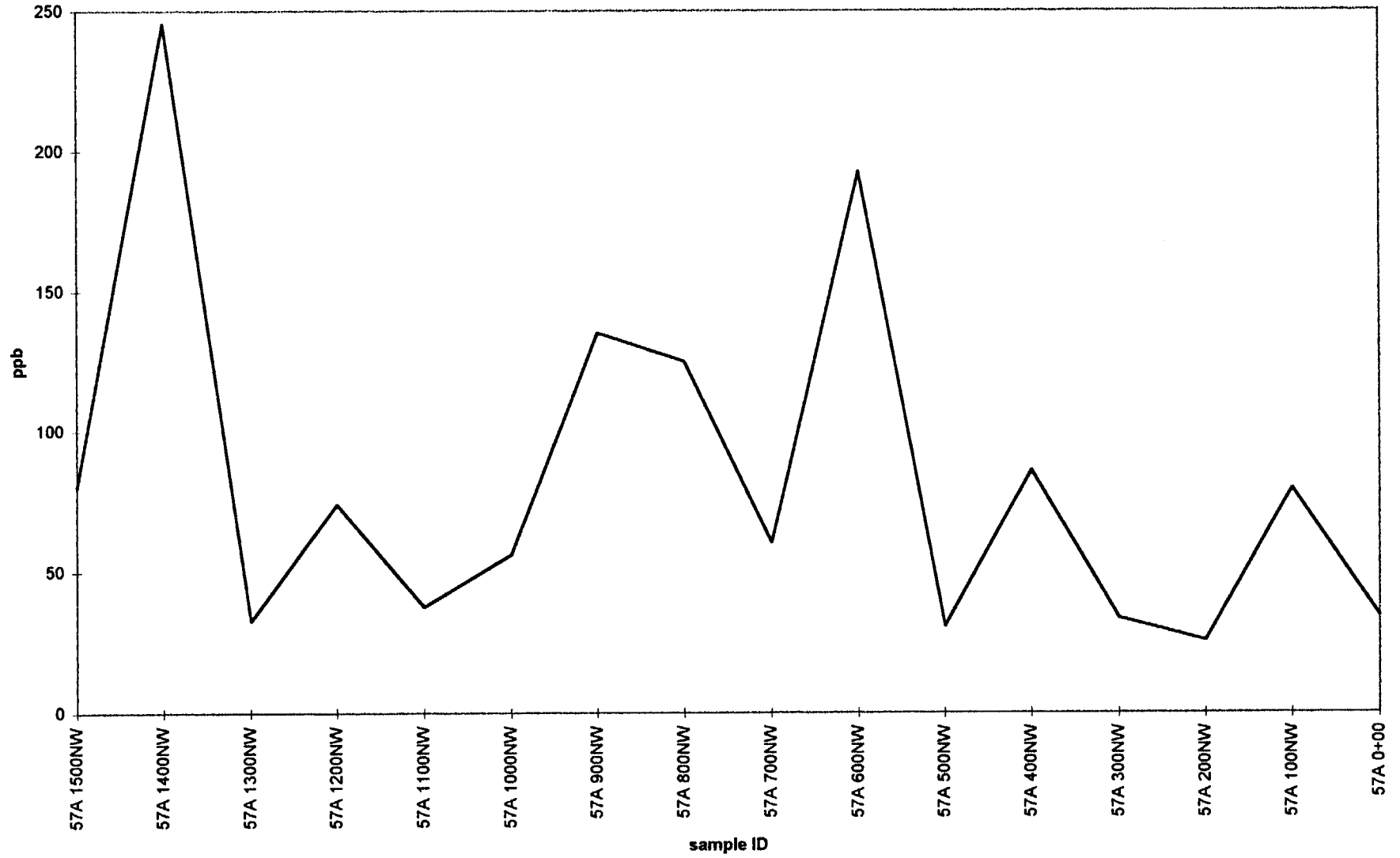
TUZEX CLAIMS Enzyme Leach (SM) data

Nd



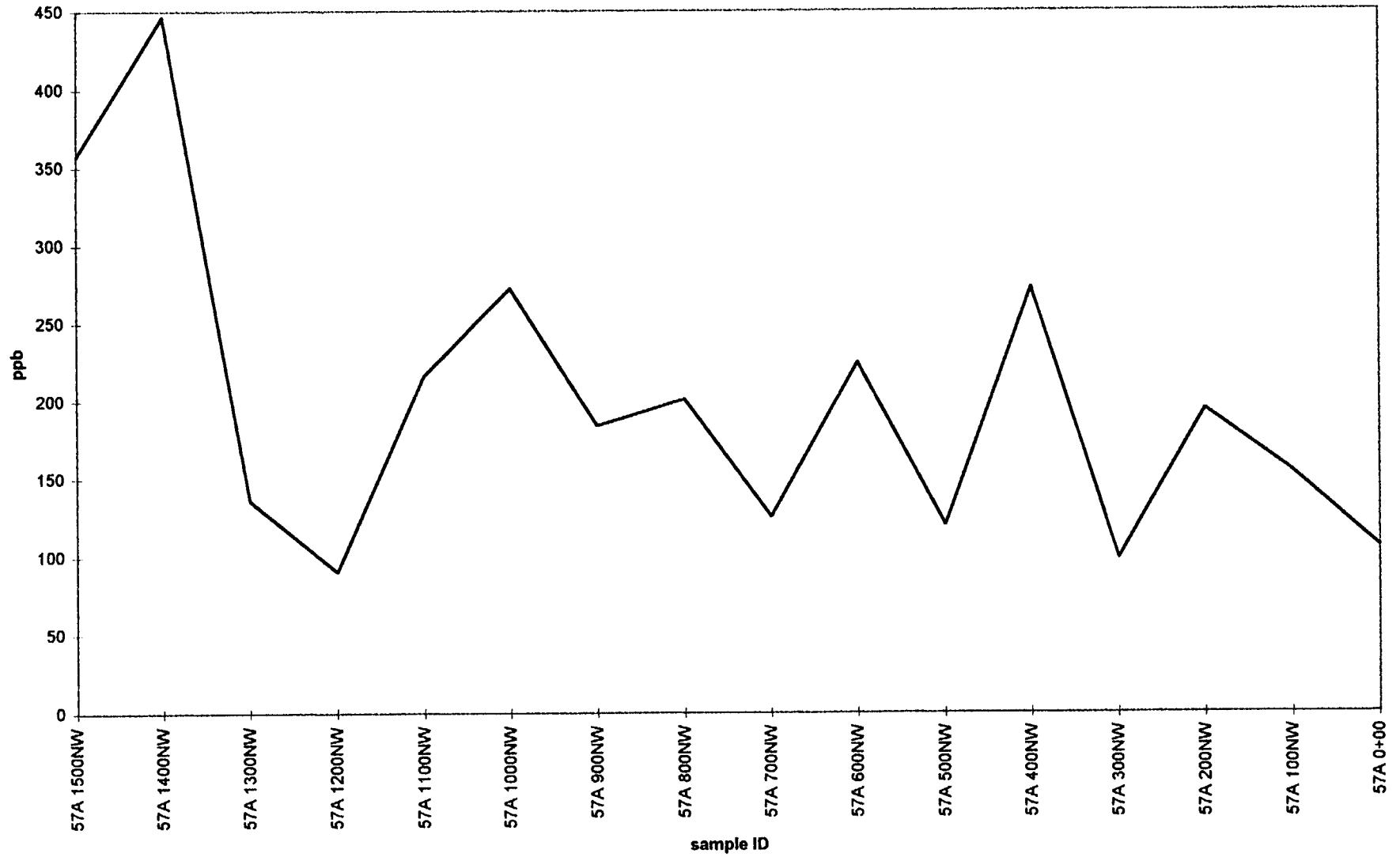
TUZEX CLAIMS Enzyme Leach (SM) data

Sr



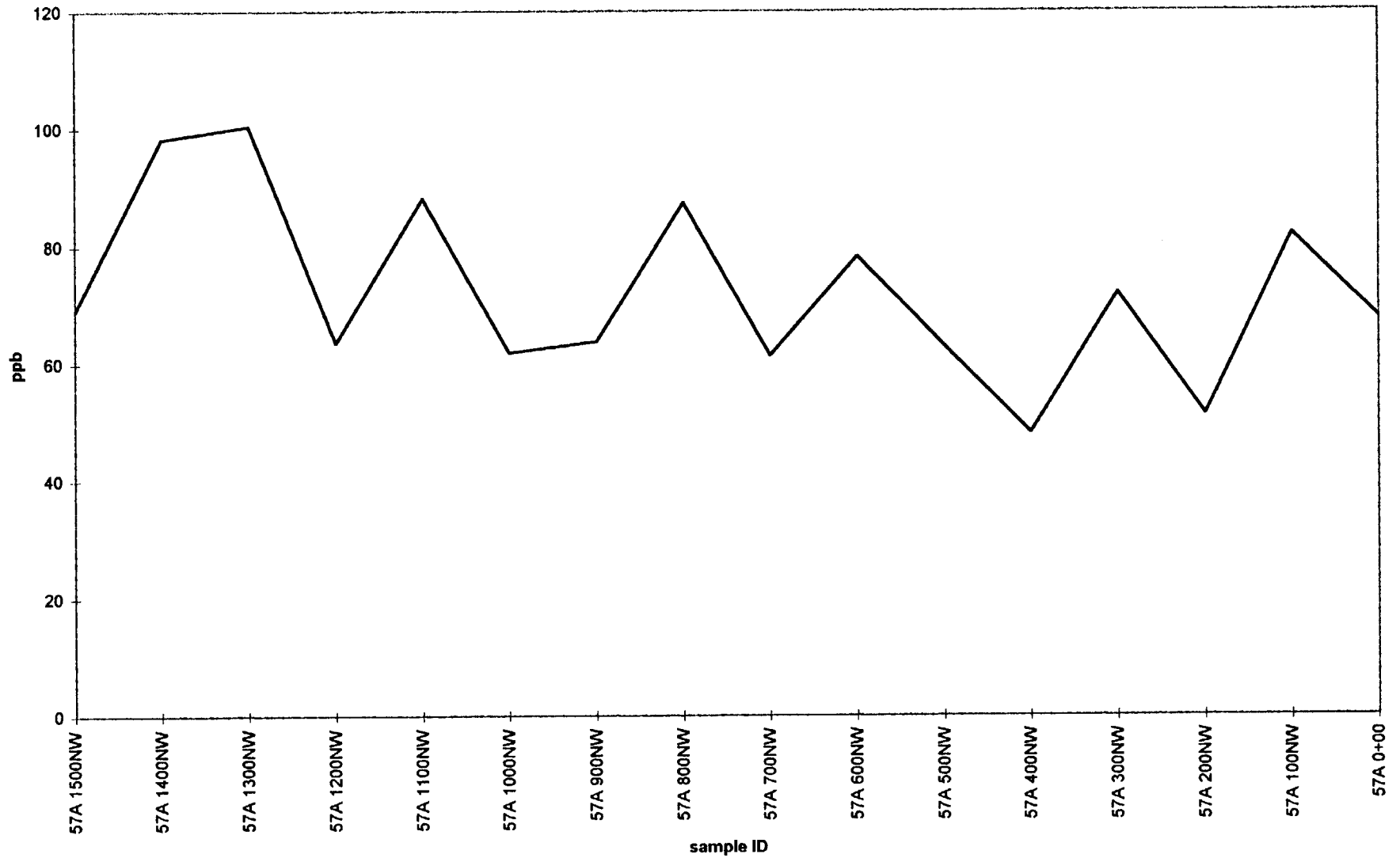
TUZEX CLAIMS Enzyme Leach (SM) data

Ba



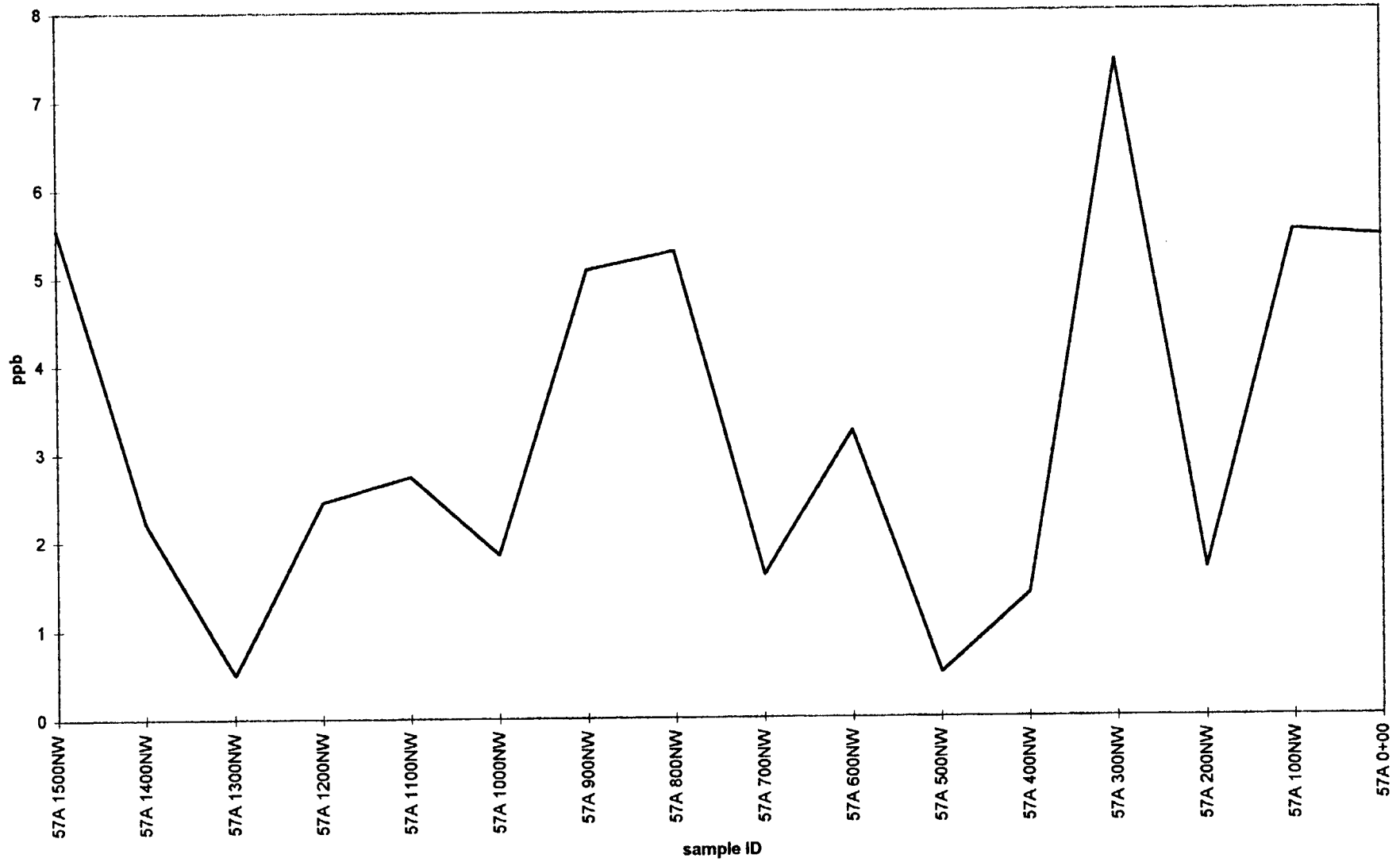
TUZEX CLAIMS Enzyme Leach (SM) data

Rb



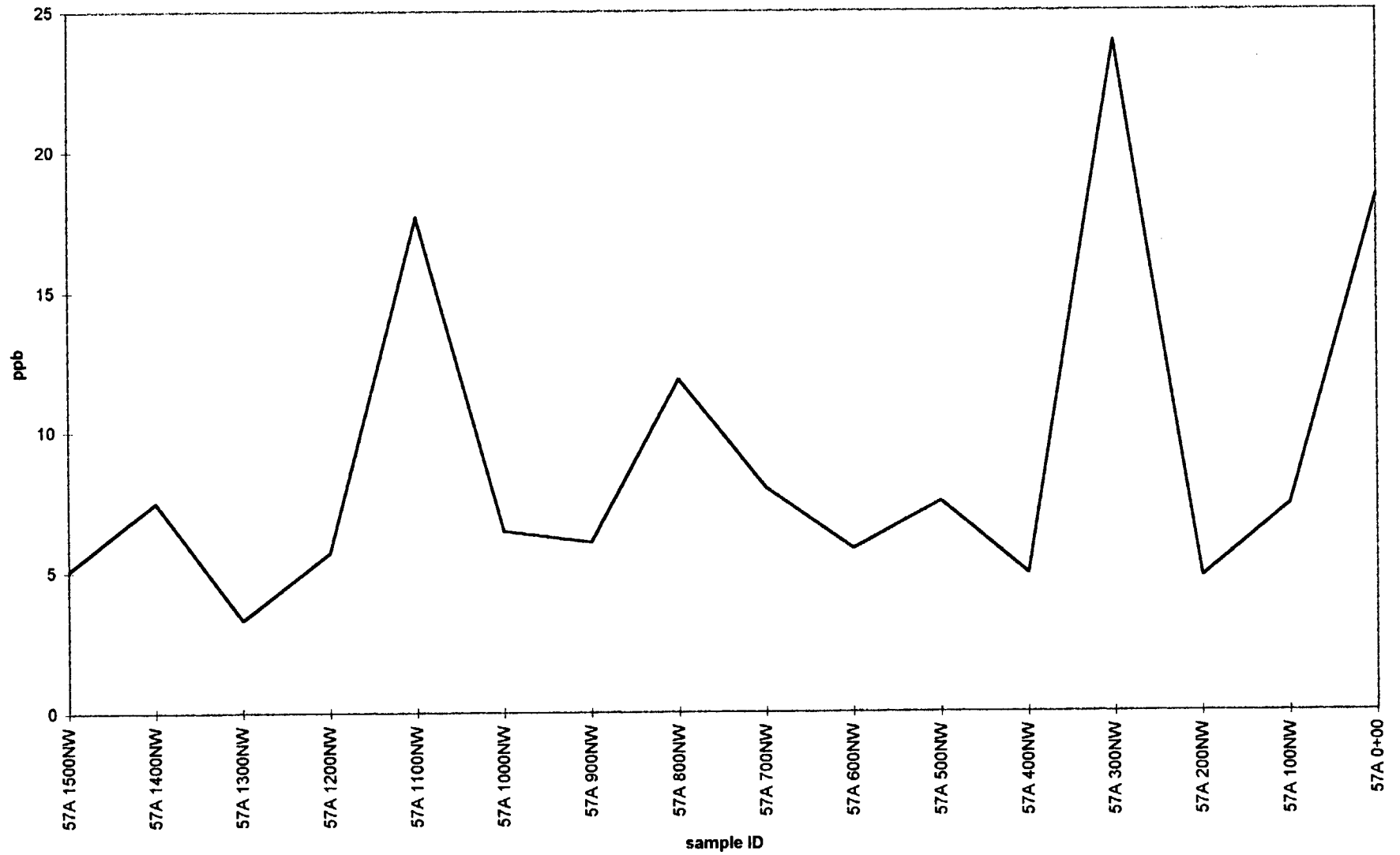
TUZEX CLAIMS Enzyme Leach (SM) data

Zr



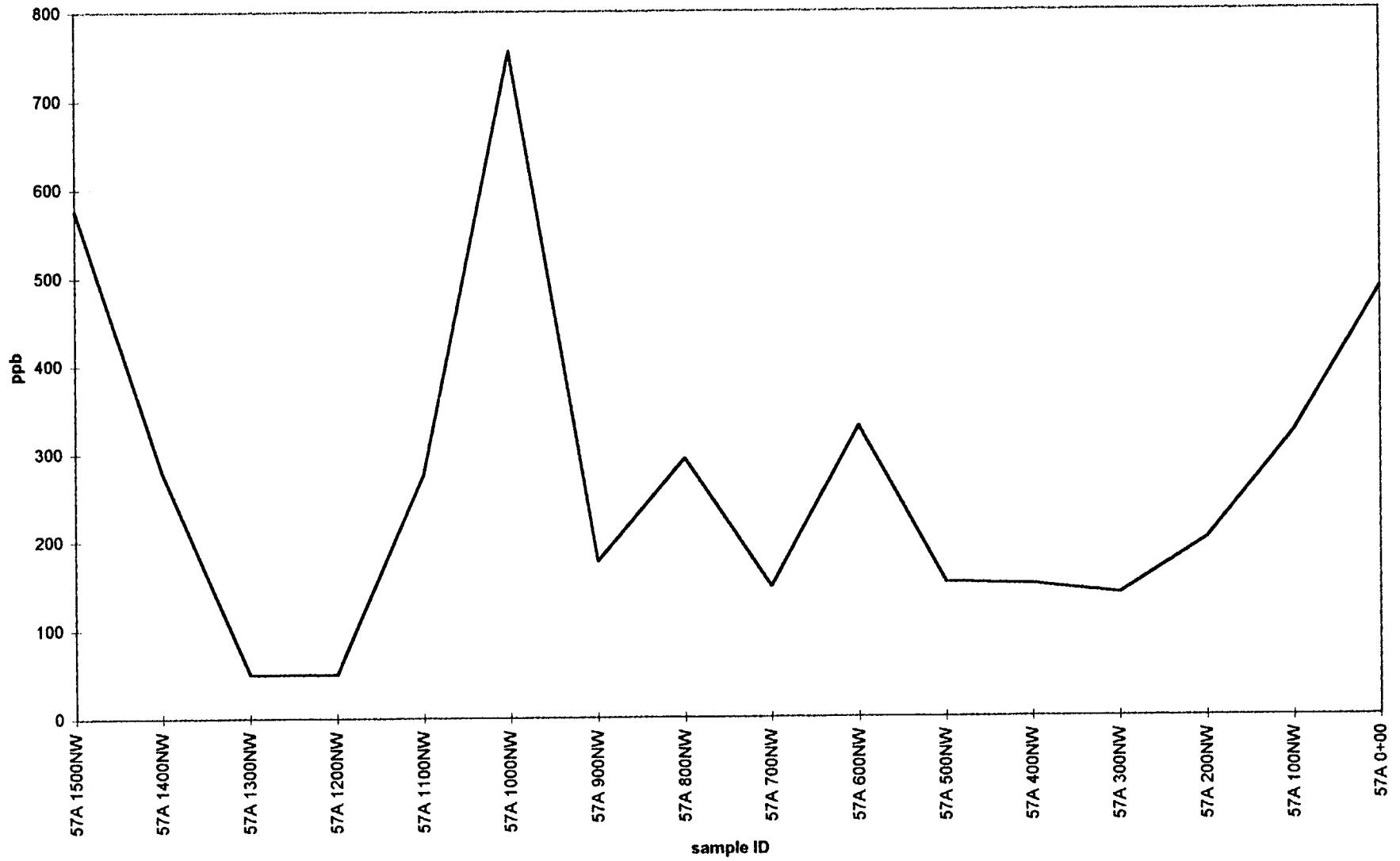
TUZEX CLAIMS Enzyme Leach (SM) data

Y



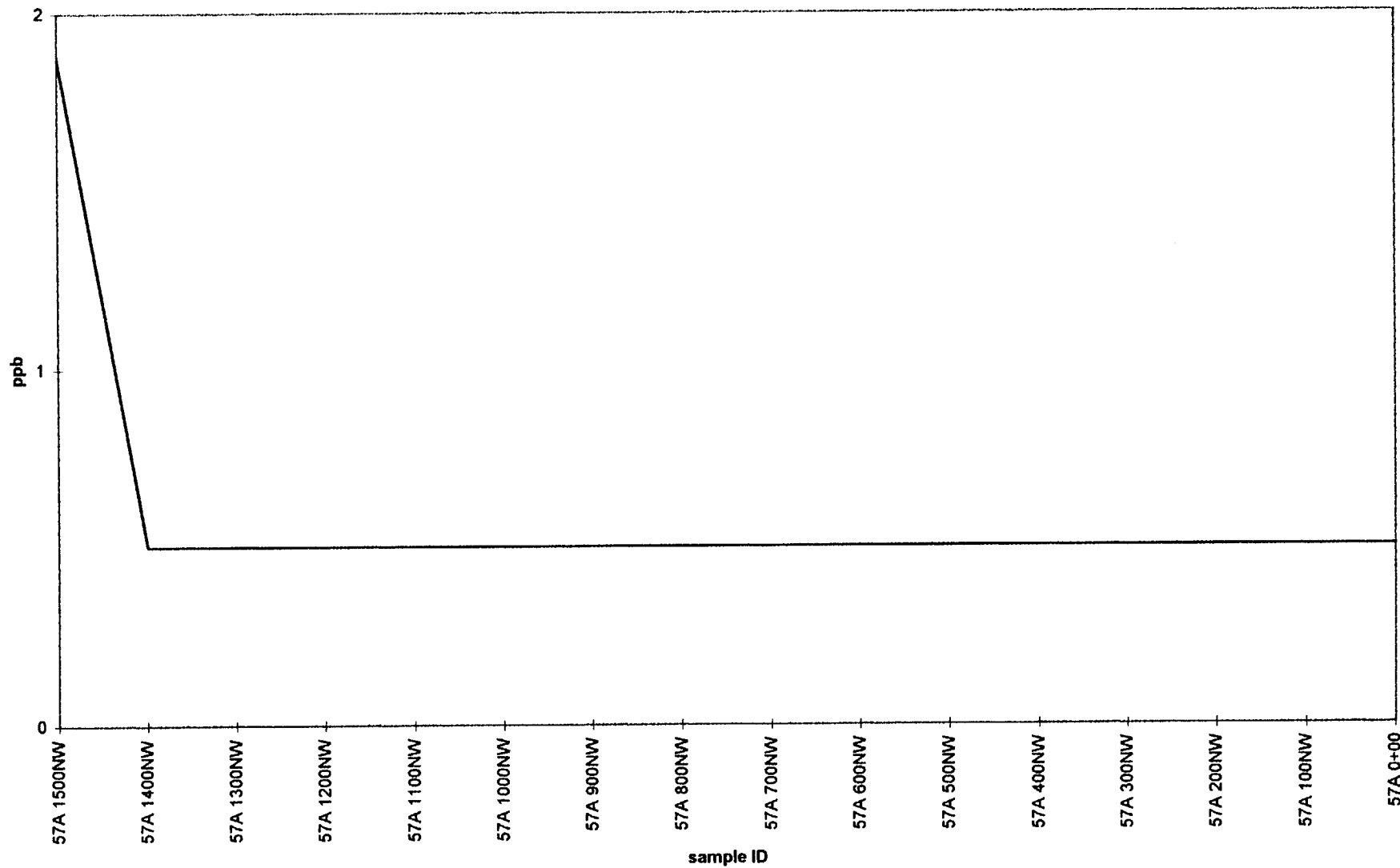
TUZEX CLAIMS Enzyme Leach (SM) data

S.Q.Ti



TUZEX CLAIMS Enzyme Leach (SM) data

Nb



TUZEX CLAIMS Enzyme Leach (SM) data